UNIVERSIDADE FEDERAL DE ITAJUBÁ - UNIFEI
PROGRAMA DE PÓS-GRADUAÇÃO EM ENGENHARIA ELÉTRICA

Framework proposal for selecting a hybrid renewable generation mix at a prosumer connecting point in the context of Micro Smart Grids

Pedro Henrique Ferreira Machado

Itajubá, February 2019

UNIVERSIDADE FEDERAL DE ITAJUBÁ - UNIFEI
PROGRAMA DE PÓS-GRADUAÇÃO EM ENGENHARIA ELÉTRICA

Pedro Henrique Ferreira Machado

Framework proposal for selecting a hybrid renewable generation mix at a prosumer connecting point in the context of Micro Smart Grids

A document presented to the Program of Post-Graduation in Electrical Engineering in fulfillment of the requirement for the degree of Doctor of Philosophy in Science in Electrical Engineering.

Concentration area: Automation and Industrial Electrical Systems

Supervisor: Prof. PhD Luiz Edival de Souza

2019
Itajubá

UNIVERSIDADE FEDERAL DE ITAJUBÁ - UNIFEI
PROGRAMA DE PÓS-GRADUAÇÃO EM ENGENHARIA ELÉTRICA

Framework proposal for selecting a hybrid renewable generation mix at a prosumer connecting point in the context of Micro Smart Grids

Pedro Henrique Ferreira Machado

Itajubá
2019

Pedro Henrique Ferreira Machado
Framework proposal for selecting a hybrid renewable generation mix at a prosumer connecting point in the context of Micro Smart Grids/ Pedro Henrique Ferreira Machado. – Itajubá, February 2019 -
122 p. : il. (algumas color.) ; 30 cm.

Supervisor: Prof. PhD Luiz Edival de Souza

Tese (Doutorado)
Universidade Federal de Itajubá - UNIFEI
Programa de pós-graduação em engenharia elétrica, February 19, 2019.

1. Optimal planning. 2. Renewable energy. 3. Microgrids. I. Luiz Edival de Souza. II. Universidade Federal de Itajubá. III. Instituto de Engenharia de Sistemas e Tecnologia da Informação. IV. A framework proposal for selecting a hybrid renewable generation mix at a prosumer connecting point in the context of Micro Smart Grids

CDU 07:181:009.3

Pedro Henrique Ferreira Machado

Framework proposal for selecting a hybrid renewable generation mix at a prosumer connecting point in the context of Micro Smart Grids

A document presented to the Program of Post-Graduation in Electrical Engineering in fulfillment of the requirement for the degree of Doctor of Philosophy in Science in Electrical Engineering.

Itajubá
2019

Acknowledgements

I thank God first, who strengthens us and keeps us up at all the time.

I thank my parents, Mariana and Nelson, for their support in every decision I have made in my life. The person I am today, I thank you.

I also thank my dear girlfriend Mayara for her patience and support, always by my side in all moments of need.

To friends, who have always encouraged and supported me in the good and bad moments of my life.

My thanks also go to my supervisor, Prof. PhD Luiz Edival de Souza, by the teachings, advice, examples, encouragement and guidance that have opened doors and brought me great knowledge. The thanks are also extended to the my tutor Prof. PhD Jean-Claude Maun for accepting and helping me in the SMART^2 project at Université Libre de Bruxelles in the PhD mobility period.

The present work was carried out with the support of Coordenação de Aperfeiçoamento de Pessoal de Nível Superior - Brazil (CAPES) - Financing Code 001.

"An investment in knowledge pays the best interest."
(Benjamin Franklin)

Abstract

Considering the thematic of climate change, numerous strategies have been adopted in order to struggle with such problem. In electrical systems and power supply, the use of clean technologies is considered the most acceptable solution. In this context, emerges the concept of microgrids (MGs). MGs are local energy providers that can potentially reduce energy expenses and emissions by utilizing distributed energy resources (DERs). Among a variety of DERs used on microgrids, it is widely accepted that renewable sources, especially solar and wind generation, play a significant role in providing sustainable energy, as they are both inexhaustible and less polluting.

Because of that, the microgrids and renewable energy sources are receiving increasing attention from power system operators, since they can aid to transform the current high pollutant power system into a "greener" system. However, there is still much to be considered and proven in relation to the implementation of such technologies. The intermittent nature and the uncertainties associated with solar and wind generation pose sufficient technological and economical challenges for system planners. Besides, the supply of electricity interferes the society as a whole, which makes the implementation of microgrids and renewable energies an even more complex problem, dependent on a wide spectrum of players, interests and constraints.

In this context, the present work is a first effort in establishing a framework that is capable of dealing with such heterogeneous problem. More than that, this thesis contributes with a broader view of microgrid implementation, suggesting a collection of tools which are suitable for observing the effects of penetration of clean technologies on society.

The proposed framework is a five stage planning strategy which allows the system planners to consider all aspects ranging from uncertainty in resources, technological feasibility, economics, and environmental impacts of the system and choose an optimal design suited to their localized conditions. The motivation behind using such strategy lies not only in the optimization of the individual systems or disciplines but also their interactions between each other.

In short, the suggested approach is an iterative procedure divided in five stages, named microgrid coordination, operation optimization, reliability assessment, contingency assessment, and searching mechanism. The microgrid coordination stage has the function of modeling the philosophy used by the energy management system (EMS) to control the power balance in microgrids. The models of EMS are developed using the Petri net formalism. Optimization stage performs a constrained cost minimization analysis of microgrid considering the operation and maintenance (O&M) cost, pollutants emission, and stochastic variables (generation and load demand). After that, it is executed the reliability assessment, where the power system reliability indexes are estimated by means of a Monte

Carlo Simulation (MCS), taking into account the EMS philosophy of microgrid in isolated mode. Next, using the reliability indexes, the contingency probability is calculated using the steady state analysis of a Markov chain, which aims to assess the distribution power system admitting all possible mode transition. Finally, since the DER selection involves multiple criteria and interests of different parts, it is required a multi-attribute decision system providing a list of possible configuration based on their relative importance as denoted by the stakeholders. Because of that, the Particle Swarm Optimization (PSO) is used to search the best DER combination using two distinct solvers - multi-objective weighted function and Pareto front. As result, the framework provides the rated power of each DER that must be installed in the microgrid in order to have an optimal balance between technical, economical, social, and environmental aspects.

Regarding the heterogeneous quality of planning problem, this strategy is effective in the sense of incorporating several aspects into the same analysis framework. In addition, the proposed framework contributes helping the planners to handle the penetration of renewable resources in a systematic way. To have realistic results, the framework is performed on a case of study of a potential campus microgrid program.

Key-words: Petri nets, microgrid design, optimal planning, renewable energy, reliability analysis, distributed energy resources.

List of Figures

List of Tables

List of Acronyms

AI	Artificial Intelligence
BESS	Battery energy storage system
COP	Constant output power
CPN	Colored Petri net
CTMC	Continuous time Markov chain
DER	Distributed energy resources
DER-CAM	Distributed energy resources customer adoption model
DG	Distributed generators
DSO	Distribution system operators
DTMC	Discrete time Markov chain
ED	Economic dispatch
EMS	Energy management system
ENS	Energy not supplied
ERM	Energy resource management
EV	Electrical vehicle
FSM	Finite state machine
GA	Genetic algorithm
GF-CL	Generate first choose later
HPN	Hybrid Petri net
ICE	Internal combustion engine
ILP	Integer linear programming
IPP	Independent power producer
LHS-CD	Latin Hypercube Sampling combined with Cholesky decomposition
LOEE	Loss of energy expectation
LOLE	Loss of load expectation
LOLP	Loss of load probability
LP	Linear programming
MCS	Monte Carlo simulation
MG	Microgrid
MILP	Mixed-integer linear programming
MOPSO	Multi-objective particle swarm optimization
MPPT	Maximum power point tracking
MTBF	Mean time between failures
MTTR	Mean time to repair
MV/LV	Medium voltage/low voltage
NIST	National Institute of Standards and Technologies

OPF	Optimal power flow
PDF	Probabilistic distribution function
PEM	Point estimation method
PN	Petri net
PSO	Particle swarm optimization
PV	Photovoltaic system
RES	Renewable energy sources
SG	Smart Grid
SGAM	Smart Grid Architecture Model
SHS	Stochastic hybrid system
SLP	Stochastic linear programming
SOC	State of charge
SS	State space
STC	Standard test conditions
TE	Transactive energy
UCP	Unit commitment problem
WT	Wind turbine

List of Symbols

Sets

T	set of indexes of time i
D	set of dispatchable generating units
R	set of renewable generators
E	set of energy storage systems

Parameters and Constants

C_i^f	fuel cost of unit i
C_i^m	maintenance cost of unit i
$C_{g,buy}$	cost of buying energy from grid
$C_{g,sell}$	cost of selling energy to grid
C_{ζ_i}	emission factor of unit i
$P_{l,t}$	forecasted load demand at time t
$E_b^{install}$	installed energy capacity of ESS
P_i^{max}, P_i^{min}	upper/lower operation generation capacity of DG i
P_b^{ramp}	maximum charge/discharge variation in storage system
T_i^{on}, T_i^{off}	minimum number of periods that unit i must be kept switched on/off
P_g^{max}	limit on transmission capacity of grid
t_i^{prev}	number of periods unit i has been on or off prior to the first period of the planning horizon

Operation Variables

P_i	power generated by unit i
P_b	charging/discharging power of storage
E_b	state of stored energy
P_{g+}	power imported from grid
P_{g-}	power exported to grid
$y_{i,t}$	1 if unit i is on in period t, 0 otherwise
$u_{i,k}^{on}$,$u_{i,k}^{off}$	1 if unit i is started/switched off in period t, 0 otherwise
y_i^{prev}	previous state of unit i (1 if on, 0 if off)

Decision Variables

x_i capacity of DER assets to be installed

Contents

1 Introduction

Climate change, scarcity of energy resources, and cost of energy are becoming increasingly important in the political agendas. The solutions to reduce energy production from traditional power systems are mainly based on three pillars: the promotion of renewable energy, energy efficiency and energy savings by behavior changes.

The development of renewable energy has seen a significant boost, remarkably because of its associated socioeconomic and environmental advantages, role in addressing climate change concerns, increased federal and state support in forms of tax credits, net metering policy, and other incentives and mandates. However, the renewable energy sources (RESs) are usually weather-dependent, which increases the variability and uncertainty in both generation sector (when appeared in the form of large-scale power plants) and load sector (when deployed by customers as distributed energy resources (DERs)). On the load side, renewable generation proliferation does not only lead to higher variability and uncertainty, hence challenging supply-load balance, but also results in sharp net load ramps that require additional investment and application of fast-response units to address abrupt load changes.

Therefore, it is not only important to adopt many kinds of renewable energy alternatives but also integrating them with public grids in order to achieve a complete energy solution, indicating a greener and reliable choice for electricity, cooling, and transportation needs of communities. So, to guarantee energy in a safe way, the hybrid energy systems stands out. The hybrid characteristic is given by the capacity of taking any combination of the different available RES including solar (photovoltaic - PV), wind, geothermal, with/without traditional diesel engine generator and storage systems, operating in both grid-connected and off-grid (isolated).

In such context, the microgrid (MG) technologies perform a significant role on RES integration. A microgrid can be regarded as a small-scale version of the centralized electricity system able to generate, distribute and regulate the electricity flow in order to satisfy the demand needs in a local and decentralized way [1]. This small-scale energy system allows a most feasible way to cope with RES penetration since it is more flexible than large-scale traditional networks. In this way, one can assumes that the microgrid implementation increases reliability and decreases the pollutants emission. However, the microgrid technologies faces a plenty of issues on implementation side, especially because of its dependency on many players and non-standardized practices. Table 1 expresses the duality on microgrid deployment [2, 3].

Table 1 – Microgrid Benefits x Drawbacks

Benefits	**Drawbacks**
Improves local energy delivery	High installation cost
Increases reliability	Necessity of improved standard legislation and regulations
Efficient energy consumption	Voltage, frequency and power quality
Generating revenue	Resynchronization with the utility grid
Makes the grid more resilient	Market monopoly
Aiding economic growth	
Helping to counter climate change	

1.1 Overview

This work is an effort to promote an appropriate collection of tools for microgrid planning and design. The investigation is largely based on previous work done on pilot and research project, which validate early ideas that may be brought to standardization or at least to common practices.

To contextualize the present work under the Smart Grid vision, the technical report of Smart Grid architectures promoted by the CEN-CENELEC-ETSI Smart Grid Coordination Group (SG-CG/RA) and the National Institute of Standards and Technologies (NIST) [4, 5] is briefly discussed below.

To achieve consistency and gradual integration of innovation in an incremental manner, two items stated in such report are essential:

- an overall high-level model that describes the main actors of the power system and their main interactions. This is captured by the conceptual model;
- a set of universal presentation schema that allow for the presentation of the power system according to a variety of viewpoints that can cope with the variety of power network stakeholders, combining power system management requirements with expanded interoperability requirements, and the possibility of allowing various levels of description from the top to down level to more detailed views. This is captured in the reference architecture that should be seen as the aggregation of several architectures (e.g. technical, economical, environmental, etc.) into a common framework.

The first item is achieved considering well-know and well-accepted models defined on Smart Grid research groups, as presented in some techinical reports [6–8]. The second item is exactly where this thesis is placed, suggesting a set of tools to deal with the new paradigms and new players of power systems. Figure 1 depicts SGAM model adapted by the NIST institute, in which it is highlighted the area where this thesis aims to achieve (distribution system operators, distributed energy resources, customer/prosumers).

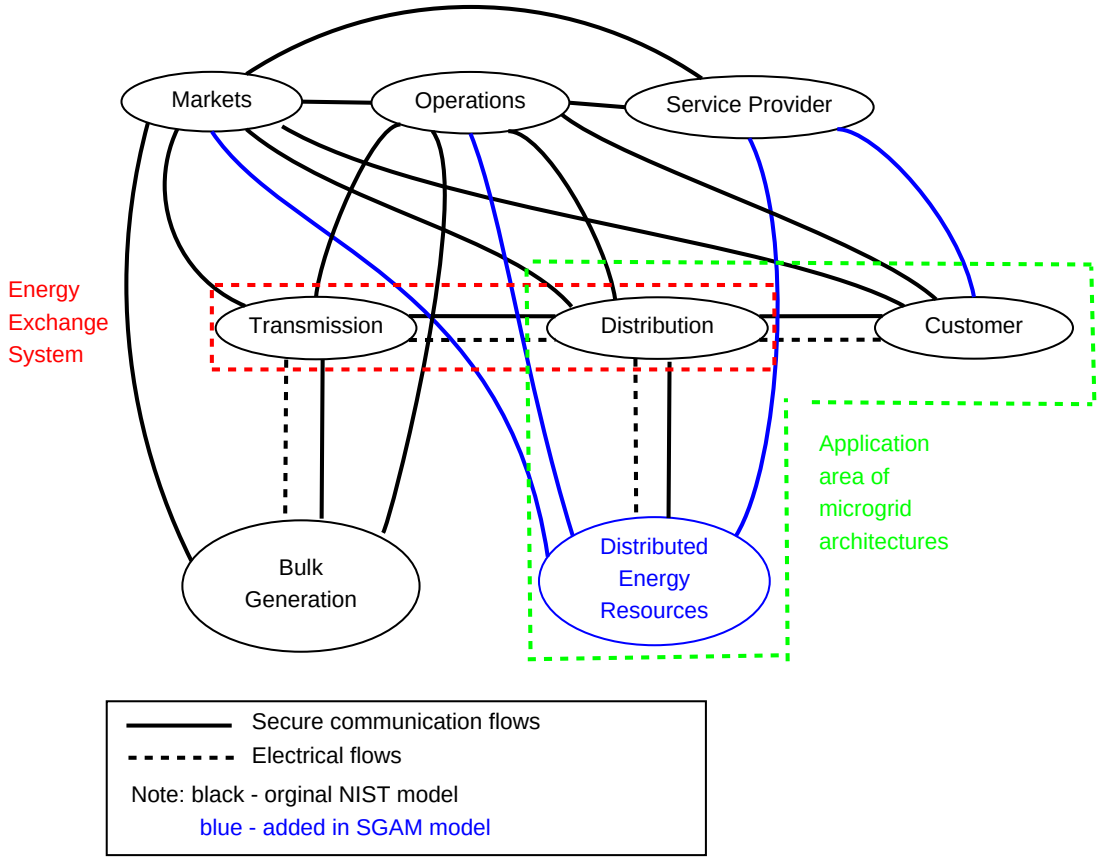

Figure 1 – Conceptual model SGAM adaptation of NIST framework (adapted from [4])

Back to the microgrid context, one may understand the MG as a complex system dependent on many players who consider distinct interests, as technical indicators (power balance, reliability), organizational aspects (business, regulation), and society/environmental issues (energy demand, greenhouse gases emission). Therefore, the investigation about planning of microgrids ponders different aspects at the same time. Here, it is considered four important aspects - energy management strategy, operational costs, pollutants emission, and reliability issues. The selection of these parameters is justified by the reason that they represent the greatest impacts in the implementation of a distribution system as suggested in the literature [9–15].

Thus, the proposed framework indicates a strategy that facilitates the development and implementation of microgrids suggesting suitable tools dealing with operational, economical, social and environmental aspects. The methodology presented in this document is a combination of well-known techniques in the microgrid planning problem, however, the concept of unifying all these techniques in only one problem is unique.

1.2 Related work

There are a significant number of relevant work regarding planning and design of microgrid. However, in order to validate the proposed framework, it is necessary to give more attention to solid solutions. In this way, two tools must be highlighted: DER-CAM [16], and HOMER Pro [17]. The first one has academic purposes, while the second is a commercial software.

Distributed Energy Resources Customer Adoption Model (DER-CAM) is a powerful and comprehensive decision support tool that primarily serves the purpose of finding optimal distributed energy resource (DER) investments in the context of either buildings or multi-energy microgrids. The problem solved by the optimization algorithm is formulated as a mixed integer linear programming (MILP) and the objective function typically consists of minimizing total annual costs of energy supply (including DER investment costs) or carbon dioxide (CO_2) emissions.

Similarly to DER-CAM, the HOMER Pro microgrid software is the global standard for optimizing microgrid design in all sectors, from village power and island utilities to grid-connected campuses and military bases. It uses a proprietary derivative-free algorithm to search for the least-costly system.

Since the present work has academic purposes, the base of comparison is the DER-CAM, which has free distribution, and its implementation is detailed in some scientific papers [18, 19]. Following, some vantages and disadvantages of DER-CAM and the proposed framework are disposed for comparison.

A) DER-CAM - ADVANTAGES AND DISADVANTAGES

The DER-CAM presents some advantages and disadvantages listed below.

ADVANTAGES

- Very accurate economic model;
- Parametric solution;
- Simple to use;
- Allows power network topology;
- Indicates the best size of distributed generators;
- Indicates best positioning of distributed generators;
- Considers power flow analysis;

DISADVANTAGES

- Does not consider the reliability as explicit variable on the objective function;
- Considers ε-constrain method for generation of Pareto front, which is an approximation method (simple approach);
- Does not allows appropriate stochastic sampling, which can lead to weak results;
- Simplifies the formulation considering a single optimization problem;
- Uses only a commercial platform of Mixed Integer Linear Program (MILP) as optimization tool – biased solutions can appear;
- Limited effectiveness in the results when considering multiple aspects, as sustainable approach;

B) PROPOSED FRAMEWORK - ADVANTAGES AND DISADVANTAGES

Thus, the proposed framework aims to face some of the issues listed above. In fact, the main focus of the present work is to develop a more complete solution for microgrid planning/design problems, regarding the concepts of multi-objectivity and sustainability. Obviously, the proposed solution has pros and cons as listed below.

ADVANTAGES

- Considers the reliability as explicit variable on the objective function;
- Uses a more appropriate optimization method for multi-objective problem, avoiding biased solution;
- Allows appropriate stochastic sampling, which gives a more robust result;
- The optimization process and the Pareto optimality is performed using a mix of different techniques (a more complete framework);
- Indicates the best size of distributed generators;
- Allows more effective solutions in the sense of sustainability.

DISADVANTAGES

- Less accurate economic model;
- Does not indicate the best positioning of distributed generators;
- Does not consider power flow analysis;
- Still under validation.

1.3 Objectives

By the way of simplification, most of previous studies on microgrid planning do not explicit consider the uncertainty on weather-dependent generators and load. Besides that, they are determined in an parametric and integrated fashion, by solving a single and complex optimization problem. This indicates a certain contradiction, since an important part of the problem is simplified, whereas the decomposition of the problem, which can decrease the complexity [20], is not examined. Furthermore, these works are mainly focused on capturing some particular aspects of a given MG, especially economic aspects, rather than a global view [21], leading to an unilateral decision.

As such, the present solution transcends the economic aspect, incorporating other aspects as pollutant emissions, reliability, and social effects into the same analysis framework, which means a more sustainable decision. To comply with this, it is developed a distributed architecture which considers uncertainty of DERs and load, and multi-criteria decisions. The proposed strategy decomposes the complex MG planning problem into smaller and easier to solve subproblems. Furthermore, the present work contributes suggesting a collection of appropriated tools for each subproblem.

Therefore, the present thesis aims to fulfill some gaps on microgrid planning problem, promoting a more complete solution in the sustainability point of view.

The list of goals proposed in this research for building the framework are:

- Develop statistical models of renewable energy resources and demand given uncertainties inherent in them;
- Investigate optimal scheduling of typical scenarios of microgrid considering the minimization of capital and operational costs subject to operational constraints;
- Assess the relation between RESs penetration and reliability issues;
- Analyze the impacts of possible microgrid configurations regarding diversified interests (environmental, technical, economical, social);
- Present a procedural design of a possible commercial software;
- Validate the PSO algorithm as a proper solver of multi-criteria microgrid planning problem.

It is necessary to clarify that the suggested framework identifies tools which can be used in a standardized way, leading to a global view of microgrid planning problem. The study does not contemplate an specific investigation of each step. Instead, it suggests a set of methods and procedures which are commonly used in academic and commercial solutions.

In specific terms, the present work aims to facilitate the planning and design of microgrids suggesting suitable tools dealing with operational, economical, social and environmental aspects. In broader terms, the proposed framework seeks to establish a knowledge base and common practices which point to multidisciplinary and flexible approach of microgrid planning, leading to a sustainable development.

1.4 Main contributions

The current PhD thesis aims at researching appropriate set of tools to deal with planning of hybrid renewable energy systems in the context of microgrids. In this way, the main contributions of the present work are disposed herein:

- Configuration of a set of tools suitable for the treatment of microgrid planning problems;
- Definition of appropriate composition of hybrid renewable generation mix at a prosumer (producer-consumer) connecting point;
- Presentation of a more heterogeneous vision of microgrid planning problem in the Smart Grid scenarios;
- Framework documentation for continuous improvement.

1.5 Document organization

This work is presented in six chapters. Chapter 2 offers a literature review of the research contributions in the area of microgrid planning. Chapter 3 presents the theory basis and tools that support the development of the proposed framework. Chapter 4 demonstrates the integration of the framework's subproblems using a comprehensive programming approach. Chapter 5 presents simulation results and analysis of possible microgrid configurations using some data available on public data sets. This chapter allows to address and comprehend each stage of the framework and to observe the effects of changing the stakeholders interests and technical parameters. Chapter 6 draws the conclusions of the work. It also lays a path for researchers to investigate new areas of microgrid planning.

2 Literature Review

An overall questionnaire made in the research undertaken in the framework of EUROPEAN MORE MICROGRIDS project [22] indicates that the customers and system operators at microgrid pilot test locations were willing to adopt the energy saving and emission reduction measures. However, they were not very enthusiastic to engage or invest in new technologies for distributed generation, without any previous experience [23]. It seems quite unlikely that the grid users will completely change their everyday habits and shift their daily energy and policies, which implies that more effort needs to be done in the area of rising awareness of overall benefits/drawbacks of microgrids concept.

The following literature review aims to point some of the particular perspectives which are still under scientific investigation.

2.1 Optimal planning of distribution systems

Studies about optimal planning of distribution systems have two main goals considering the time horizon of observation (short-term and long-term horizon). Short-term problems deals with scheduling of power generation and demand response in day-ahead or few-hours-ahead energy trading, while long-term take charge of optimal sizing and/or location of generators. Both approaches mainly aims to provide good quality and reliable energy while minimizing costs and pollutants emission. The minimization process is subject to a group of constraints, which forces the optimal solution to obey some rules such as the generator and grid limitations, acceptable level of pollutant emission, social and political restrictions, reliability level, meteorological parameters, and so on.

The uncertainty and intermittence of renewable energy sources places as a challenge to generation scheduling of microgrids. In [24], it is developed a hierarchical framework to handle an economic generation microgrid scheduling considering the intermittent energy sources. The lower level combines a battery energy-storage system (BESS) with renewable energy sources, targeting maximal utilization of renewable power and minimal deviation from the schedule, providing an optimal generation plan in the day-ahead market. The upper level minimizes the total cost of the microgrid by means of genetic algorithm (GA) to yield an economic generation plan of dispatchable distributed generators (DGs) based on the lower level. Similarly, [25] addresses a Multi-Objective Particle Swarm Optimization (MOPSO) methodology to solve Energy Resource Management (ERM) problem in buildings with penetration of Distributed Generation (DG) and Electric Vehicles (EVs), considering the uncertainty of photovoltaic (PV) generation. The methodology aims to maximize profits while minimizing CO_2 emissions. In [26], the authors assess the benefits

for the distribution system of scheduling flexible residential loads focusing on electric vehicles (EV). It is proposed an extensive load model and a formulation of a bilevel Mixed Integer Linear Programming (MILP) optimization problem. The lower level minimizes individual household electricity bills using dynamic pricing, while the upper level intends to smooth the power load curve of a typical MV/LV transformer.

For the optimal design problem, the authors in [12] present a mathematical model and optimization algorithm to identify the optimal microgrid configuration (in terms of the installed capacities of the generators) and its respective optimal scheduling generation. The optimal design and placement of DERs is also treated in [10]. The microgrid decision support tool Distributed Energy Resources Customer Adoption Model (DER-CAM - [27]) is used to determine the optimal installation place, size and type of distributed energy resources (DERs) while minimizing cost and emission. Similar strategy is seem in [11–13]. The work presented in [11,14,15] executes the planning/design of microgrid also including indexes of system reliability and equipment outages.

In [28], a possibilistic–probabilistic model was proposed to address the impact of EVs in distribution systems. The proposed methodology is based on the combination of fuzzy theory and probability distribution functions (pdfs) employing Monte Carlo simulation (MCS) to model the load in an uncertain manner. After that, an optimal wind distributed generation planning was investigated employing an intensified hybrid PSO/GA. Still considering the topic of penetration of EV in distribution systems, the papers [29] and [30] address the problem of insertion of electric vehicles from the economic dispatch (ED) point of view, indicating the relevance of vehicle batteries on microgrid operation optimization.

The economic dispatch, based on unit commitment problems (UCP), and optimal power flow (OPF) are frequently considered in planning process where uncertainties are present. Probabilistic methods as Point Estimation Method (PEM) [31, 32] and Latin Hypercube Sampling combined with Cholesky decomposition (LHS-CD) [33] are some of the proposed solutions. Besides probabilistic strategies which usually perform a Sequential Monte Carlo algorithm, a formal approach can aid the process of modeling and simulation of a microgrid. Highlighted in [21], a MG model is developed based on Stochastic Hybrid Systems (SHS), capturing the interaction between probabilistic elements and discrete and continuous dynamics.

2.2 Social aspects of microgrid

Seeking to provide energy to remote and isolated areas, the microgrid appears as a feasible solution. Traditional efforts to reach these remote communities through centralized grid are expensive, logistically complex, time consuming, and ultimately unprofitable

in many cases. Decentralized microgrids, however, provides a financially feasible solution [34].

The implementation of microgrids in remote and/or poor places, where the electricity is low-quality or even non-existent, promotes the discussion upon the benefits that the MGs technologies bring to sustainable communities, balancing and integrating four main components: environment, economy, society and culture [35].

As real examples, Brazilian Amazon forest and Red Lake community in Canada are areas of study in [36] and [35], respectively.

Still considering sustainable solutions, the paper [37] assesses consumer valuation of different attributes of electricity supply to elucidate the conflict between solar microgrids and the centralized utility grid in India. Besides that, such paper provides an insight to support government policies and infrastructures deployment. The study also contributes significantly to understand the role of microgrids in complementing a centralized system and its value as a sustainable energy solution for development. Electricity reliability, power, price, and hours availability are studied through a choice experiment, a method uniquely able to disaggregate the willingness to pay for each attribute.

In the matter of good-quality energy brought by MG implementation, in [38] is conduced an evaluation over reliability and economic indexes considering penetration of renewable energy in microgrid power systems. The results obtained from this study have established the substantial influence of renewable sources and storage systems on the reduction of annualized energy costs and reliability improvement of power system, representing significant benefits to society. A similar approach is proposed in [39], where it was identified the most prominent problems and challenges that the electric power systems faces in developing countries, influencing the decision making process. The authors have identified two major factors, namely, reliability and cost. To connect these factors, the authors suggest the reliability parameter of energy not supplied (ENS) and outages charge rates to monetize the deficit between power generation and demand consumption.

Besides that, some of these before mentioned renewable energy sources will be installed directly at the premises of the end consumers (e.g. photovoltaic systems), transforming their role to prosumers (producers-consumers) [40]. In summary, the era of renewable energy, decentralized energy sources and smart grid technologies will empower all prosumers, from households to small and medium sized enterprises, as well as larger companies, to integrate their consumption and production of energy in networks that would function more like ecosystems than markets. This situation will undoubtedly challenge conventional power generated by centralized power and unidirectionally distributed by utility companies [41].

Hence, the direction of future research is to conceptualize a model of the electricity

prosumers and to model prosumer behaviors through computational simulation method where, by applying different energy policy and intervention into the virtual environment it is possible to observe and analyze prosumer behavior when changing different inputs. Such new computational simulation strategies that incorporates social aspects, more specifically prosumers behavior, in the microgrid planning problem is one of the objectives proposed in this thesis.

2.3 Microgrid - business case

In general, the microgrid can be owned by the distribution system operator (DSO) or utility, the customer, or an independent power producer (IPP). In each case, benefits will be valued differently; the DSO would tend to value technical benefits such as reduced peak loading, whereas the customer would likely value energy cost reduction [42]. On the other hand, a free-market IPP-owned model can be operated with the interests of all stakeholders.

The multi-party energy market, also referred as new paradigm of transactive energy (TE), is illustrated in [43]. The authors suggest that the IPP-owned microgrid will be able to participate in retail, wholesale, and bilateral markets when operating in a grid-connected mode.

There are two major energy transaction-based benefits for microgrids. The first is based on the fact that wholesale energy prices may be significantly lower than retail prices, the difference being made up by charges for network usage, service fees, market charges, retail charges, and taxes. Since the microgrid can deliver power directly to its local loads without using the main network, this power is not subjected to the same additional fees, and may be offered to customers at a rate that is higher than wholesale (providing additional revenue to the IPP) and lower than retail price (providing cost savings to the customer) [44]. The second major benefit is based on fluctuations in wholesale prices on the energy market. Microgrids can use intelligent controls to provide peaking power when market demand and energy prices are high, and they can purchase power from the grid when demand and energy prices are low.

Following the case of IPP-owner, the authors in [13] propose a systematic approach and methodology for formulating and quantifying different microgrid business cases. Two main cases are suggested: (i) IPP owns and runs their own utilities including the electrical system; (ii) there are three stakeholders, named the urban residents acting as both customers and society, IPP who owns the microgrid system, and the utility or Distributed System Operator (DSO) who regulates the bidirectional power flow. Also, the proposed framework defines what are the benefits and beneficiaries of each case. Furthermore, it investigates the dependency of chosen business case on microgrid technologies and oper-

ation.

Different from most of the operational microgrids with single owner, [45] focuses on community based multi-party microgrids which involves critical loads and generators of multiple owners, who has different structures, but, unique operating objectives as cost reduction, decreasing of pollutants emission, revenues, reliability, remote area electricity supply, and so on.

2.4 Microgrid to enhance distribution system resilience

Thanks to smart grid (SG) technologies, the conventional power system is about to transition from a static and centralized grid to a reconfigurable and decentralized grid. In this context of reconfigurable networks, SG use remotely controlled switches to control and change the network topology to ensure that desired objectives can be achieved. SG can provide customers with a greater degree of reliability, and power quality. In this context, the microgrids appears as an effective solution to sustain the reconfigurable grids, since it can provide energy to a group of load when an abnormal event occurs at the main grid.

A microgrid can be implemented by using the four-stage approach: demand reduction, on-site generation and storage, advanced controls, and grid independence. Local and master controllers work together to optimize the operation of a microgrid and its interaction with the main grid, enhancing the reliability and resilience of power generation. The hierarchical control diagram (primary, secondary, and tertiary control level) is responsible in islanding operation, grid-connected operation, and the smooth transition between these two operation modes [46].

In practical meanings, [15] presents a framework for analyzing the resilience of an electric power grid with integrated microgrids in extreme conditions. The objective of this paper is to demonstrate that controllable and islandable microgrids can help improve the resiliency of power grids in extreme conditions. The Markov chain is utilized to represent the state transition of a power grid with integrated microgrids in these conditions, and calculate the probability of the system being at contingency state.

The resiliency-oriented MG is also addressed in [47], in which it is presented a two-stage stochastic linear programming (SLP) framework for optimal scheduling problem. Stage one characterizes the uncertainties, and stage two generates the possible scenarios. After that, the SLP is solved using commercial softwares (IBM CPLEX and GAMS IDE). The optimization process tries to minimize the socioeconomic cost of MG while taking into account the operation constraints considering two groups of uncertainties, categorized as: I) normal operation uncertainties (including errors in forecasting wind data, EV operation, and real-time market prices), and II) contingency-based uncertainties (including random forced outages, unintentional islanding, and resynchronization events).

In a more technical programming issue, the paper [48] indicates that sampling strategies influences the reliability indexes in a power system including RES. Because of that, an appropriate Monte Carlo simulation using Latin hypercube sampling techniques are investigated, showing that different techniques can lead to different results and errors. In the phase of microgrid implementation, these planning errors could reflect in over or under sized MG systems.

For the specific case of remote microgrids, the reliability assessment is the priority aspect on the planning process. Regarding the isolated mode of operation, the author's work presented in [49], assesses the reliability of a microgrid operating in such mode. It was used the colored Petri net (CPN) formalism in order to model and simulate the proposed hybrid microgrid, gathering the reliability indexes.

2.5 Energy management system - suitable formalisms

Two of the key functionalities in microgrid's energy management system (EMS) are the optimal scheduling and coordinated operation. Optimal scheduling includes optimal unit commitment of all dispatchable generation resources, as well as demand management of flexible load, and coordinated operation. Coordinated operation aims to supervise some control parameters in order to manage or to constrain power flow in multi-source power system based on certain generation policy (*e.g.* lower pollutant emission, lower cost, use of energy storage system, etc.). Existing EMS functionalities and architectures for microgrids are extensively investigated and reviewed in [50], which could be classified as centralized and distributed EMSs. A centralized EMS is especially suitable for a single owner microgrid with adequate system observability and consistent operation goal, while decentralized EMS works for community multi-party microgrids.

Since a while, Petri net (PN) modeling has been applied in many specific areas of power systems, such as power system restoration, protective relay algorithm modeling, fault diagnosis, reliability analysis, and distribution network reconfiguration. A survey with these applications can be found in [51]. In the context of microgrids, the PN is used as formal tool to design and simulate energy management strategies of distribution systems [52, 53]. The objective of energy management modeling is to validate certain energy policy by means of numerical simulation before experimental tests.

In [54], the power system modeling and power balancing control for grid-connected mode is studied. To do so, the PN modeling is used as a formalism to interpret such scheme. It identifies the constraints of microgrid and presents a coordinated operation in order to establish an overall power balancing control strategy considering all the different sources. Similar approach is used in [9] and [55] in which a building integrated photovoltaic system with energy storage is considered. In these papers, the behavioral

modeling of multi-source power system components is based on discrete PN state modeling. Identification of discrete states of each multi-source subsystem allows the subsequent design of energy management.

Following the same perspective of using Petri net to model coordination, [56–58] includes a multi-agent event-triggered control for intelligently restructuring the operating mode of a microgrid ensuring the energy supply with high security, stability and cost effectiveness. On Petri-net model, the operational mode switching process of each unit agent depends on, not only its own event-driven discrete behavior, but also on interactive behaviors with other agents. For instance, when a unit agent needs to change its operation mode, it needs to send a request to other agents in order to deliberate if its switching request can be implemented at that time. The interactive behaviors are implemented based on Foundation for Intelligent Physical Agents - Agent Communication Language (FIPA-ACL) messages. Such multi-agent approach seems promising for real MG scenarios implementation.

Considering other formalisms than PN, [21] puts forward a model of a MG that is based on the framework of Stochastic Hybrid Systems (SHS). It shows that SHS models can capture the interaction between probabilistic elements and discrete and continuous dynamics, and thus promise to be able to tame the complexity of distribution systems. Similar approach is shown in [59], where an hybrid Petri net (HPN) modeling method is able to describe the discrete and continuous dynamic of microgrid elements. The reachability graph of the resulting HPN is generated and used to list all the possible options/choices at a EMS decision. The formalisms can also aid the deployment process of a EMS controller as shown in [60, 61], in which a finite state machine (FSM) model supports the development of a software used to control the energy in the microgrid.

As suggested, the EMS is a specific or a group of controllers which aim to coordinate the MG operation in a optimized way. To do that, it is necessary a communication system to support the interaction among the elements of the microgrid. In this way, the recent author's work [62] investigate the impacts of communication network in a microgrid context. Such paper, presents a proper CPN modeling and simulation of the islanding process over the communication point of view. It is observed from this work, modifying some parameters of critical message transmission can lead a stable operation of EMS to an unsafe condition.

3 Fundamentals and Theory Basis

In order to have a solid framework, there is the need of convenient description of mathematical fundamentals, programming tools, and system modeling. Thereby, this chapter aims to expose the necessary background concerning the proposed framework stages.

3.1 Monte Carlo simulation for reliability assessment

Monte Carlo simulation (MCS) generates a random sample of N points for each uncertain input variable of a model. It selects each point independently from the probability distribution for that input variable. It generates a sample of N values or scenarios for each result variable in the model using each of the corresponding N points for each uncertain input. From this random sample for each result, it estimates statistical measures such as mean, standard deviation, and probability density curves.

There are two basic techniques utilized in Monte Carlo applications to power system reliability evaluation. These are known as the sequential and non-sequential techniques. In the non-sequential method, the states of all components are sampled and a non-chronological system state is obtained. In the sequential approach, the uncertainty cycles of all components are simulated and a system operating cycle is obtained by combining all the component cycles. Sequential technique permits chronological issues to be considered and distributions of the reliability indexes can be calculated. This method, usually requires a larger investment in computing time and effort compared to the non-sequential technique [63].

Sequential simulation provides the ability to consider the chronological time varying load and generation profiles, and can be used to obtain extra information that other techniques are unable to produce, such as probability distributions.

The sequential Monte Carlo approach can be used to model all contingencies and operating characteristics inherent in the system. The major steps in using the sequential procedure with time varying loads and generation for composite system reliability assessment, are as follows:

1. The chronological hourly probabilistic models give the load and generation for the simulated hour.

2. The simulated operation of the system is assessed.

3. Steps 1-2 are successively performed for the entire sequence of system states over a year. The yearly adequacy indexes are accumulated as $F(X_j)$ where X_j is the sequence of system states in year j and $F(X_j)$ is the reliability index function over the year j. In order to evaluate the loss of load probability (LOLP) for instance, $F(X_j)$ is the sum of durations of all failure states divided by the number of hours in a year (8760 hours) in the year j.

4. If the coefficient of variation of the chosen index is greater than the tolerance level, steps 1 - 3 are repeated until convergence is achieved. The coefficient of variation (β) is calculated as shown in [64]:

$$\beta = \frac{\sqrt{V(F)/NS}}{E(F)} \tag{3.1}$$

where:
V(F) is the variance of the test function;
E(F) is the expected estimate of the test function;
NS is the number of simulated years.

5. The adequacy indexes are estimated as follows, also presented in [64]:

$$\text{Expected value} = \frac{\sum_{j=1}^{NS} F(X_j)}{NS} \tag{3.2}$$

In [63, 65] a proper description is given with a good practical example of MCS in power system reliability.

3.2 Microgrid composition and modeling

Figure 2 displays the composition of the proposed MG which is considered in the present work. The MG is connected to the main distribution grid, which feeds the local power network with electricity. In this work it is assumed that the main distribution grid is operated by a distribution system operator (DSO). Three local generation sources are additionally considered: diesel generation set, wind turbine, and photovoltaic (PV) generation system. The diesel generators are controllable devices, while wind turbine and PV represent uncontrollable generation devices with a stochastic behavior. Furthermore, an electrical energy storage is considered in order to give higher flexibility for power balancing. Also, several electrical loads are connected to the local power network. These loads are stochastic in nature, but they are controllable, which allows the implementation of energy shedding policies.

To coordinate the microgrid operation, the energy management system (EMS) communicates to all the elements in order to observe the state of each subsystem and execute certain control action. The EMS will be better discussed in section 4.1. For sake of simplification, no network topology is discussed in the present thesis.

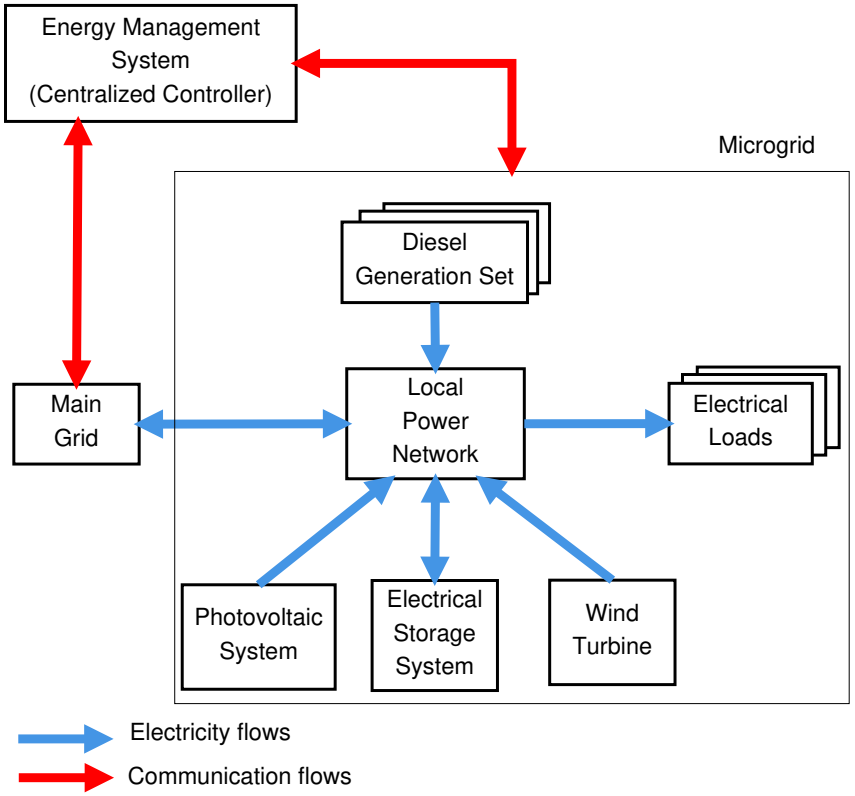

Figure 2 – Microgrid composition - prosumer connecting point (adapted from [21])

3.2.1 Wind generation

The output of a wind generator is determined by the average hourly wind speed at the hub height and the output characteristics of the wind generator. Since wind speed is a stochastic parameter, the probability of a given wind speed can be estimated if the probability distribution is known. Once the wind speed is known, the power injected into the grid can be calculated by means of certain probabilistic model of wind turbine (WT) power generation. This information is useful for planners to predict accurately wind power available at the site.

As deduced in [66], hourly wind speed v is considered as a random variable and is modeled using the Weibull probability distribution function (pdf). The mathematical expression is given by (3.3), where k is the shape parameter ($k > 0$) and c is the scale parameter ($c > 0$). The parameters k and c can be approximated by (3.4).

$$f(v) = \frac{k}{c}\left(\frac{v}{c}\right)^{k-1} \exp\left[-\left(\frac{v}{c}\right)^{k}\right] \tag{3.3}$$

$$\begin{cases} k = \left(\frac{\sigma}{v_{mean}}\right) \\ c = \frac{v_{mean}}{\Gamma(1+1/k)} \end{cases} \tag{3.4}$$

where v_{mean} is the annual mean speed, σ is the standard deviation based on historical data of wind speed for a particular site, and $\Gamma(\cdot)$ represents a Gamma function. For stochastic sampling process, it is necessary the usage of cumulative distribution function (cdf) which can be mathematically represented by (3.5).

$$F(v) = 1 - \exp\left[\left(-\frac{v}{c}\right)^k\right] \tag{3.5}$$

The wind turbine power output P_{WT}, dependent of wind speed v, follows 3.6, which is better described in [67]. From such equation, the profile of a wind turbine generated power related to wind speed can be better understood in Figure 3. Also, the values for v_{in}, v_r, and v_{out} are adopted from [68], where the values for these parameters are 3 m/s, 11 m/s, and 22 m/s, respectively.

$$P_{WT}(v) = \begin{cases} 0, & v < v_{in} \quad (a) \\ a + b.v + c.v^2, & v_{in} \leq v \leq v_r \quad (b) \\ P_r, & v_r \leq v \leq v_{out} \quad (c) \\ 0, & v > v_{out} \quad (d) \end{cases} \tag{3.6}$$

where:
P_r is the wind turbine rated power;
v_{in} is the cut in wind speed;
v_{out} is the cut out wind speed;
v_r is the wind speed for rated power;

The terms a, b and c of (3.6) can be calculated using (3.7):

$$\begin{aligned} a + b.v_{in} + c.v_{in}^2 &= 0 \quad (a) \\ a + b.v_r + c.v_v^2 &= P_r \quad (b) \\ a + b.v_c + c.v_c^2 &= P_r.\frac{v_c^3}{v_r^3} \quad (c) \end{aligned} \tag{3.7}$$

where:

$$v_c = \frac{v_{in} + v_r}{2} \tag{3.8}$$

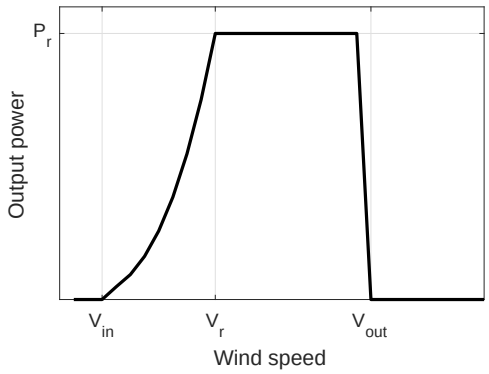

Figure 3 – Wind turbine output power profile

3.2.2 Solar generation

The power output of PV system is dependent on stochastic variables as well. For solar generators, the variables of interest are the radiation and temperature of specific site.

For long-term planning analysis, the solar radiation is considered as a beta random variable [32, 69, 70]. Beta distribution model works to describe the stochastic vibration of the hourly solar radiance around its mean value.

$$f(s) = \frac{\Gamma(\alpha+\beta)}{\Gamma(\alpha)+\Gamma(\beta)} \times s^{\alpha-1} \times (1-s)^{\beta-1}, \quad 0 \leq s \leq 1, \alpha \text{ and } \beta > 0 \tag{3.9}$$

where s represents the solar radiance (kW/m^2), α and β (refer to (3.10)), which are parameters of Beta pdf, are derived as follows:

$$\begin{cases} \beta = (1-\mu) \times \left(\frac{\mu(1-\mu)}{\sigma^2} - 1\right) \\ \alpha = \frac{\mu \times \beta}{1-\mu} \end{cases} \tag{3.10}$$

The calculation of how much power a PV can generate in one hour is exposed by 3.11, which is adapted from [71]. In [71] it is considered the minute-by-minute DC output of the solar array. However, since the proposed microgrid (refer to Figure 2) is an AC network, it was necessary to adapt what was suggested in [71] imposing the inverter efficiency (n_{inv}) and the photovoltaic panel efficiency (f_{PV}). Such adaptation is first presented in [68]. It is important to mention that this formulation of power generated by solar arrays does not consider the geographical aspects nor installation angle of each PV panel.

$$P_{PV} = n_{inv}.f_{PV}.P_{STC}.\frac{G_A}{G_{STC}}.(1 + (T_C - T_{STC}).C_T) \tag{3.11}$$

In this equation the term n_{inv} is the inverter efficiency, once the PV energy production is DC power. f_{PV} is the photovoltaic panel efficiency, P_{STC} is the PV rated power

in kW_{peak} on Standard Test Conditions (STC). G_A is the incident radiation measured in kW/m^2, and G_{STC} is the incident radiation over test conditions with the value of 1 kW/m^2. The cells temperature is given by T_C, and T_{STC} assumes 25 °C. C_T, which assumes the value of -0.004, is the temperature coefficient given in / °C. This coefficient is applied because the dusty and aging.

All this terms are constants, except the cells temperature, which follows the equation bellow, exposed in [68]:

$$T_C = T_a + \frac{(NOCT - 20)}{0.8}.G \tag{3.12}$$

where T_a is the ambient temperature, given in °C , and G (in kW/m^2) is the global radiation. $NOCT$ is the Normal Operational Condition Temperature (NOCT), which is usually 48 °C [68].

3.2.3 Electrical energy storage system

Weather-dependent renewable generation has high variability due its random variables *e.g.* wind speed, sun radiation, rain, clouds. In order to overcome power generation variability, energy storage system can be used to make the power system more dispatchable and reliable [72]. Because of that, the storage system is included in the MG.

A simplified storage model is considered, which the storage energy E_{ESS} is expressed as:

$$E_{ESS}(t+1) = E_{ESS}(t) + \eta \Delta P_E(t) \tag{3.13}$$

where η denotes the power exchange efficiency, and P_E is the power exchanged between the storage device and the local power network.

3.2.4 Load demand

Electrical loads can also be characterized as a stochastic variable. For the present work, demand is represented by a normal distribution function $N(\mu, \sigma^2)$ [32], where μ and σ are the mean and standard deviation of the total load, respectively.

To have representative values of demand of real system, it is used the dynamic established in the IEEE Reliability Test System (IEEE/RTS) 1996 report [73].

The load profile information provided in IEEE/RTS can be used to calculate system hourly loads for one year on a per unit basis, expressed in a chronological fashion. So, daily, weekly and seasonal patterns can be developed. The load model is sufficient

for generating capacity and reliability studies such as loss of load or energy expectation analysis [63].

3.2.5 Diesel generator

A diesel generator consists of an internal combustion engine (ICE) and a synchronous generator coupled on the same shaft. Such systems are widely used as backup or emergency power in commercial and industrial installations. Diesel generators are also heavily used in remote locations where it is impractical or expensive to connect to utility power. They are typically designed to operate at higher efficiencies since, in the long run, the fuel costs will dominate the initial capital costs.

The generator is either a permanent magnet or a wound-field synchronous machine. In the case of a permanent magnet generator, the front end consists of a rectifier and a voltage-source converter to provide the necessary AC voltage at the desired frequency. The presence of a power electronics front end increases the overall cost of the system and decreases its fault tolerance. However, the presence of the inverter enables non-synchronous operation of the engine which makes it possible to achieve increased power density and higher efficiency [74].

For the proposed microgrid, the use of diesel generators is justified by the fact of their dispatchability feature, which guarantees flexibility and increases the reliability of the system.

3.3 Petri nets

A Petri net (PN) is an abstract, formal model of information flow. The properties, concepts and techniques of Petri net are being developed in a search for describing and studying information processing systems that may exhibit events which are concurrent, asynchronous, distributed, parallel, nondeterministic, and/or stochastic [75].

The representation of a Petri net model is made by means of a bipartite graph, comprising two types of nodes, named places and transitions . A place is represented by a circle and a transition by a filled rectangle (see Figure 4). Places and transitions are connected by arcs. An arc is directed and connects either a place to a transition or a transition to a place [76]. The PN graph models the static properties of a system, similarly to a flowchart. In this context, what distinguishes PN graphs from typical flowcharts is the capacity of abstraction. Such capacity must be understood as the ability of impose some interpretation of meaning on each PN element. A common practice is to use the places as states and the transitions as events. To illustrate this concept, a PN interpretation of a simple product selling process is demonstrated in Figure 5.

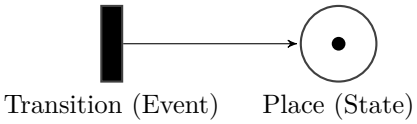

Figure 4 – Petri net formalism

In addition to the static properties represented by the graph, a Petri net has dynamic properties when assuming the execution of the flowchart. The dynamics of a PN model is represented by the movement of markers, also referred as *tokens*, between the places according to the occurrence (firing) of events defined in the transitions. Because of this, a Petri net with tokens can be defined as *marked Petri net*. Tokens, which are graphically represented by filled circles, are information assigned to places to represent the situation (state) of the network at any given time. The distribution of the tokens in the places is formalized by the notion of *marking*, which can be seen either as a function *m(p)* representing the number of tokens in place p or as a vector $m = (m_1, m_2, \ldots, m_n)$, where m_i is the number of tokens in place p_i. To facilitate the understanding of the present work, hereafter, the terminology *Petri net* is used to refer to both static and the dynamic graph (*marked Petri net*).

Still regarding the PN dynamics, a transition can only be fired if each of the input places of this transition contains at least one token. The transition is then said to be enabled. Firing of a transition t_j consists in withdrawing a token from each of the input places of transition t_j and in adding a token to each of the output places of transition t_j. Figure 5 exemplifies a simple dynamic of firing a transition. As can be seen, there is 2 tokens in place p_1 and 4 tokens in place p_2 at the initial marking (Figure 5a). When t_2 fires, it is removed one token from each input place (p_1 and p_2) and is inserted one token in the output place p_3 (Figure 5b). To this example, the initial marking M_0 is (2, 4, 0), and next marking M_1 is (1, 3, 1). The observation of all possible markings correspondent to all possible transition firings allows a comprehension of how the PN model behaves [75]. Such study is made by what is defined as reachability tree, and it is in the scope of state space analysis. In section 4.1, the state space analysis will be discussed again.

A formal definition for Petri nets is shown [77]. It is defined that the PN is a 5-tuple, $PN = \{P, T, F, W, M_0\}$ where

- $P = \{p_1, p_2, \cdots, p_m\}$ is the finite set of places;
- $T = \{t_1, t_2, \cdots, t_m\}$ the finite set of transitions;
- $F \subseteq (P \times T) \cap (T \times P)$ is a set of arcs (flow relation);
- $W : F \to \{1, 2, 3, \cdots\}$ is a weight function (indicates the number of tokens produced or removed after firing a transition);

- $M_0 : P \to \{0, 1, 2, 3, \cdots\}$ is the initial marking;
- $P \cap T = \emptyset$ and $P \cup T \neq \emptyset$.

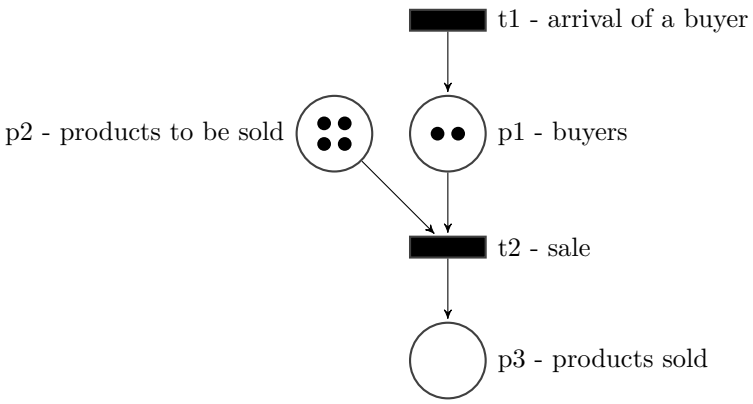

(a) Before firing

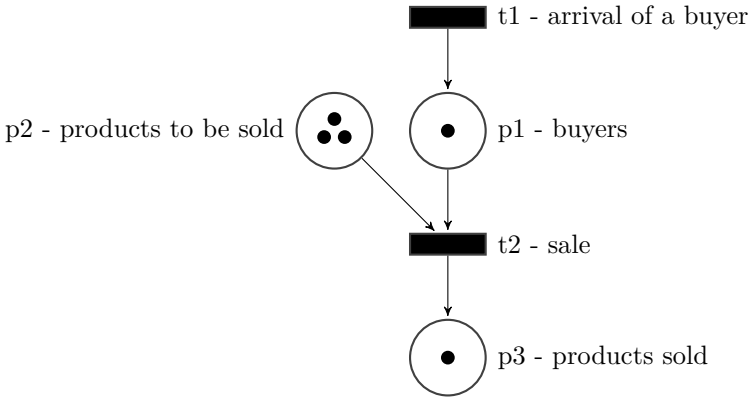

(b) After firing

Figure 5 – Petri net dynamics

3.4 Markov Chain

The term "Markov model" is referred to mathematical discrete models in which the future state of a system depends only on its current state, not on its past history. This "memoryless" characteristic, called markovian property, implies that all transitions from one state to another occur at constant rates. Much of the practical importance of Markov models for reliability analysis is due to the fact that a large class of real-world devices and systems exhibit essentially constant failure rates, and can therefore be effectively represented and analyzed using Markov models.

For any given system, a Markov model consists of a list of the possible states of that system, the possible transition paths between those states, and the rate parameters of those transitions. For reliability analysis, the transition usually consist of failures and

repairs. Graphically, a Markov model is composed by two elements named state (bubble) and transition paths (arrow). Such structure is depicted on Figure 6.

A classical usage of Markov chain in power system is the calculation of reliability indexes based on generator and/or grid outages [78]. Usually, the two state-model represents the outage scenario by means of up and down condition of the element, and the transition between this states is dependent on the mean time between failures (MTBF) and the mean time to repair (MTTR). After that, the steady-state calculation is performed in order to have the probability of being in each state.

Following, a brief introduction on Markov chains analysis is conduct in order to review some concepts that support the development of this work. For a better understanding of the topic, it is suggested the readings of [79] and [80].

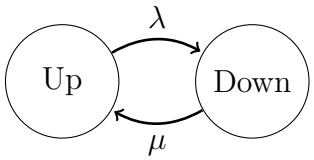

Figure 6 – Two state Markov chain

3.4.1 Discrete time Markov chain (DTMC)

A Markov process X_t is a stochastic process with the property that given the value of X_t, the values of X_v for $t < v$ are not influenced by the values of X_u for $u < t$. That means, assuming a set of states S=$\{s_1,s_2,...s_r\}$, the markovian process starts in one of these states and moves successively to another regardless of its previous state. For instance, if the process is currently in state s_i, then it can moves to state s_j at the next move with a probability denoted by p_{ij}. The process can also remain in the state it is in, and this occurs with probability p_{ii}. These probabilities are called transition probabilities, and they do not depend upon which states the process was before the current state.

For a discrete time (discrete time Markov chain (DTMC)), this property is given by (3.14), and the probability after *n-steps* is given as (3.15).

$$P[X_{n+1} = j|X_n = i, X_{n-1} = i_{n-1}, \cdots, X_0 = i_0] = P[X_{n+1} = j|X_n = i]; P_{ij} \geq 0 \quad (3.14)$$

$$p_{ij}^{(n)} = P(X_{m+n} = j|X_m = i) \quad (3.15)$$

where, $p_{ij}^{(n)}$ is the probability of transition between the states i and j in *n-steps*.

A Markov chain X_t with the space of states S, which means, S is the set of possible values of X_i, and assuming the probability of transition $P_k(\cdot,\cdot)$, it is given that

the probability of transition in *n-steps* can be find from any intermediate state, including the initial state. Equation (3.16) indicates such relation.

$$p_{ij}^{(n)} = \sum_{k \in S} p_{kj}^{n-1} p_{ik} \tag{3.16}$$

This equation is interpreted in two parts:

- the first part of summation represents the probability of moving in *(n-1)* steps from state k to state j
- the second part of summation represents the probability of transition in just one step to intermediate state k;

Joining all possible *k-states*, it is obtained the path from state i to state j in *n-steps*. This recursive equation is known as identity of Chapman-Kolmogorov. Another important notation is the transition matrix P, which gives all the information about the state transition.

$$P = \begin{pmatrix} p_{11} & p_{12} & \cdots & p_{1j} \\ p_{21} & p_{22} & \cdots & p_{2j} \\ \vdots & \vdots & \ddots & \vdots \\ p_{i1} & p_{i2} & \cdots & p_{ij} \end{pmatrix}$$

In case the probabilities of P be stationary, it is defined that the Markov chain is homogeneous. Thus, assuming $\pi = [\pi_1 \pi_2 \cdots \pi_j]$ as the vector of state probabilities, where π_j with $j = 1, 2, ..r$ is the probability of being in state s_j, it is possible to prove that:

$$\pi_n = \pi_0 \prod_{i=1}^{n} P_i \tag{3.17}$$

An analogous form for (3.17) is $\pi_n = \pi_0 P^{(n)}$. These equations represent that the future state depends on the initial probability distribution and the exponentiation of P.

3.4.2 Continuous time Markov chain (CTMC)

The continuous time Markov chain (CTMC) has an analysis similar to DTMC provided that the markovian property (3.14) be satisfied.

Given the general case (3.18), and considering $t = t + \tau$, then, the relation (3.19) comes up.

$$p_{ij}(s,t) = P[(X_t = j | X_s = i)], s \leq t \tag{3.18}$$

$$p_{ij}(s, t+\tau) = P[(X_{t+\tau} = j | X_s = i)], \forall t \tag{3.19}$$

So, from a stochastic process $X(t), t \geq 0$ in continuous time, such process is a CTMC if: (i) the transition probability does not depend on the instant that the counting time started; (ii) the past information are irrelevant; (iii) the time that the process is at current state is irrelevant. Based on this, a homogeneous Markov chain is that one in which the probabilities $p_{ij}(s, t+\tau)$ depend just on τ and not on the instant that it has occurred. In this case, it is possible to find the probability of the system being on state j given that at instant t it was on state i. The equation (3.20) shows this consideration.

$$p_{ij}^{(\tau)} = P[(X_{t+\tau} = j | X_s = i)], \forall t \tag{3.20}$$

So, from (3.20), it is necessary to reconsider the Chapman-Kolmogorov observing the effects that parameter τ causes. Admitting the time interval $s \leq t \leq t+\tau$, the Chapman-Kolmogorov can be rewritten as (3.21). Using the infinitesimal statement on each probability transition, the rate transition (λ_{ij}) can be defined as shown in (3.22). Derivating (3.21) in relation to τ, and assuming that the time t is equal to the initial time s, it reaches the relation (3.23). Thus, the concept of transition probability is replaced by the concept of transition rate, and in a similar way, the matrix of probability transition P, is replaced by the transition rate matrix Q.

$$p_{ij}^{(s,t)} = \sum_{k \in S} p_{kj}^{(t,t+\tau)} p_{ik}^{(s,t)} \tag{3.21}$$

$$\lambda_{ij} = \frac{dp_{ij}^{(\tau)}}{d\tau}\bigg|_{\tau=0} \tag{3.22}$$

$$\frac{dp_{ij}^{(s,t+\tau)}}{d\tau} = \frac{dp_{ij}^{(\tau)}}{d\tau} = \sum_{k \in S} p_{ik}^{(s,t)} \frac{dp_{kj}^{(\tau)}}{d\tau} = \sum_{k \in S} p_{ik}^{(s,t)} \lambda_{kj} \tag{3.23}$$

$$Q = \begin{pmatrix} \lambda_{11} & \lambda_{12} & \cdots & \lambda_{1j} \\ \lambda_{21} & \lambda_{22} & \cdots & \lambda_{2j} \\ \vdots & \vdots & \ddots & \vdots \\ \lambda_{i1} & \lambda_{i2} & \cdots & \lambda_{ij} \end{pmatrix}$$

Another important property for CTMC is the correlation between mean time that stochastic process stays on state i before making a transition to other state j, and the transition rate λ_{ij}. Admitting that T_{ij} is the time that the a stochastic process stays on state i before making a transition to other state j, and also assuming that this time

spent in i obeys a negative exponential distribution (3.24), then, there exists the relation $\overline{T_{ij}} = 1/\lambda_{ij}$. This condition can be observed in (3.25) and (3.26).

$$f(t) = \lambda e^{(-\lambda t)} \tag{3.24}$$

$$\int_0^\infty f(t)dt = 1 \tag{3.25}$$

$$\overline{T}_{ij} = \int_{-\infty}^{\infty} \lambda_{ij} e^{(-\lambda_{ij} t)} dt = \frac{1}{\lambda_{ij}} \tag{3.26}$$

3.4.3 Steady state analysis

The steady state analysis consists in observing the stochastic process considering $t \to \infty$, in which there is no variation on the probabilities of staying in each state.

3.4.3.1 Steady state for DTMC

An initial probability distribution, defined on S, specifies the starting state probability distribution P. Usually it is of interest to consider the next possible states, defined by the analogous transition matrix $P^{(n)}$, which indicates the probability for the process in the n_{th} step. The particular case described by $n \to \infty$ is called steady state. Moreover, the main objective of the steady state analysis is check the probability of the system to be in certain state of S after a long period of observation. This condition is defined by a probability vector named steady state vector π.

The steady state vector represents the stationary condition for a Markov chain. So, to calculate it, the linear problem (3.27), derived from Champman-Kolmogorov equation, has to be solved. (3.27) express the relation between the steady state vector π and the probability transition matrix P. Besides, since π is a probabilistic solution, it is a simple conclusion that the summation of π must be equal one, as shown in (4.29). So, to calculate the steady state vector, it is necessary to solve this system of equation.

$$\pi = \pi P \tag{3.27}$$

$$\sum_{j \in S} \pi_j = 1 \tag{3.28}$$

3.4.3.2 Steady state for CTMC

Assumes that $\pi_j^{(t)}$ the probability of being on state j after the system has operated t time unities as shown in (3.29), and $\pi^{(t)} = [\pi_0^{(t)} \pi_1^{(t)} \pi_2^{(t)} \cdots]$ is the vector of probability

states. Considering the convenient time $t + \tau$, then, Chapman-Kolmogorov can be expressed as (3.30). When this equation is derivated in relation to τ, it results in (3.31) with its matrix form expressed in (3.32).

$$\pi_j^{(t)} = P(X_t = j) \tag{3.29}$$

$$\pi_j^{(t+\tau)} = \sum_{k \in S} p_{kj}^{(\tau)} \pi_k^t \tag{3.30}$$

$$\frac{d\pi_j^{(t+\tau)}}{d\tau} = \sum_{k \in S} \lambda_{ik}^{(\tau)} \pi_k^t \tag{3.31}$$

$$\frac{d\pi_j^{(t+\tau)}}{d\tau} = \pi^{(t)} Q \tag{3.32}$$

$$lim_{t \to \infty} \frac{d\pi^{(t+\tau)}}{d\tau} = 0 \tag{3.33}$$

For steady state observation ($lim_{t \to \infty} \pi^{(t)}$), it is expected that $\pi^{(t)}$ stabilizes, and therefore, there is no dependency of τ anymore, resulting in (3.33). As conclusion, applying this result in (3.32), the steady state probability vector is given solving the system formed by (3.34) and (3.35).

$$0 = \pi Q \tag{3.34}$$

$$\sum_{j \in S} \pi_j = 1 \tag{3.35}$$

A numerical example is given below in order to demonstrate the steady state assessment. Regarding a Markov model for reliability analysis as shown in Figure 6, assumes a MTBF equals to 10 hours, returning $\lambda = 0.1$ ($\lambda = 1/MTBF$), and a MTTR equals to 1 hour, returning $\mu = 1$ ($\mu = 1/MTTR$). Thus, the matrix Q (transition rate matrix) is:

$$Q = \begin{pmatrix} -\lambda & \lambda \\ \mu & -\mu \end{pmatrix} = \begin{pmatrix} -0.1 & 0.1 \\ 1 & -1 \end{pmatrix}$$

Substituting such matrix in (3.34) and considering the condition of normalization presented in (3.35), the following mathematical system is established:

$$\begin{cases} -0.1\pi_1 + \pi_2 &= 0 \\ 0.1\pi_1 - \pi_2 &= 0 \\ \pi_1 + \pi_2 &= 1 \end{cases} \tag{3.36}$$

Solving (3.36), the final probability distribution is shown by the vector $\pi = [0.91, 0.09]$, indicating that the steady state probability of the system being UP is 91%, and 9% of being DOWN.

3.5 Mixed Integer Linear Programming (MILP)

Mixed integer linear programming is a subset of the broader field of mathematical programming, which provides a mechanism for optimizing decisions that take place in complex systems [81].

MILP formulations include a set of variables, which represent actions that can be taken in the system being modeled. Then, one attempts to optimize (either in the minimization or maximization sense) a function of these variables, which maps each possible set of decisions into a single score that assesses the quality of the solution. These scores are often in units of currency representing total cost incurred or revenue gained. The limitations of the system are included as a set of constraints, which are usually stated by restricting functions of the decision variables to be equal to, not more than, or not less than, a certain numerical value. Another type of constraint can simply restrict the set of values to which a variable might be assigned. Several applications involve decisions that are discrete (e.g., which generator unit should be committed or decommitted), while some other decisions are continuous in nature (e.g., determining how much energy each generator must dispatch). Evidently, the ability to enumerate all possible values that a discrete decision can take seems appealing; however, in most applications, the discrete variables are interrelated, requiring an enumeration of all combinations of values that the entire set of discrete variables can take. Observe all possible combination is very time consuming and sometimes impractical.

Therefore, a more efficient technique is required to solve problems containing discrete variables. MILP techniques do not explicitly examine every possible combination of discrete solutions, but, they examine a subset of possible solutions instead, and use optimization theory to prove that no other solution can be better than the best one found. This type of technique is referred to as implicit enumeration.

The name integer linear programming (ILP) refers to the class of combinatorial constrained optimization problems with integer variables, where the objective function is a linear function and the constraints are linear inequalities [82]. The ILP optimization problem can be stated in the following general form:

$$\text{Minimize or maximize} \quad cx \tag{3.37}$$

$$\text{subject to:} \quad Ax \leq b \tag{3.38}$$

$$x \in Z^n \tag{3.39}$$

where the solution $x \in Z^n$ is a vector of n integer variables: $x = (x_1, x_2, \ldots, x_n)^T$, and the data are rational given by the $m \times n$ matrix A, the $1 \times n$ matrix c, and the $m \times 1$ matrix b. This formulation includes also equality constraints, since each equality constraint can be represented by means of two inequality constraints like those included in (3.38).

Considering the before mentioned ILP definition, comes that a mixed integer linear program (MILP) is a linear program with the added restriction that some, but not necessarily all, of the variables must be integer-valued. Several studies also replace the term "integer" with "0-1" or "binary" when variables are restricted to take on either 0 or 1 values.

There are, at least, three different approaches for solving integer programming problems, although they are frequently combined into "hybrid" solution procedures in computational practice (refer to [82]):

- Cutting planes algorithms based on polyhedral combinatorics;
- Enumerative approaches and Branch-and-Bound, Branch-and-Cut and Branch-and-Price methods;
- Relaxation and decomposition techniques.

To exemplify the concept of solving a mixed integer linear-programming, a basic branch-and-bound algorithm is described as follows.

The algorithm starts with the original MILP, not knowing how to solve this problem directly, it is removed all of the integrality restrictions. As integrality, one can understand that only integer values are accepted as feasible solution. The resulting LP is called the linear-programming relaxation of the original MILP. Then it is solved this LP. If the result satisfies all the integrality restrictions, even though these were not explicitly imposed, then the MILP is solved. If not, as it is usually the case, the normal procedure is to pick some variable that is restricted to be integer, but whose value in the LP relaxation is fractional (unfeasible solutions). For the sake of argument, suppose that this variable is x and its value in the LP relaxation is 5.7. One can excludes this value by, in turn, imposing the restrictions $x \leq 5.0$ and $x \geq 6.0$.

If the original MILP is denoted P_0, then it is possible to denote these two new MIPLs by P_1, where $x \leq 5.0$ is imposed, and P_2, where $x \geq 6.0$ is imposed. The variable x is then called a branching variable, and it is said the MILP have been branched on x,

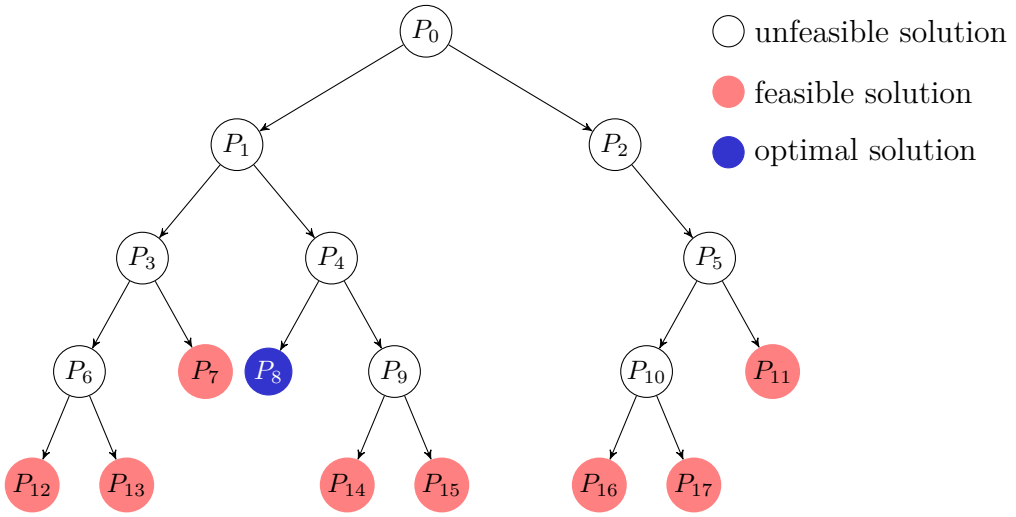

Figure 7 – The search space of a mixed integer linear program - MILP tree

producing the two sub-MILPs P_1 and P_2. It should be clear that if one can computes optimal solutions for each of P_1 and P_2, then it is possible to take the better of these two solutions, and it will be optimal to the original problem, P_0. In this way P_0 is replaced by two simpler (or at least more-restricted) MILPs. Applying the same idea to these two MILPs, solving the corresponding LP relaxations and, if necessary, selecting branching variables, it is generated what is called a search tree as shown in Figure 7. In other words, the branch-and-bound algorithm solves a mixed integer linear program by dividing the search space and generating a sequence of subproblems. The subproblems generated by the search procedure are called the nodes of the tree, with P_0 designated as the root node. The leaves of the tree are all nodes that have been branched from P_0. In general, if one reaches a point at which it is possible to solve or to dispose all leaf nodes, which means that one can evaluate all feasible solutions, then the solution of original MILP can be computed (optimal solution). Refer to Figure 7.

For better understanding, it is proposed an example in the context of microgrid planning. This example is adopted from [81].

The problem is to minimize the capital costs of acquiring equipment for installing a photovoltaic system for a residence. The equipment is sold in kits ready for installation, which are composed of inverters and photovoltaic panels. In addition, there are some specifications and requirements for the project, as shown below:

- There are two vendors available: X and Y;
- The equipment is sold in kits that cost \$4,000.00 in seller X and \$6000.00 in seller Y;
- It is required 5 kits for the residence project;

- It is required an even number of kits purchased from each seller;
- It is required that the difference of kits purchased in X and Y be less than or equal to 1. This restriction may be justified on the grounds that the quality of kits provided by Y are greater than those provided by X.

The prices of kits and the capital costs are considered in thousands of dollars to facilitate the modeling and solution of the problem. In this way, the mathematical model can be formulated as follows:

$$\begin{aligned} \text{Minimize} \quad & z = 4x + 6y && \text{(3.40a)} \\ \text{subject to:} \quad & 2x + 2y \geq 5 && \text{(3.40b)} \\ & x - y \leq 1 && \text{(3.40c)} \\ & x, y \geq 0 && \text{(3.40d)} \end{aligned}$$

The first concept that is discussed in solving MILPs is the relaxations. A relaxation of a MILP is a problem such that (a) any solution to the MILP corresponds to a feasible solution to the relaxed problem, and (b) each solution to the MILP has an objective function value greater than or equal to that of the corresponding solution to the relaxed problem. The most commonly used relaxation for an MILP is its LP relaxation, which is identical to the MILP with the exception that variable integrality restrictions are eliminated.

So, returning to the proposed problem of installing a photovoltaic system on a residence, graphically, Figure 8 illustrates the feasible region (set of all feasible solutions) to the LP relaxation of formulation (3.40). Considering such region, the optimal solution is found at the point (1.75, 0.75).

Solving the LP relaxation has yielded a fractional, not integer, solution. Thus, such point (1.75, 0.75) is not a MILP feasible solution. In fact, all feasible solutions have the characteristic that either $x \leq 1$ or $x \geq 2$. Therefore, one can split the problem (3.40) into two subproblems: one in which $x \leq 1$ (called region 1), and one in which $x \geq 2$ (called region 2). All the solutions to the original MILP are contained in exactly one of these two new subproblems. This is called *branching*, and one could also has branched the variable y instead, by requiring that either $y \leq 0$ or $y \geq 1$.

The feasible region of the two new subproblems are depicted in Figure 9. When $x \leq 1$, the optimal solution is (1, 1.5) with the objective function value 13. When $x \geq 2$, the optimal solution is (2,1) with the objective function value of 14. So, since the best solution happens to be an integer solution in the $x \geq 2$ region, then, there is no need

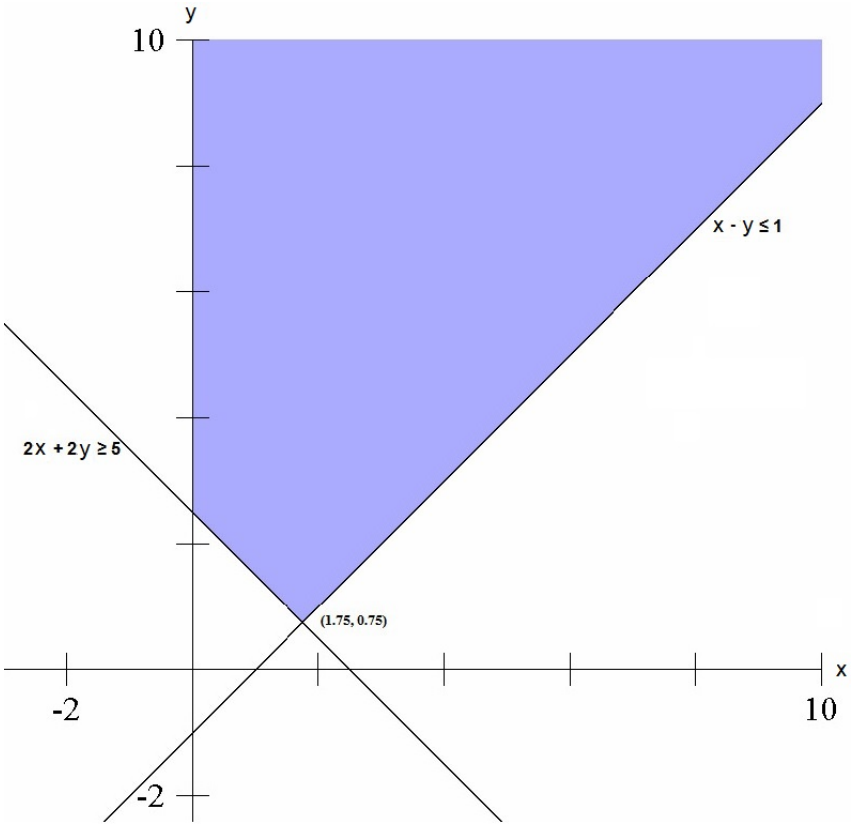

Figure 8 – Feasible region for LP problem (adapted from [81])

for further search in such region. This region is said to be fathomed by integrality. The solution (2, 1) is stored, and it is called *incumbent solution*. If no better solution is found, it will become our optimal solution.

At this point, there is one *active* region (or "active node" in the context of branch-and bound trees, which we will describe shortly), which is region 1. An active region is one that has not been branched on, and that must still be explored, because there is a possibility that it contains a solution better than the incumbent solution. The region 1 is recursively divided, in which $x \leq 1$. Since the optimal solution in this region was a non-integer solution (1, 1.5) , one must branch it, creating two new subproblems: one in which both $x \leq 1$ and $y \leq 1$ (called region 3), and one in which $x \leq 1$ and $y \geq 2$ (called region 4).

However, note that region 3 is empty, because the stipulation that both x and y are no more than 1 makes it impossible to satisfy (3.40b). Therefore, there are no integer solutions in this region either, and the searching in region 3 stops. This region is said to be fathomed by infeasibility. The optimal solution for the linear relaxation of region 4 is (0.5, 2), with objective function value 14. Still the fact that no best integer solution was found over region 4, it is known that the best integer solution (if one even exists) has already an objective function value of 14 or more. However, the incumbent solution has an objective function value of 14, which allows to say that the best solution in region 4

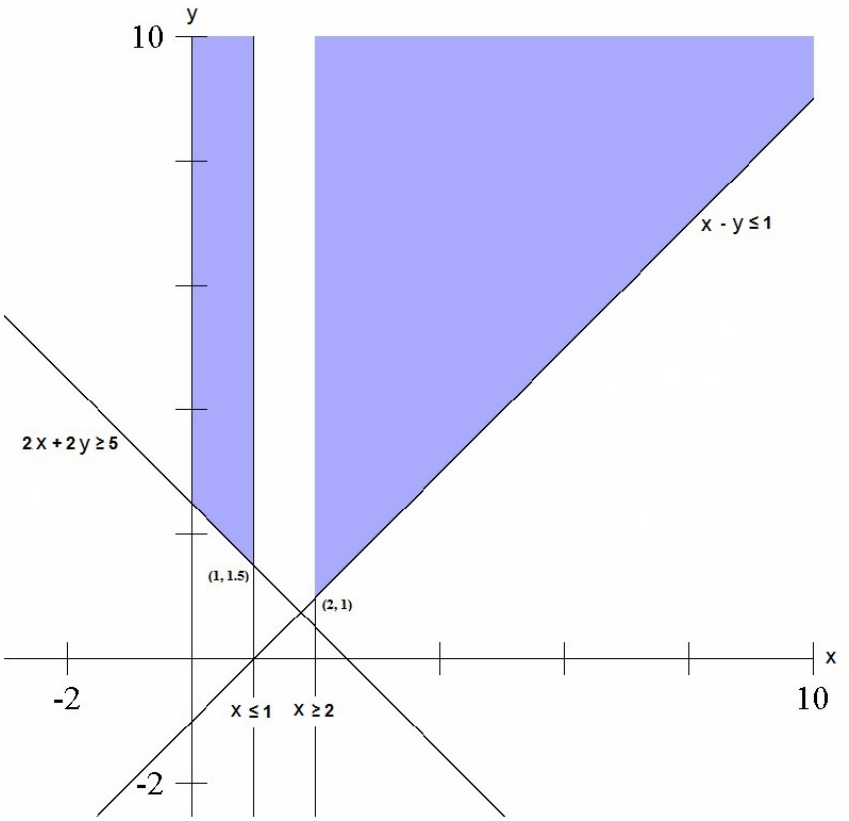

Figure 9 – Feasible region of subproblems (adapted from [81])

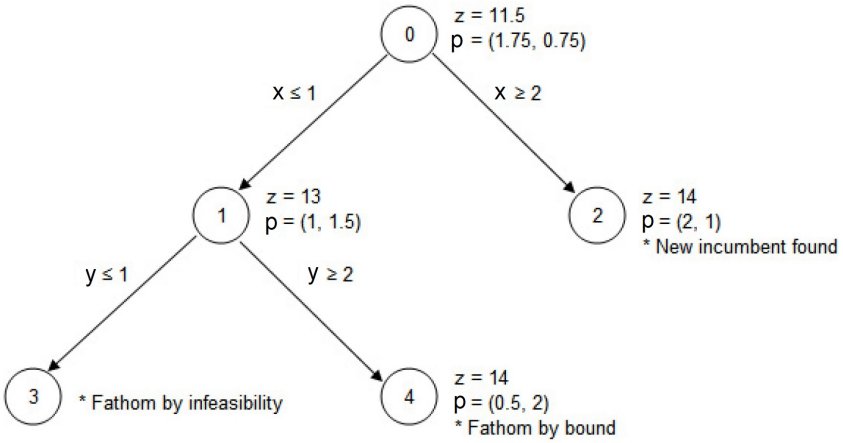

Figure 10 – Branch-and-bound tree (adapted from [81])

will not improve the incumbent solution that was previously found. Thus, the searching for the best solution over region 4 stops. Region 4 is said to be fathomed by bound.

Figure 10 depicts a tree representation of this search process, which is called the "branch-and-bound tree." Each node of the tree represents a feasible region. Now, there are no more regions to be examined (no more active nodes), and the algorithm terminates with the incumbent solution, (2, 1), as an optimal solution. In summary, the decision-maker must buy 2 kits from seller X and 1 kit from seller Y to guarantee all the requirements of the residential project, representing an optimized investment of $14,000.00.

3.6 Particle Swarm Optimization (PSO)

Many different artificial intelligence (AI) techniques have been applied on microgrid planning, each one dedicated to solve a specific problem. Genetic algorithm (GA), PSO and hybrid approaches mixing both techniques, are commonly used on optimization problems as economic dispatch, microgrid optimal design, and optimal positioning of DERs [11, 25, 28, 83, 84]. Artificial neural networks (ANNs) are useful in solving data-intensive problems where the algorithm or rules to solve the problem are unknown or difficult to express. For instance, ANN is used to estimate microgrid maximum power provided by solar [85] and short-term load forecasting [86]. Fuzzy systems use fuzzy sets to deal with imprecise and incomplete data. In this way, in [87] fuzzy is used to capture nonlinearities and systematically represent the uncertainties associated with renewable resources at a certain confidence level, and in [28] it has the function of classify a specific stochastic parameter, more specifically, traveled distance of electrical vehicles. Also, Fuzzy techniques can be applied to support a decision-making process in microgrid planning as shown in [88].

Regarding that the major issue of the proposed framework is establishing the size of DERs in a manner that the operation costs, reliability and pollutants are minimum, the PSO seems quite promising, since it is widely applied for global minimization problems [89]. Besides, the PSO is a technique with versatile algorithms, simple enough to be accessible for practical applications and easy to implement.

The traditional PSO, a form of swarm intelligence, is a population-based dynamic optimization algorithm. The objective of computational swarm intelligence is to model the collaborative behavior of biological populations (behavior of insect colonies and other animal societies) used to solve complex problems, generally optimization problems [90].

PSO is inspired by the ability of flocks of birds, schools of fish, and herds of animals to adapt to their environment, find rich sources of food, and avoid predators by implementing an "information sharing" approaches, hence, developing an evolutionary advantage [91].

In PSO, the initialization process starts with the generation of a fixed number of randomly generated particles (potential solutions) scattered in a multidimensional solution space. A swarm of particles moves around in a multidimensional search space until they find the optimal solution. Each particle in the swarm represents a candidate solution to the problem and moves towards the optimal point by appending a velocity with its position. Using its own experience (pbest) and the experience attained by the neighboring particles in the swarm (gbest), each particle updates its position during its moving. In this way, each particle makes use of the pbest and gbest. The update mode is termed as the velocity of particles. Particles update their positions and velocities in a heuristic

manner [92].

Suppose that the search space is D dimensional, the $i-th$ particle of the population can be represented by a *D-dimensional* vector $X_i = (x_i^1, x_i^2, \ldots, x_i^D)^T$. The velocity of this particle can be represented by another *D-dimensional vector* $V_i = (v_i^1, v_i^2, \ldots, v_i^D)^T$. The previously best visited position of $i-th$ particle is denoted by $P_i = (p_i^1, p_i^2, \ldots, p_i^D)^T$ and the best particle in the swarm is denoted by $P_g = (p_g^1, p_g^2, \ldots, p_g^D)^T$. The update of the particle position is accomplished computing the following equations (3.41) and (3.42) [91]. (3.41) calculates a new velocity for each particle based on its previous velocity, and (3.42) updates each particle position in search space.

$$V_{id}^{k+1} = wV_{id}^k + c_1 r_1[p_{id}^k(t) - x_{id}^k(t)] + c_2 r_2[p_g^k(t) - x_{id}^k(t)] \tag{3.41}$$

$$x_{id}^{k+1} = x_{id}^k(t) + v_{id}^{k+1}(t+1) \tag{3.42}$$

where $k = 1, 2, 3, ...$ is the iteration number; $d = 1, 2, 3, ..., D$ is the space dimension; $i = 1, 2, 3, ..., N$ is the particle index; N is the swarm size, w is the inertia weight, which controls the momentum of particle by weighting the contribution of previous velocity; c_1 and c_2 are positive constants called acceleration coefficients; r_1 and r_2 are random numbers uniformly distributed between [0,1].

The complete procedure for PSO is:

Step P0: Initialize each solution by randomly generating its position X_i^0 and velocity V_i^0, and then calculate the fitness function $F(X_i^0)$;

Step P1: Let gen=1 and $P_i^0 = X_i^0$, and then find gbest such that $P_{gbest}^0 \geq P_i^0$ for all i;

Step P2: Update the velocity and move to the next position for each solution using (3.41) and (3.42);

Step P3: If the fitness value of solution j is better than pbest, then set the current fitness value to the new pbest for solution j;

Step P4: If any pbest is updated and is better than the current gbest, then set gbest to the current best;

Step P5: If gen $<$ N, then let $gen = gen + 1$ and go back to Step P2; otherwise, stop.

3.7 Pareto frontier - intuitive approach

One way to find good solutions to multi-objective problems is with Pareto optimality, named after economist Vilfredo Pareto. Pareto noticed that many economic solutions helped some people while hurting others. He was interested in finding solutions that helped some people without hurting anyone else. Solutions like this are now called "Pareto improvements" [93].

To find such solutions, the first step when solving a multi-objective problem is to get a handle on the feasible region (design space). After graphing the feasible region and finding its boundaries in design space, the next step is to convert it to criterion space (refer to Figure 11). In criterion space, the axes are no longer decision variables $(x_1, x_2, \ldots x_i)$, but objective functions $((f_1, f_2, \ldots f_n))$. As last stage, the Pareto points (frontier) is characterized using the concept of dominating points. There is no mathematical "best" point along the Pareto front. Decision makers would have to get together and figure out how they wanted to balance their priorities. Another implication of the Pareto front is that any point in the feasible region that is not on the Pareto front is a bad solution [94–96].

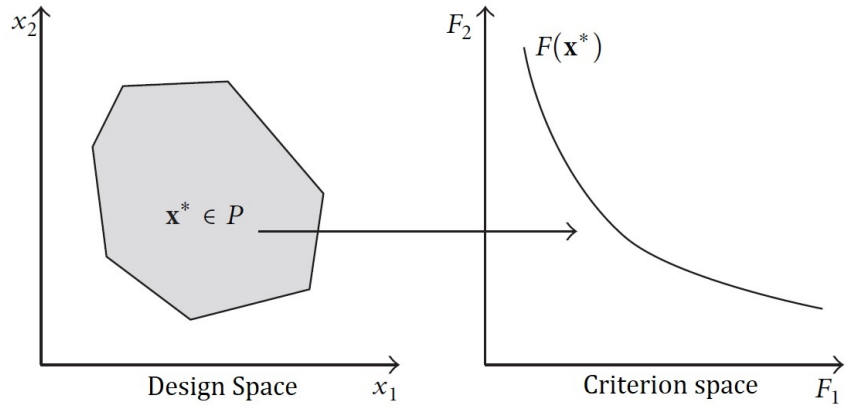

Figure 11 – Design space and criterion space for 2-dimensional problem (adapted from [97])

A multi-objective optimization problem can be formulated as (3.43) and (3.44):

$$\text{minimize} \quad F(x) = (f_1(x), \ldots, f_m(x))^T \tag{3.43}$$

$$\text{subject to } x \in S, \tag{3.44}$$

where *F(x)* is an objective vector, consisting of m-objective functions $f_i : \Re^n \to \Re$ for all $i \in \{1, \ldots, m\}$. $S \subset \Re$ is called the design variable space and is defined as (3.45)

$$S = \{x \in \Re^n | g_j(x) \leq 0 \, (j = 1, \ldots, l), h_k(x) = 0 \, (k = 1, \ldots, p)\} \tag{3.45}$$

Here, $g_j(x)$ and $h_k(x)$ are inequality and equality constraints, respectively. Multi-objective optimization problems consist of two definitions that handle the trade-off among the multiple criteria (objectives). Notably, these definitions are prescribed for minimization problems.

Definition 1 (Pareto dominance). For x_1 and x_2 ($x_1 \neq x_2$), x_1 is said to dominate x_2 if for at least one $i = 1, \ldots, m$, $f_i(x_1) \leq f_i(x_2)$ and $f_i(x_1) < f_i(x_2)$.

Definition 2 (Pareto optimality). Let $x_0 \in S$. Then, x_0 is *Pareto optimal* when there are no other solutions in S dominating x_0.

Based on these definitions, the Pareto solution set or non-dominated solution is a subset of all the Pareto-optimal solutions. So, the basic definition of the Pareto frontier is that it consists of exactly those alternatives that are not dominated by any other alternative.

To illustrate such concept, imagine a problem with two objectives (cost and time). It is said that an alternative A dominates B if A outscores B regardless of the trade-off between cost and time — that is, it does not matter if A is both cheaper and faster than B. Obviously, both the cheapest and fastest alternative always belong to the Pareto frontier, and in fact, they are its endpoints. A simple algorithm to find the other alternatives (if any) on the Pareto frontier is first sort the alternatives according to one of the objectives — say, cost. One then starts with the cheapest alternative (which, as noted, always belongs in the Pareto frontier) and skips successive alternatives in order of increasing cost until one finds a solution with a higher value. This alternative is then added to the frontier and the search is restarted from it.

Similar to Figure 11, the Figure 12 illustrates the Pareto front for a 2-dimensional problem composed by two objective functions (F_1 and F_2), which represents the cost and time in the example above.

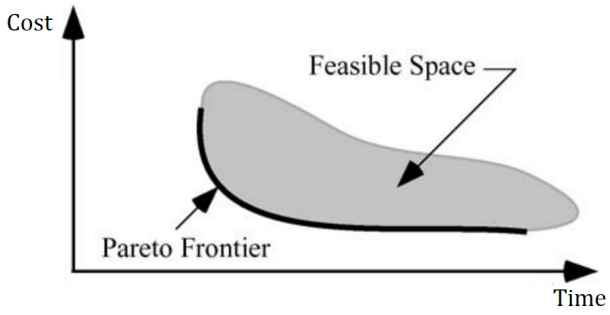

Figure 12 – Pareto frontier for 2-dimensional problem (adapted from [93])

A step-by-step description of the algorithm, assuming that A1,. . . ,An are the alternatives in increasing order of cost, goes like this:

1. Let $i := 1$;

2. Add A_i to the Pareto frontier;
3. Find smallest $j > i$ such that value $(A_j) >$ value (A_i);
4. If no such j exists, stop. Otherwise let $i := j$ and repeat from step 2

4 Proposed Framework

The microgrid planning usually considers long-term forecasting and long-term investments [98]. Because of that, the time to make a decision in such problem is non-critic. Thus, the planning process can be executed off-line, and the final decision can be taken in few minutes, hours or days. However, it is necessary to enumerate a large number of combined hypothetical situations, leading to an explosion-state problem. In other words, such problem may become impractical to solve.

The models and searching techniques used on microgrid planning must be appropriate in the sense of examining only a preselected set of possible candidate solutions, avoiding unpractical situations. Briefly explaining, the microgrid planning is a complex and non-convex problem, requiring some assumptions in order to simplify it.

To illustrate such complexity, the work presented in [20] takes 118–155 min to run each simulation of a microgrid planning problem which considers investments, operation, and reliability costs, using commercial software on a high-performance computing server consisting of four 10-core Intel Xeon E7-4870 2.4 GHz processors. Although the simulation response time presented in [20] seems quite attractive for the performance point of view, the authors also identifies the drawbacks of their planning model. In their solution, they have not considered forecast errors, which could potentially alter the microgrid planning results. Also, the proposed formulation is determined in an integrated fashion by solving a single optimization problem. A decomposition method could be employed in this case to convert such problem into a set of smaller and easier to solve, yet coordinated, subproblems.

The framework proposed in this thesis decomposes the microgrid planning/design problem on specific subproblems, which are solved separately by a number of appropriated tools. After that, the subproblems are associated on a multi-objective function which is solved using a meta-heuristic approach.

Thus, the present work establishes two main coordinated problems, named operation optimization and reliability/contingency assessment. The former is based on classical unit commitment problem (UCP), and the latter is a system reliability analyses. Both are NP-hard problems [99,100], which means an even more complex problem if reliability and UCP are considered at the same tool. Because of that, the problems are separated in two district procedures. UCP is solved usign a MILP approach while reliability problem uses a combination of Monte Carlo simulation (MCS) and steady state Markov chain analysis.

The proposed framework is an iterative procedure divided in five stages, named microgrid coordination, operation optimization, reliability assessment, contingency assess-

ment, and searching mechanism as shown in Figure 13.

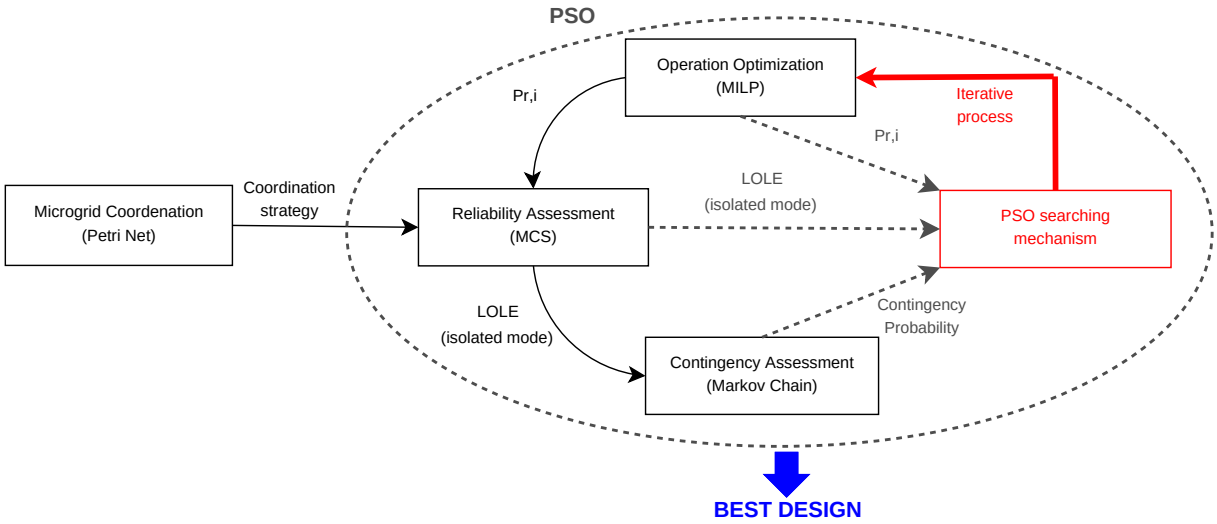

Figure 13 – Microgrid planning framework

The microgrid coordination stage has the function of modeling the philosophy used by the energy management system (EMS) to control the power balance when the microgrid is operating on isolated mode. The models of EMS are developed using the Petri net formalism. Optimization stage performs a minimization of the operation cost and pollutants emission considering the stochastic variables (generation and load demand) and operational constraints in grid-connected mode. After that, for given DER composition ($P_{r,i}$), it is estimated the reliability indexes by means of a Monte Carlo Simulation (MCS) considering the EMS philosophy in isolated mode. From the loss of load expectation (LOLE) reliability index, the contingency probability is calculated using the steady state analysis of a Markov chain, assessing the distribution power system admitting all possible mode transition. Finally, the PSO is responsible for searching the best microgrid design considering a multidimensional space formed by all DER combination.

In this study, it is considered a high-level microgrid system design (tertiary control). Since the balance of current and voltage is managed at a lower level (primary control), their associated balance equations are not explicitly shown in the following discussions.

The author's paper [101] was the first effort to validate the proposed framework, trying to join the most important aspects of planning and design of microgrids, as mentioned above. In general, the present thesis is a more accurate framework proposal than such previous work.

4.1 Microgrid coordination - Energy management system

The main function of this stage is to make a state observation and an event-based behavior analysis of each component in the microgrid. To do so, the microgrid composed by a wind turbine (WT), a photovoltaic system (PV), a energy storage system (ESS), a set of diesel generators, and a group of local loads as already depicted in Figure 2, is modeled using Petri nets (PN). The models presented here are adapted from [55] and [58].

Besides the individual elements, the PN modeling process aims to demonstrate the event-based microgrid operation by means of a model which shows the philosophy of coordinated control. In this way, the microgrid coordinator tries to satisfy the objective of the microgrid which is the lower emission and economical generation avoiding load shedding.

4.1.1 PN models of microgrid components

Starting with the wind turbine, it is assumed a three state model. One is the STOP MODE, in which the generator is off. This state is achieved when the wind speed is under or above certain limit. The second is defined as Maximum Power Point Tracking (MPPT), when the turbine power is dependent of wind speed. The last one is the Constant Output Power (COP), when the wind speed is higher than the rated wind speed and lower than maximum allowable wind speed. Figure 14 illustrates the PN model while Table 2 describes it.

Table 2 – Wind turbine model description

PN instance	**Functionality description**
Pwt1	Stop Mode
Pwt2	MPPT Operating Mode
Pwt3	Constant Output Power
Twt1	Wind speed$_{min}$ < Wind speed < Wind speed$_{rated}$
Twt2	Wind speed$_{min}$ > Wind speed or Wind speed > Wind speed$_{max}$
Twt3	Wind speed$_{min}$ < Wind speed < Wind speed$_{rated}$
Twt4	Wind speed$_{rated}$ < Wind speed < Wind speed$_{max}$
Twt5	Wind speed$_{min}$ > Wind speed or Wind speed > Wind speed$_{max}$

Photovoltaic generators are described with two states as shown in Figure 15. The states are MPPT and STOP MODE. The MPPT state has similar meaning as presented on the wind turbine, but for solar system the power generation is dependent on solar radiation. Besides that, the PV power output does not have upper solar radiation limits. Table 3 indicates its dynamics.

In the same way, the diesel generator is represented only by two states (refer to Figure 16). But, unlike the PVs, diesel generators have a WORKING MODE instead of a

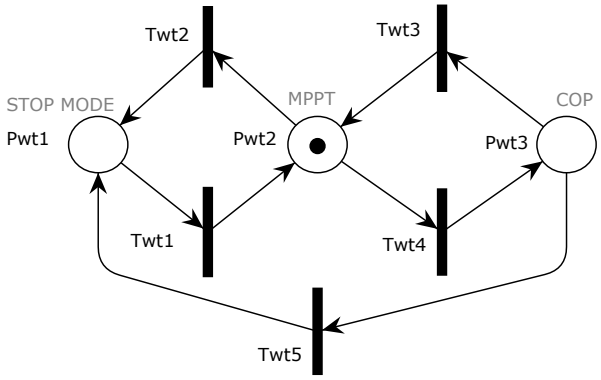

Figure 14 – Petri net model of wind turbine

Table 3 – PV Petri net model description

PN instance	**Functionality description**
Ppv1	MPPT mode
Ppv2	Stop Mode
Tpv1	Solar radiation $<$ Solar radiation$_{min}$
Tpv2	Solar radiation $\geq$ Solar radiation$_{min}$

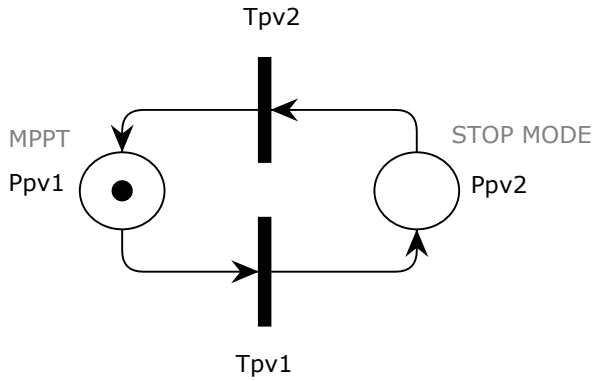

Figure 15 – Petri net model of photovoltaic panel

MPPT state. That is because they have a dispatchable behavior, which means that they are controllable elements. Because of such behavior, their operation are dependent on the microgrid power balance, which means that the diesel generators need to receive the information from the EMS to turn on or turn off. The Table 4 shows the description for this model, indicating the dependency of power balance on its dynamics. The variables P_{WT}, P_{PV}, P_{ST} and P_{LO} represents the produced or consumed power of wind turbine, photovoltaic system, storage system and load demand, respectively.

The dynamics of energy storage system (ESS) is modeled by a three states Petri net. The states are named CHARGING, DISCHARGING and IDLE. Its operation is simple. Whenever the power balance of the renewable generators (P_{Gr}) and load (P_{LO}) is positive, the storage assumes the charging mode absorbing the surplus energy, and whenever the balance is negative, it assumes the discharging mode delivering the required

Table 4 – Diesel generator model description

PN instance	**Functionality description**
Pmt1	Working mode
Pmt2	Stop Mode
Tmt1	$P_{WT} + P_{PV} + P_{ST}$ - $P_{LO} \leq 0$
Tmt2	$P_{WT} + P_{PV} + P_{ST}$ - $P_{LO} > 0$

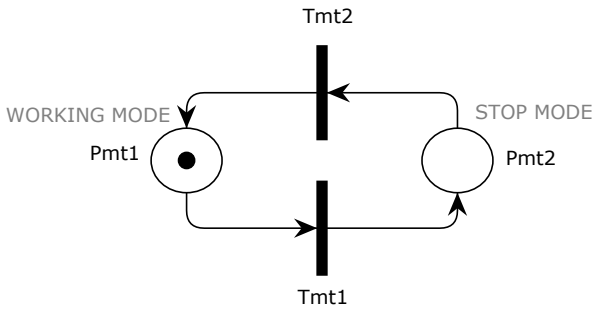

Figure 16 – Petri net model of diesel generator

energy. The IDLE state can be reached by two different events, one when the storage system reaches its maximum capacity, and another when it reaches the minimum capacity. The capacity of the storage is indicated by the state of charge (SOC) index. The description and logic of ESS operation is shown in Table 5 and Figure 17.

Table 5 – Storage model description

PN instance	**Functionality description**
Pst1	Charging operating mode
Pst2	Discharging operating mode
Pst3	Idle mode
Tst1	$SOC > SOC_{min}$ & $P_{Gr} < P_{LO}$
Tst2	$SOC < SOC_{max}$ & $P_{Gr} > P_{LO}$
Tst3	$SOC \leq SOC_{min}$
Tst4	$SOC > SOC_{min}$ & $P_{Gr} < P_{LO}$
Tst5	$SOC < SOC_{max}$ & $P_{Gr} > P_{LO}$
Tst6	$SOC \geq SOC_{max}$

Last, the load is represented by two states. It is considered only the normal operation and load curtailment states. The normal condition is assumed when the generation is higher than the consumption, otherwise the system is put in load shedding state. The model description is presented in table 6 and the PN dynamics is shown in Figure 18.

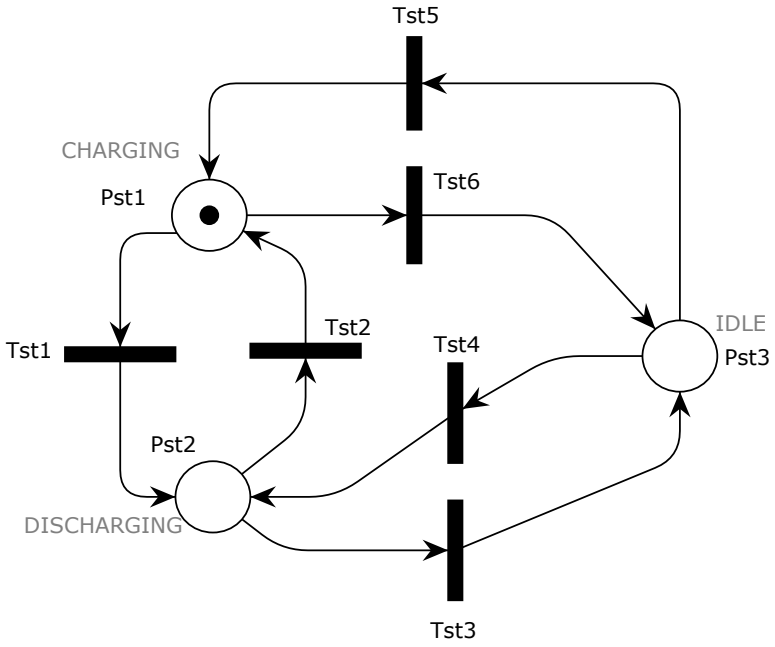

Figure 17 – Petri net model for energy storage system

Table 6 – Load model description

PN instance	**Functionality description**
Plo1	Normal load
Plo2	Cut load
Tlo1	$P_{WT} + P_{PV} + P_{ST} + P_{DG}$ - $P_{LO} < 0$
Tlo2	$P_{WT} + P_{PV} + P_{ST} + P_{DG}$ - $P_{LO} \geq 0$

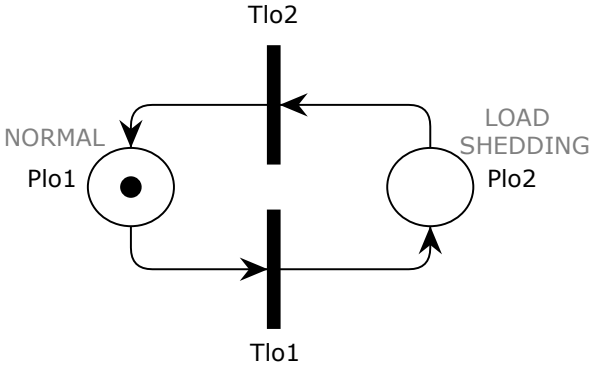

Figure 18 – Petri net model of load demand

4.1.2 PN model of microgrid coordinated control - EMS philosophy

4.1.2.1 EMS PN modeling

The coordinated control executed by the energy management system has the function of manage and control the microgrid operation in isolated mode. In fact, depending on the event and the current state of MG elements, the coordinator performs some actions in order to maintain the power balance security, trying to avoid the load curtailment.

The proposed philosophy of EMS strategy follows the concept of low emission of pollutants, avoiding the use of fossil fuel in energy generation process (mainly CO_2). For this reason, the first attempt of power balance is using the renewable energy. In case of power mismatch, the storage system acts, and if the power balance is still negative, as last resource, the diesel generator is turned on. If all the available generation sources are not enough to maintain the load balance, the system is placed in the load curtailment mode.

From the PN modeling of microgrid elements, one can note that the discrete modes of each element affect the whole system. So, the discrete modes of each device can be understood as a subset of a global set denominated microgrid. Because of that, the EMS needs to receive the actual operational mode of all elements in order to execute some action.

In this way, the subsets with the respective operation mode can be summarized as follows:

- WT → Wind Turbine {Stop: 0; MPPT: 1; COP: 2};
- PV → Photovoltaic system {Stop: 0 ; MPPT: 1};
- DG → Diesel generator {Stop: 0 ; Working: 1};
- ST → Storage {Discharging: -1; Idle: 0; Charging: 1};
- LO → Load {Economic: -1; Normal: 1};

The complete microgrid set, defined as M^S, is a combination of all subsets ($WT \times PV \times ST \times DG \times LO$). Considering this, the complete M^S set is formed by $3 \times 2 \times \times 3 \times 2 \times 2 = 72$ operative modes. But, for the proposed EMS philosophy only a small number of combination is possible. Actually, the microgrid set is reduced to M^{S*} which has five operating modes ($M^{S*} = \{m_1, m_2, m_3, m_4, m_5\}$). Table 7 shows the new microgrid set M^{S*}.

Table 7 – Set of microgrid operating modes (M^{S*})

Microgrid mode	**WT mode**	**PV mode**	**ST mode**	**DG mode**	**LO mode**
m_1	Unknown	Unknown	1	0	1
m_2	Unknown	Unknown	-1	0	1
m_3	Unknown	Unknown	0	1	1
m_4	Unknown	Unknown	0	1	-1
m_5	Unknown	Unknown	0	0	1

After defining the set of microgrid operating modes M^{S*}, the PN model of EMS coordinated control is described as shown in Figure 19. The description of the event-based

coordinated control is demonstrated in Table 8. As remarkable note, one can verify that the proposed model is a Finite State Machine (FSM) since it is in only one state at a time, which facilitates the model analysis.

Table 8 – Microgrid management model description

PN instance	**Functionality description**
Pco1	Only renewable
Pco2	Discharging storage
Pco3	Diesel generator on
Pco4	Load shedding
Pco5	Full storage (SOC_{max})
$Tco_{1,2}$	$P_{WT} + P_{PV}$ - $P_L < 0$
$Tco_{1,5}$	$SOC = SOC_{max}$
$Tco_{2,1}$	$P_{WT} + P_{PV}$ - $P_L > 0$
$Tco_{2,3}$	$P_{WT} + P_{PV} + P_{ST}$ - $P_L < 0$
$Tco_{3,1}$	$P_{WT} + P_{PV}$ - $P_L > 0$
$Tco_{3,4}$	$P_{WT} + P_{PV} + P_{ST} + P_{DG}$ - $P_L < 0$
$Tco_{4,3}$	$P_{WT} + P_{PV} + P_{ST} + P_{DG}$ - $P_L > 0$
$Tco_{4,1}$	$P_{WT} + P_{PV}$ - $P_L > 0$
$Tco_{5,2}$	$P_{WT} + P_{PV} + P_{ST}$ - $P_L > 0$
$Tco_{5,3}$	$P_{WT} + P_{PV} + P_{ST}$ - $P_L < 0$

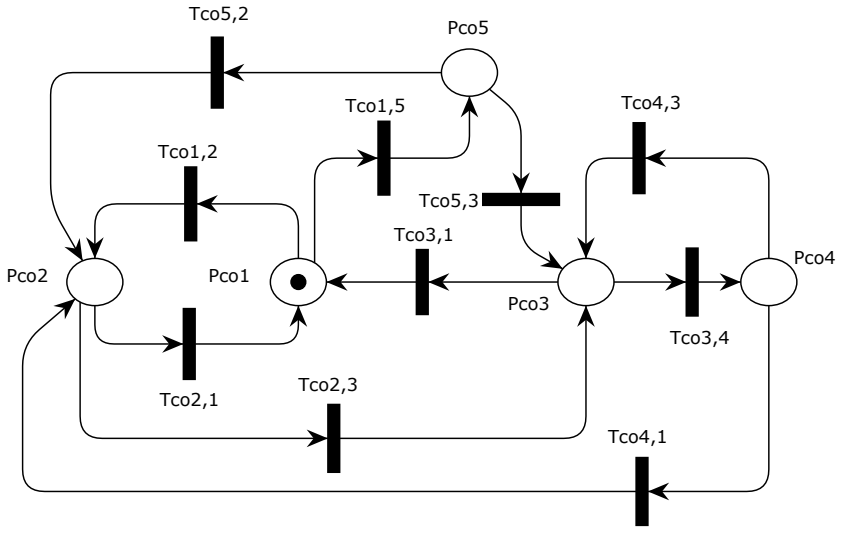

Figure 19 – Petri net model for microgrid energy management system

4.1.2.2 EMS PN analysis

A relevant analysis considering the Petri net formalism is the state space (SS) assessment, which helps the study of dynamic behavior of a PN model. In order to exemplify the dynamics of proposed EMS philosophy, two state transition paths are simulated, indicating that two different paths reach the same final state (reachability property). Figure 20 and Figure 21 show the graphics that relates the state path with the elapsed time

and the fired transition which triggers the state changing. Under these circumstances, the figures indicate two distinct paths that end up in the same state (place **Pco4** - load shedding).

Describing the first path (Figure 20), the system initializes at place **Pco1**, indicating that the microgrid power balance is dependent only of renewable sources (state *Only renewable*); after that, the system goes to *Discharging storage* state (place **Pco2**), since at this time (*T1*), the renewable sources were not enough to maintain the power balance; next, it returns to state *Only renewable* at *T2*; then, the system is conduced to state *Full storage (SOCmax)*, representing that there was more generation than consumption, besides, it indicates that the excess of produced energy was enough to fulfill the storage system; at time *T4*, the demand was bigger than the combination of renewable and storage, and there was the necessity of turning on the diesel generator; finally, it was observed at time *T5* that the system was conduced to place **Pco4**, showing that the combination of all renewable sources, storage system, and dispachable generation was not enough to keep the positive power balance of microgrid. Similar interpretation can be done for the second path on Figure 21.

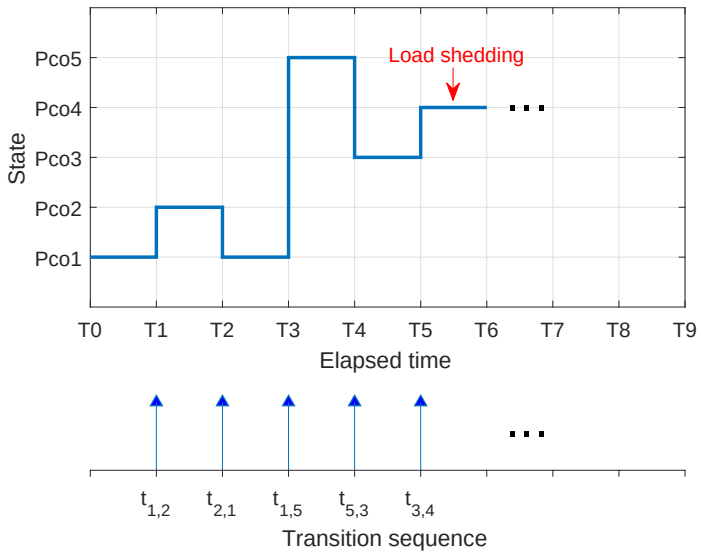

Figure 20 – State dynamics - path 1

So, the dynamics of the EMS philosophy can be investigated over a state space. The observable state space is defined by means of a reachability tree which is obtained from the exhaustive search of all possible markings of PN model starting at the initial marking M_0. For the suggested model, the reachability space is a finite state space composed by five states, and its dynamics can be evaluated considering any sequence of transition firing.

As suggested, the behavioral properties can be investigated by means of reachability tree, as shown in Figure 22. Assuming the definitions presented in [77] and considering the system as a FSM, it is guaranteed that the system is bounded and conservative, since the number of tokens does not change for all possible markings, and has no dead-locks,

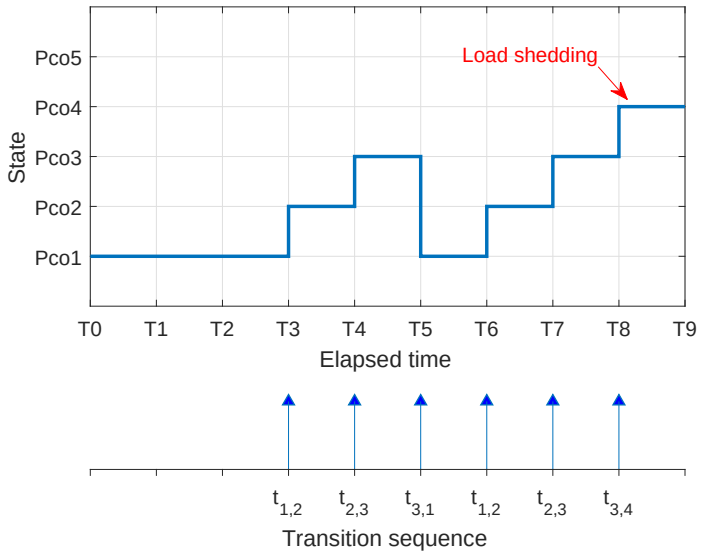

Figure 21 – State dynamics - path 2

which means that for all possible markings the system has at least one enabled transition. Such concept can be cleared up observing the dynamics exposed on the reachability graph (refer to Figure 23).

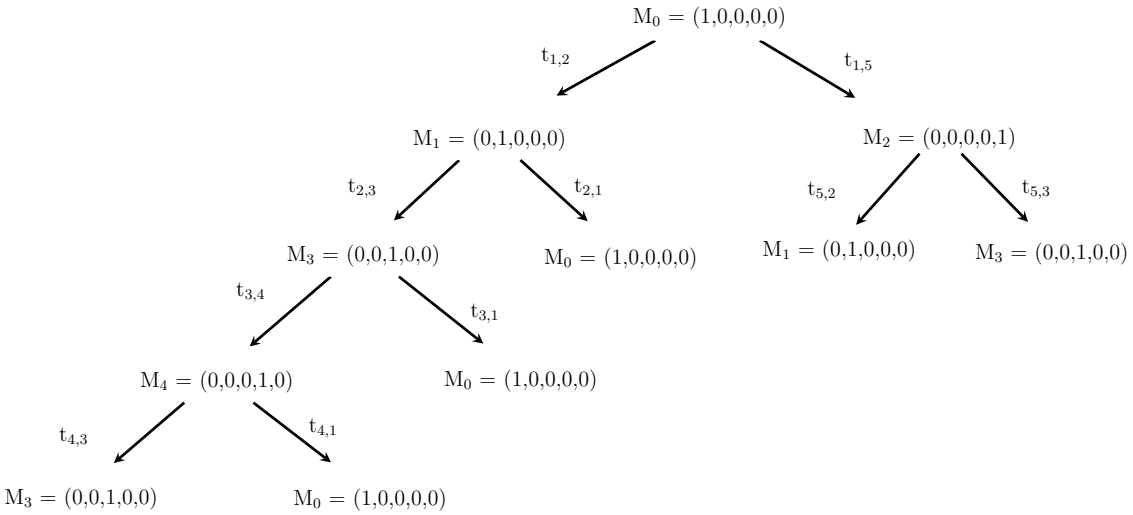

Figure 22 – Reachability tree of EMS coordinated control philosophy

From the non-deterministic behavior of the proposed EMS power balance strategy, it is necessary the usage of an appropriate technique that deals with such characteristic. Because of that, the Monte Carlo simulation (MCS) is adopted herein. The reliability assessment using the MCS based on the EMS strategy defined by the PN models will be better discussed in section 4.3.

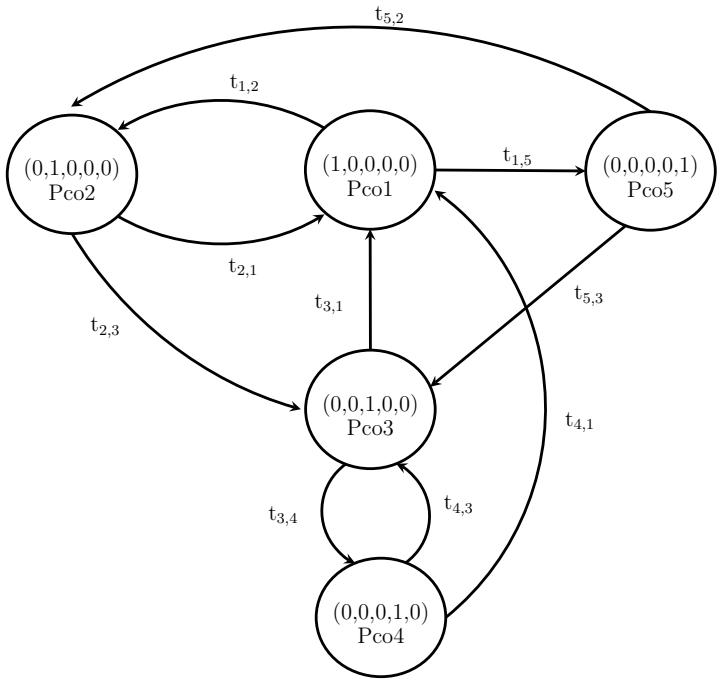

Figure 23 – Reachability graph of EMS coordinated control philosophy

4.2 Optimization of microgrid operation

The optimization of microgrid operation has two main procedures, named stochastic modeling and optimization. The modeling refers to create a representative probabilistic model of generation and load demand based on historical data and realistic system parameters. This probabilistic model is iteratively used to sample the stochastic scenarios that will be applied on optimization process. Besides, the modeling stage concerns on a exhaustive investigation to promote a proper database of weather variables, electricity tariffs, capital and maintenance costs of power system equipments and infrastructure, environmental taxes, fuel costs, and other technical data. The optimization stage is responsible for executing the mixed integer linear programming (MILP) in order to have quantitative results for decision making. The MILP program will adjust the microgrid power generation to minimize the costs and CO_2 emission without violating some constraints. Figure 24 illustrates these two procedures and the relationship between them.

4.2.1 Stochastic modeling - historical data, curve fitting and sampling

The modeling process of optimization problem consists on observe historical data (hourly data of weather and load), fit a probabilistic distribution function (pdf) for each hour of four representative days (one day per year season), and then sample the stochastic variables which will be inputs to the optimization tools. Similar procedure is seen in [72].

First, it is built a histogram for each hour of certain season day following the historical data of weather and load demand. From this histogram, it is fitted a probabilistic

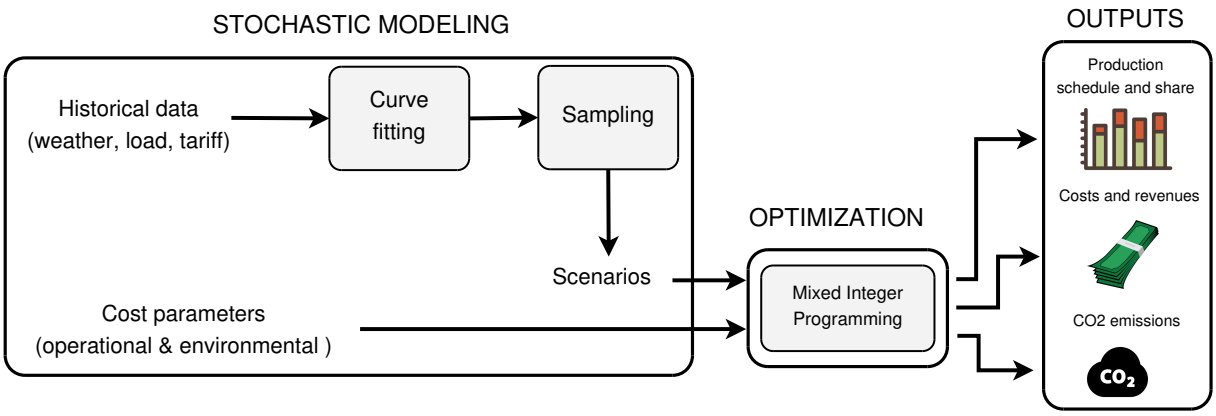

Figure 24 – Microgrid optimal operation stage

distribution function considering the appropriate pdf for each stochastic variable as already discussed in the Section 3.2. Figure 25 shows the histogram and curve fit for the solar radiation of the 12th hour of a summer day. In the same way, Figure 26, Figure 27, and Figure 28 represents the histograms and curve fitting of temperature, wind speed, and load demand respectively. This procedure of curve fitting is made for all 24 hours of each representative day, which means that such operation is repeated 96 times (24 hours $\times$ 4 season days = 96 hours). Observing such profiles, the results indicates some agreement with what is suggested in the literature [32, 102–104], in which a *Beta* distribution is suitable for radiation, a *Normal* distribution for temperature and load demand, and *Weibull* distribution for wind speed.

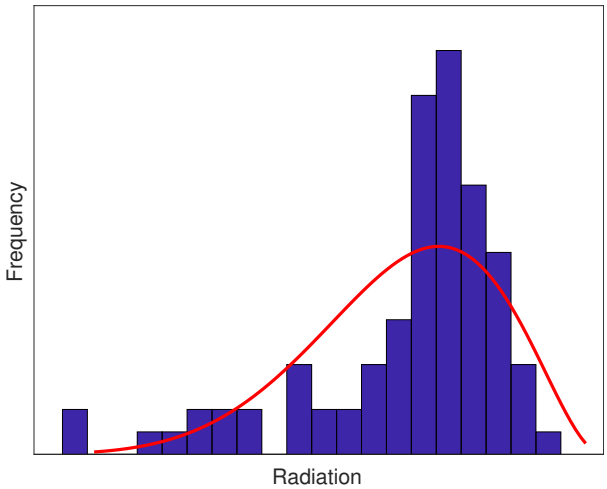

Figure 25 – Histogram of radiation of 12th hour of summer day based on historical data

Usually, traditional stochastic programming uses a large time-consuming sampling process, and because of that it was necessary to found an efficient and low latency sampling strategy. That is why the concept of representative days was used in this work. Such approach is already used and disseminated in academia, as shown in papers [28, 105].

Real information of wind speed, temperature, and radiation are used to calculate

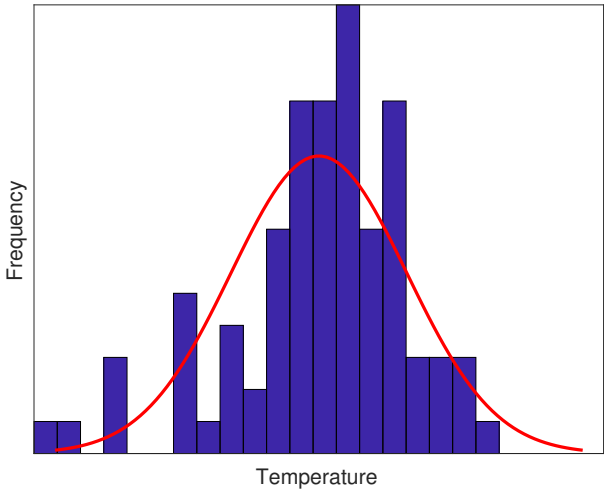

Figure 26 – Histogram of temperature of 12th hour of summer day based on historical data

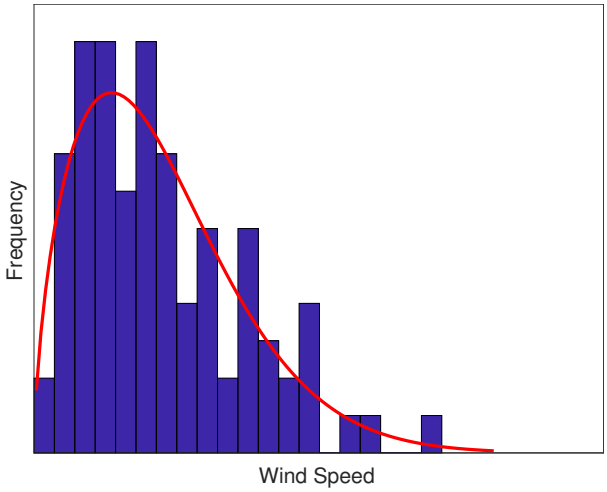

Figure 27 – Histogram of wind speed of 12th hour of summer day based on historical data

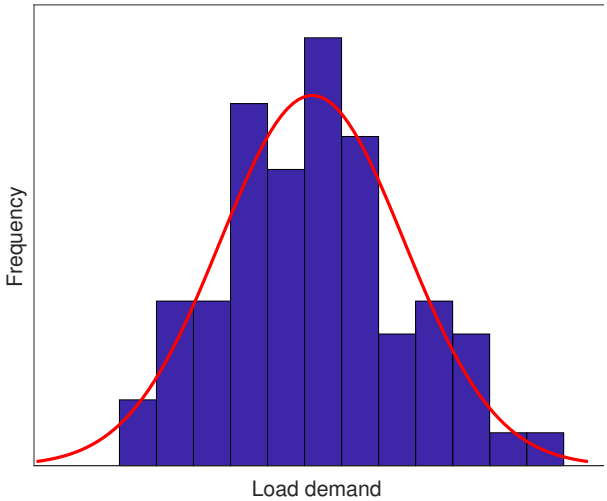

Figure 28 – Histogram of load demand of 12th hour of summer day based on historical data

the generated power of renewable sources. The data were provided by Centro de Estudos e Previsão do Tempo e Clima de Minas Gerais - CEPreMG/UNIFEI. In order to evaluate the whole year, it was used the 8760 hourly information of wind speed, temperature, and radiation of the year 2015 in the city of Itajuba - Brazil.

From this database, the curve fitting process is performed and then the stochastic generation is calculated using the formulation presented in 3.2. The load profiles are sampled directly from the curve fitting made over the IEEE/RTS database [73]. The seasonal daily profile of photovoltaic system, wind turbine, and the load consumption is demonstrated in Figure 29, Figure 30, and Figure 31 respectively.

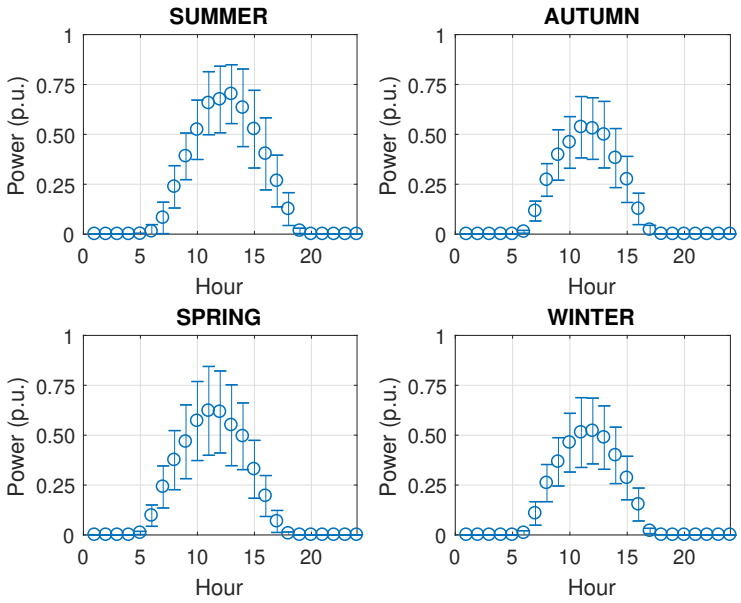

Figure 29 – Daily profile of PV output power for each year season

4.2.2 MILP to solve economic power generation

The MILP optimization stage is responsible for the economic microgrid generation dispatch aiming to reduce the microgrid operational cost and emission. In this way, it is proposed an objective function which is an attempt to express the business and environmental goals in mathematical terms. Such function, composed by decision variables (power output of dispatchable generators), is subject to a group of operational and technical constraints. In the present study, the dispatchability is guaranteed by three diesel generators and the main grid. The size of each diesel generator, as well as the renewable generators (solar and wind), are defined in each iteration of the PSO procedure, while the main grid is a fixed parameter. In this way, the economic microgrid generation dispatch is continuously calculated for each particle of the PSO algorithm.

The MILP process is performed on a horizon of 96 hours (4 days $\times$ 24 hours), using a representative day of each year season (summer, autumn, winter, spring). In practical

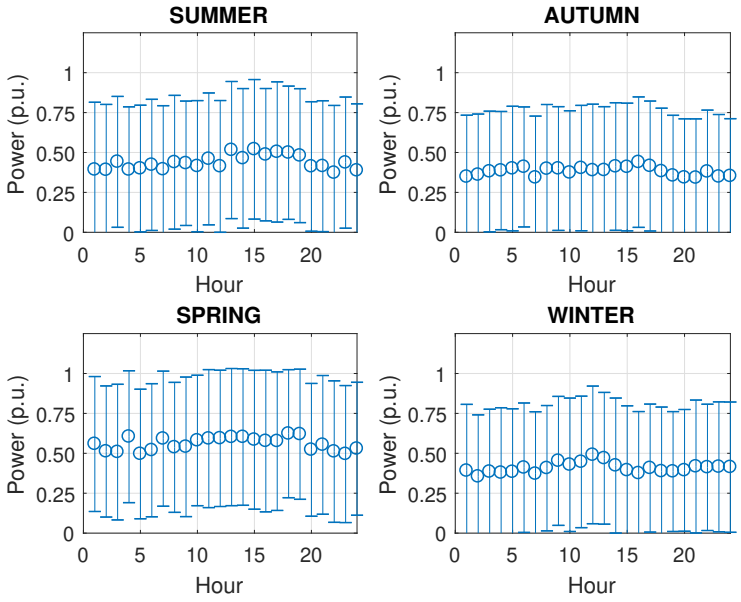

Figure 30 – Daily profile of wind turbine output power for each year season

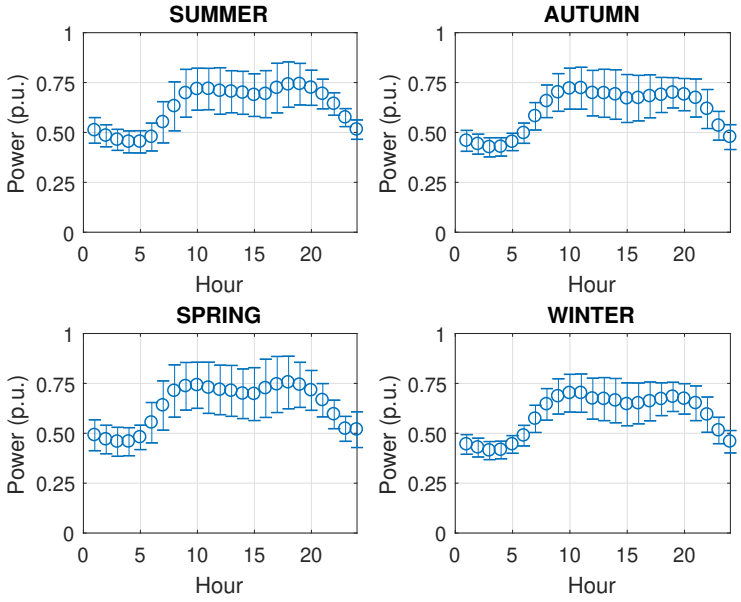

Figure 31 – Daily profile of load demand for each year season

meanings, the IBM CPLEX software [106] (embedded MILP solver) will try to find the best dispatchable generation combination over the 96 hours horizon, returning the lowest value of objective function.

Briefly describing, the following MILP problem was solved with MATLAB using the CPLEX solver and the YALMIP [107] interface.

A) Objective function

Following, it is presented the objective function which models the economical, technical and environmental interest factors. All parameters and variables are treated as integer-valued or restricted integer ("binary 0-1" integer).

$$min \sum_{t \in T} f_{cap}(t) + f_{ope}(t) + f_{grid}(t) + f_{main}(t) + f_{emi}(t) \tag{4.1}$$

where

$$f_{cap}(t) = \sum_{i \in D,E,R} \frac{C_{cap,i}}{T_i} \cdot f_{cr}(r, n_i) \tag{4.2}$$

$$f_{ope}(t) = \sum_{i \in D} C_i^f \cdot P_{i,t} \tag{4.3}$$

$$f_{grid}(t) = C_{g,buy} \cdot P_{g+,t} - C_{g,sell} \cdot P_{g-,t} \tag{4.4}$$

$$f_{main}(t) = \sum_{i \in D,E,R} C_i^m \cdot x_i \tag{4.5}$$

$$f_{emi}(t) = \sum_{i \in D} \zeta_i^m \cdot P_{i,t} \tag{4.6}$$

where $f_{cap}(\cdot)$ is the capital cost function of DERs, which accounts for the payback for initial outlay of devices; $f_{ope}(\cdot)$ is the operational cost function of DGs, including the fuel cost; $f_{grid}(\cdot)$ is the energy purchase/sell cost function, and it includes the costs of exchanging power with the grid; $f_{main}(\cdot)$ is the maintenance cost of each DER unit x_i; $f_{emi}(\cdot)$ represents the tax cost of CO_2 emission coming from fossil fuel generators. The parameter $C_{cap,i}$ is the initial capital cost of device i; T_i is the yearly operating hours of device i; f_{cr} is the capital recovery factor; r is the interest rate; and n_i is the depreciation period i in years.

To evaluate the hourly value capital cost, the initial capital cost is converted to annual cost with the capital recovery factor, and then to hourly cost with the yearly operating hours. The capital recovery factor is used to calculate the present value of annuity, and it is expressed as

$$f_{cr}(r, n_i) = \frac{r(1+r)^{n_i}}{(1+r)^{n_i} - 1} \tag{4.7}$$

B) Constraints

For the constraints, it is admitted the power balance constraint in (4.8), the unit generation limitation in (4.13), the grid limit energy importation/exportation in (4.14), and the storage operation constraints in (4.15), (4.16), (4.17), (4.18), (4.19), (4.20).

$$\sum_{i \in D,E,R} P_{i,t} + P_{g+,t} - P_{g-,t} = P_{l,t} \quad \forall t \in T \tag{4.8}$$

For the unit constraint, when a unit i is switched on (off), it must remains for at least T_i^{on} (T_i^{off}) consecutive periods. Constraints (4.9) and (4.10) model this aspect for the initial state, while the constraints (4.11) and (4.12) do the same for the remaining planning horizon. In (4.9) θ_i^{on} represents $max\{0, T_i^{on} - t_i^{prev}\}$, and θ_i^{off} in (4.12) stands for $max\{0, T_i^{off} - t_i^{prev}\}$ [99].

$$y_{i,t} = 1, \quad \forall i \in D : y_i^{prev} = 1, for\ t = 0, \ldots, \theta_i^{on}, \tag{4.9}$$

$$y_{i,t} = 0, \quad \forall i \in D : y_i^{prev} = 1, for\ t = 0, \ldots, \theta_i^{off}. \tag{4.10}$$

In (4.11) and (4.12), $\tau_{i,t}^{on}$ and $\tau_{i,t}^{off}$ stand for $max\{t - T_i^{on} + 1, 1\}$ and $max\{t - T_i^{off} + 1, 1\}$, respectively.

$$\sum_{k=\tau_{i,k}^{on}}^{t} u_{i,k}^{on} \leq y_{i,t}, \quad \forall i \in D,\ \forall t \in T; \tag{4.11}$$

$$\sum_{k=\tau_{i,k}^{on}}^{t} u_{i,t}^{off} \leq 1 - y_{i,t}, \quad \forall i \in D,\ \forall t \in T; \tag{4.12}$$

$$P_i^{min} y_{i,t} \leq P_{i,t} \leq P_i^{max} y_{i,t} \quad \forall t \in T \tag{4.13}$$

$$0 \leq P_{g+,t}, P_{g-,t} \leq P_g^{max} \quad \forall t \in T \tag{4.14}$$

$$E_{b,0} = 0.5 \cdot E_b^{max} \tag{4.15}$$

$$P_{b,0} = 0 \tag{4.16}$$

$$-E_b^{install} \leq P_{b,t+1} \leq E_b^{install} \quad \forall t \in T \tag{4.17}$$

$$-P_b^{ramp} \leq P_{b,t+1} - P_{b,t} \leq P_b^{ramp} \quad \forall t \in T \tag{4.18}$$

$$E_b^{t+1} = E_{b,t} - P_{b,t+1} \cdot \Delta t \quad \forall t \in T \tag{4.19}$$

$$0.2 \leq \frac{E_{b,t}}{E_b^{install}} \leq 1 \quad \forall t \in T \tag{4.20}$$

4.3 Reliability analysis - Monte Carlo simulation

The reliability analysis stage has the function of estimating the distribution power system reliability indexes when it is operating in isolated mode, especially the loss of load expectation (LOLE). For this procedure, it is used the Monte Carlo simulation (MCS) and the EMS philosophy given by the PN model. The suggested MCS approach is simple, and follows the Algorithm 1. Summarizing, it repeatedly does: (i) sampling of stochastic data based on distribution probability curve fitting; (ii) executes the power balance analysis considering the coordinated control modeled by Petri net; (iii) estimates reliability indexes; (iv) verify stop criteria; (v) estimates the value of transition rate $\lambda_{2,3}$ (markovian transition between the isolated mode to contingency state - refer to Figure 33) based on LOLE index.

Following [78], the LOLE indicator express the expected hours per year during which a system capacity shortage occurs. The equation 4.21 denotes the index calculation, where P_G and P_L, are the hourly generation and load consuming, respectively. Also, in this stage other two reliability indexes are calculated. They are the Loss of Energy Expectation (LOEE) expressing the expected energy not supplied by the generating units per year, and Loss of Load Probability (LOLP) which designates the percentage of power balance mismatch during a certain period, in this case a year. These indexes are calculated as demonstrated in (4.22) and (4.23).

$$LOLE(t) = \begin{cases} 0, & if \quad P_G \geq P_L \\ 1, & if \quad P_G < P_L \end{cases} \tag{4.21}$$

$$LOEE(t) = \begin{cases} 0, & if \quad P_G \geq P_L \\ \delta E(t), & if \quad P_G < P_L \end{cases} \tag{4.22}$$

$$LOLP = LOLE/8760 \tag{4.23}$$

4.4 Contingency analysis - steady state Markov chain

The contingency analysis indicates the impact that the grid and microgrid failures/repair rates represents to the reliability of whole distribution system. A Markov

Input : Stochastic data: weather, load; Stop criteria: Δ
Output: Estimated $\lambda_{2,3}$ transition rate
Stochastic data curve fitting;
while *NOT Stop Criteria* **do**
  for *z = 1 to 1000* **do**
    for *y = 1 to 8760* **do**
      Stochastic variables random sampling based on curve fitting parameters;
      Coordinated power balance strategy;
      Verify states and actions applied;
    end
    $S(z) \leftarrow$ computation of yearly LOLE;
  end
  if *std (S(z)) / mean(S(z))* $< \Delta$ **then**
    Stop Criteria $\leftarrow$ TRUE;
  end
end
$\lambda_{2,3} \leftarrow mean(S(z))$;
return $\lambda_{2,3}$

Algorithm 1: Monte Carlo algorithm

chain model is suggested to observe such impacts. In order to compare the effects of inserting a microgrid in the traditional power system (two state Markov chain - Figure 32), a three state homogeneous Markov chain model is suggested as Figure 33. From the homogeneous property, it is possible to say that the transition between each state obeys a negative exponential distribution with rate parameter $\lambda_{i,j}$ or $\mu_{j,i}$, where λ indicates the failure rate and μ indicates the repair rate.

Considering the model with microgrid incorporation (Figure 33), the transition from the grid-connected to isolated mode ($\lambda_{1,2}$) represents the failure of the main grid due to an abnormal event, as a fault or an extreme condition such as tropical storms and flood. Similar concept is applied to the transition between the isolated mode to contingency state ($\lambda_{2,3}$), which implies on load curtailment. If the system is on isolated microgrid mode, then it will return to normal state (grid-connected) with a repair rate of $\mu_{2,1}$. If it is on contingency state, the microgrid will return to isolated mode or to grid-connected with rate repair of $\mu_{3,2}$ and $\mu_{3,1}$, respectively. The transition rates $\lambda_{1,2}$, $\mu_{2,1}$, $\mu_{3,1}$, and $\mu_{3,2}$ assumes typical values of a distribution system, while $\lambda_{2,3}$ comes from the reliability procedure presented in the section 4.3.

In possession of all markovian transition rate, the steady state analysis is performed, allowing the evaluation of final probability distribution of the system being in each mode. The final probability distribution is found solving the linear system composed by the equations (4.24) and (4.25), where Q is the transition rate matrix and

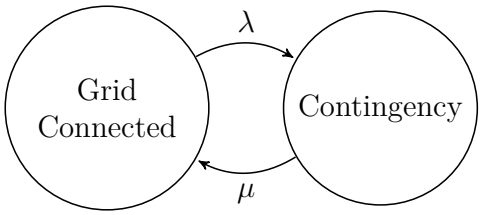

Figure 32 – Markov model for contingency analysis - traditional power system

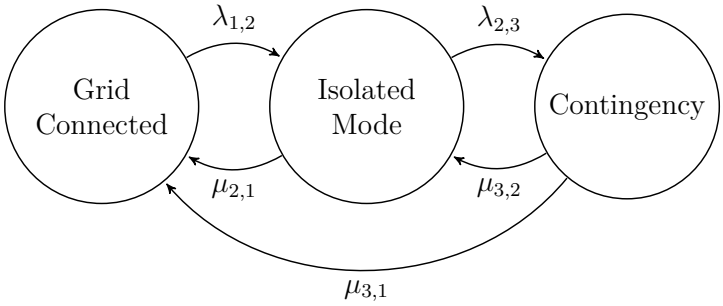

Figure 33 – Markov model for contingency analysis - incorporating microgrid to power system

$\pi = [\pi_1, \pi_2, \ldots, \pi_j]$ is the stationary vector [108].

$$0 = \pi Q \tag{4.24}$$

$$\sum_{j \in S} \pi_j = 1 \tag{4.25}$$

4.5 Particle swarm optimization (PSO) - finding the optimal microgrid design

Synthesizing the framework proposal, it tries to found the best DER combination (α_i) in which exists an appropriate balance between operation costs (C), pollutants emission (E), and unreliability (U).

$$f(\alpha_i) = C(\alpha_i) + E(\alpha_i) + U(\alpha_i) \tag{4.26}$$

So, in practical terms, the PSO will continuously run searching for the best particle α_i, returning an appropriate value for fitness function (4.26). When the stop criteria is reached, the PSO returns the best DER composition, in other words, the best particle α_i.

Each particle of the PSO is a vector composed by five continuous variables as shown in (4.27). The position of vector α_i represents, respectively, the rated power of

wind turbine (WT), photovoltaic system (PV), diesel generator 1 (DG1), diesel generator 2 (DG2), and diesel generator 3 (DG3).

$$\alpha_i = \langle WT, PV, DG1, DG2, DG3 \rangle \tag{4.27}$$

Considering the multi-objective function (4.26), it is proposed two methodologies using the PSO for defining the best solution. The first one presents the classical weighted fitness function, where the PSO returns only one best solution based on such function. The second performs the PSO to create the design space that will be used to take the Pareto front.

4.5.1 PSO - weighted fitness function

The particle swarm technique optimizes the planning problem by iteratively trying to improve a candidate solution with regard to a given measure of quality, also named as fitness function.

The fitness function indicated in (4.28) is dependent on the DER combination (α_i) of each particle i, and it ponders three different variables - operation cost $C(\alpha_i)$ (MILP solution); CO_2 emission $E(\alpha_i)$ (MILP solution); reliability/ contingency $U(\alpha_i)$ (MCS and Markov chain solutions). The parameter w_j is the weight given to each parcel of the equation. The use of a weighted fitness function is justified since there are important differences in the willingness and motivations of the stakeholders.

$$\min f(\alpha_i) = w_1 C(\alpha_i) + w_2 E(\alpha_i) + w_3 U(\alpha_i) \tag{4.28}$$

The upper ($\overline{X}(\alpha)$) and lower ($\underline{X}(\alpha)$) limits are calculated in an extensive simulation that runs the entire PSO algorithm, searching for all possible values that $f(\alpha_i)$ can assume. Then, each variable is normalized in order to have the same base of comparison. The normalization process is shown in (4.29).

$$X_{norm}(\alpha_i) = \frac{X(\alpha_i) - \underline{X}(\alpha)}{\overline{X}(\alpha) - \underline{X}(\alpha)} \tag{4.29}$$

Although the simplicity of the method, the classical approach of combinatorial weighting [109] is suggested in this work because it presents low computational time and solution effectiveness in linear problems [110,111], which is the case of microgrid planning. Besides, since the concept of the present work is to present some guidelines for microgrid planning, and not to demonstrate the best techniques, such approach is convenient.

Summarizing, the PSO procedure tries to find the best DER combination (α_i) that results in the minimum value of the fitness function, which ponders some weights

defined by the decision maker. As an acknowledgment, it is important to clarify that the definition of weights is absolutely subjective to each stakeholder, which means that the final decision may not please all parties.

4.5.2 PSO - Pareto front

In this approach, the PSO creates a plenty of feasible solutions (design space) which is then transformed into the criterion space. After that, the intuitive Pareto front method is performed in order to take the set of possible solutions. Pareto front characterizes fundamental tradeoffs between operational costs, CO_2 emission, and system reliability.

The usage of Pareto front to find optimal points of multi-objective problems is widely used as seen in [112–116], supporting its implementation on the proposed approach.

Here, the Pareto based decision-making approach involves generating many potentially preferable Pareto optimal designs, followed by choosing the most attractive one. This approach has been called Generate First—Choose Later (GF-CL) [93, 117]. An important benefit of the GF-CL approach is that by generating numerous Pareto solutions a designer can compare a range of design alternatives, where the range covers different levels of tradeoff between objectives. One drawback to GF-CL is that generating many Pareto solutions may be too computationally expensive to justify. For the present work, the GF-CL approach is performed as shown in Algorithm 2.

Summarizing, the algorithm establishes the set of dominating points (Pareto frontier). Here, one can understand dominating point as the solution which has at least one negative value when comparing to all feasible solution. Considering two feasible solutions X and Y, where $X - Y < 0$, it is assumed that X dominates Y ($X \prec Y$).

Input : PSO design space S_d (set of feasible solution)
Output: Pareto solutions M_p
for *j = 1 to number of feasible solution in S_d* **do**
  $s(j) \leftarrow$ one solution selected from design space;
  for *i = 1 to number of feasible solution in S_d* **do**
    if $i \neq j$ **then**
      $c(i) = s(j) - S_d(i)$ ▷ Comparison of solutions;
    end
  end
  if *$s(j)$ dominates all answers* **then**
    $s(j)$ is a Pareto solution;
    Save it into output matrix M_p;
  end
end
return M_p;

Algorithm 2: Pareto front generation - Generate first-Choose later approach

The PSO algorithm is the main program of the framework, and it controls the relationship among each stage. PSO procedure is shown in Figure 34.

4.6 Framework Implementation - Procedural Design

In practical meanings, the framework is a MATLAB-built program, considering a modular approach. The main program named *Particle Swarm Optimization (PSO)*, has five modules, called *Stochastic Modeling*, *Sampling*, *Optimization*, *Reliability*, and *Selection*, and the user interface. Some modules also have submodules. The complete procedural design of this software is presented in Figure 35, which shows the relationship that each module/submodule has with the user and the PSO main program.

The connection among each module, the user and the main program is made by means of a simple communication scheme. The communication has three types of messages. The first one is the *user input data*, which are vectors and/or matrices with specific meteorological data, demand profiles, economical data, etc. The second type of message is the *request/reply* mechanism, in which the module or the main program requires the execution of certain function, and it has as reply certain parameter. Such message is seem, for instance, in the relation between the PSO main program requesting the stochastic models of load and renewable sources. The last type of message is the *data flow*, which has the purpose of transferring certain type of data in the form of matrices or vectors. This data can be as sampled data, scheduled microgrid generation, best microgrid configuration, etc. Please, refer to Figure 35 for better understanding.

Until the present moment, this implementation has only academic purposes, and because of that, no software interface was created. The software was developed using simple MATLAB scripts. Hence, in the following sections, only the outlines of each module are described.

4.6.1 Stochastic Modeling

The *Stochastic Modeling* provides the parameters of a probability distribution function (pdf) which proper fits to the input data given by the user. Input data refers to local wind speed, temperature, radiation, and energy consumption. In this work, the data is hourly sampled. As output, this module returns the pdf parameters.

As shown in Figure 35, these parameters are transfered to the PSO main program by means of request/reply mechanism. The probabilistic models are used in the *Sampling* and *Reliability* modules to generate random scenarios. *Stochastic Modeling* module is executed only once, in the beginning of the *PSO* main program.

A simple pseudocode (Algorithm 3) is presented in order to demonstrate imple-

mentation aspects.

Input : User input data (weather or load data (representative days))
Output: Parameters pdf
Parameters pdf ← fit probabilistic distribution function;
return Parameters pdf;

Algorithm 3: *Stochastic Modeling* module pseudocode

4.6.2 Sampling

The parameters generated by the curve fitting in *Stochastic Modeling* (*Parameters pdf*) procedure are used in the *Sampling* module. Here, a matrix 4x96 is generated every time the *Optimization* module requests. It is formed by 96 representative values of four stochastic variables: wind speed, radiation, temperature, and load. Such matrix represents the data flow between *Sampling* and PSO main program. The *Sampling* module is executed for each particle in each PSO iteration. Because of that, the number of particle must be appropriate, otherwise, the time to execute this stage will be impractical.

Once again, it is necessary to remember that the sampling procedure can be very time-consuming, and because of that, it was used the approach of representative days (refer to Section 4.2.1). Algorithm 4 indicates its pseudocode.

Input : Parameters pdf
Output: Sampled data
for *i = 1 to 4* **do**
  for *j = 1 to 96* **do**
    Sampled data(i,j) ← generate random(pdf, Parameters pdf);
  end
end
return Sampled data;

Algorithm 4: *Sampling* module pseudocode

4.6.3 Optimization

The optimization module executes the MILP program as previously stated. Before the MILP execution, it is necessary to call the submodule *Power Profile* in order to provide the power generated by the wind turbine and photovoltaic array, and the power consumed by the load. These stochastic generation and consumption are calculated considering the formulation presented in Section 3.2, for the 4x96 matrix given by the *Sampling* procedure.

The *Power Profile* submodule uses some data given by the user: minimum/maximum rated power of wind turbine, photovoltaic array and diesel generators, and maximum peak load. As output, *Power Profile* returns a 3x96 matrix with the generation profile of wind

turbine and photovoltaic array, and the consumption profile of load demand. The MILP program is executed by the IBM CPLEX platform, and its outputs are the microgrid operational daily costs and emission. The MILP submodule also uses information provided by the user as economical data (tariffs, DER investment cost, etc.) and DER technical data (generator ramp, SOC limits, generator limits, etc.)

This procedure is performed for each particle in each PSO iteration. The Algorithm 5 indicates the implementation of the *Optimization* module.

Input : Sampled data, Rated Power Wind Turbine, Rated Power Photovoltaic Array, Peak Load, Economical data, DER techinical data
Output: Daily Operational Costs, Daily Emission
WT ← Power Profile (WT) ▷ equation (3.6);
PV ← Power Profile (PV) ▷ equation (3.11);
LOAD ← Power Profile (Peak Load);
Daily Operational Costs and Daily Emission ← MILP program (WT,PV,LOAD);
return Daily Operational Costs, Daily Emission;

Algorithm 5: Optimization module pseudocode

4.6.4 Reliability

The reliability module calculates the probability of the system being in contingency, and also calculates the reliability indexes. It executes two procedures that are connected. First, it performs the *Monte Carlo Simulation* submodule in order to obtain the microgrid reliability indexes, especially, the LOLE index. It uses the pdf parameters calculated in *Stochastic Modeling* module for sampling the probabilistic scenarios. The parameters, once again, are transfered by means of request/reply mechanism.

The LOLE index is passed to the *Markov Chain Analysis* module which calculates the contingency probability by means of Markov Chain steady state analysis. The MCS is performed exactly as described in Section 4.3, and the Markov Chain analysis follows the formulation presented in (4.24) and (4.25). The *Reliability* module is executed for each particle in each iteration.

Following, it is presented a pseudocode that implements this module (refer to Algorithm 6).

Input : Parameters pdf, transition rate $\lambda_{j,i}$ and $\mu_{j,i}$
Output: Contingency probability, Reliability Indexes
Reliability Indexes ← Monte Carlo Simulation ▷ algorithm 1;
Contingency Probability ← Markov Chain Analysis ▷ equations (4.24), (4.25);
return Contingency probability, Reliability Indexes;

Algorithm 6: Reliability module pseudocode

4.6.5 Selection

At last stage, the module *Selection* performs the PSO searching algorithm, which is solved by means of weighted sum or Pareto front. To do so, it is used the concepts presented in Section 4.5.1 or Section 4.5.2.

After this procedure, the optimal design of the microgrid is finally found. So, the input data for this module is the operational daily cost, daily emission and contingency probability of each particle in each iteration. The *Selection* module refers to the last stage of the PSO procedure, as indicated in Figure 34.

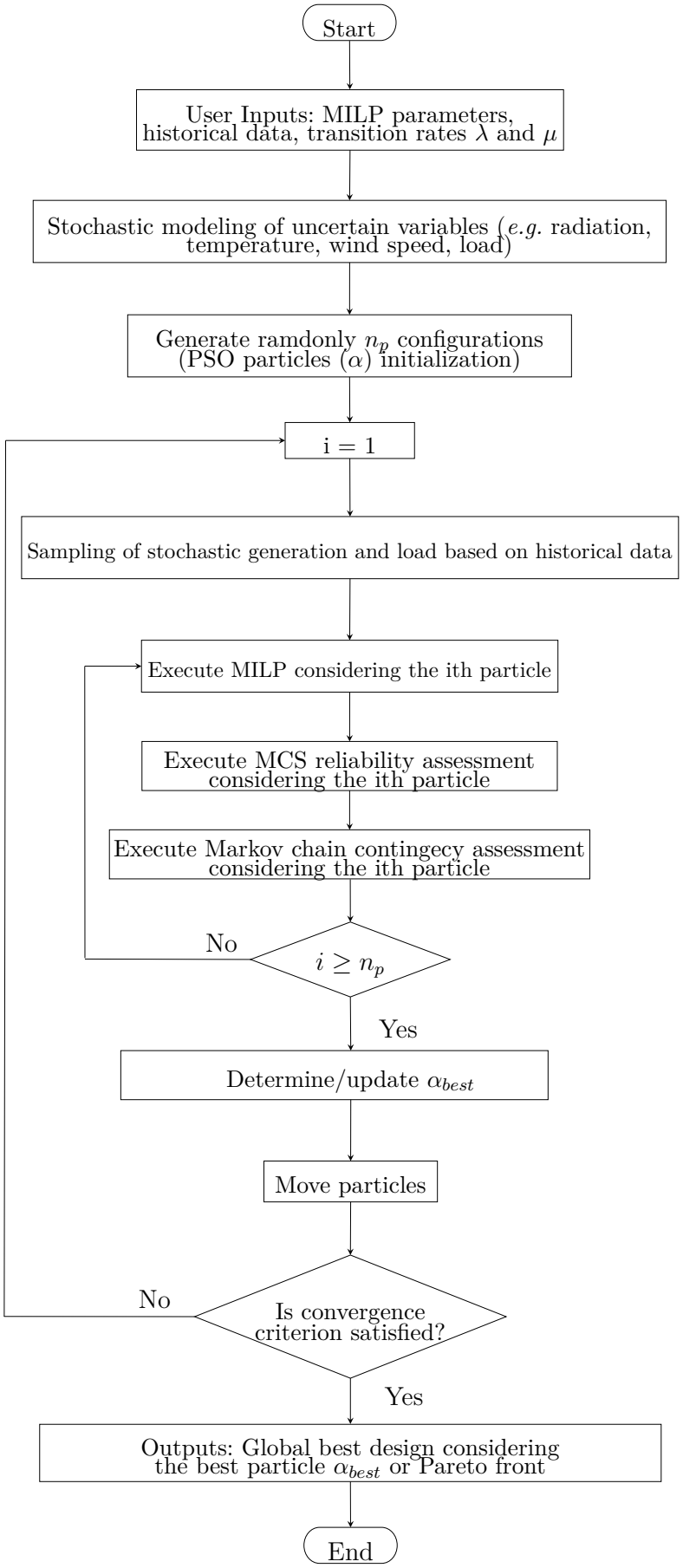

Figure 34 – PSO procedure - framework main program

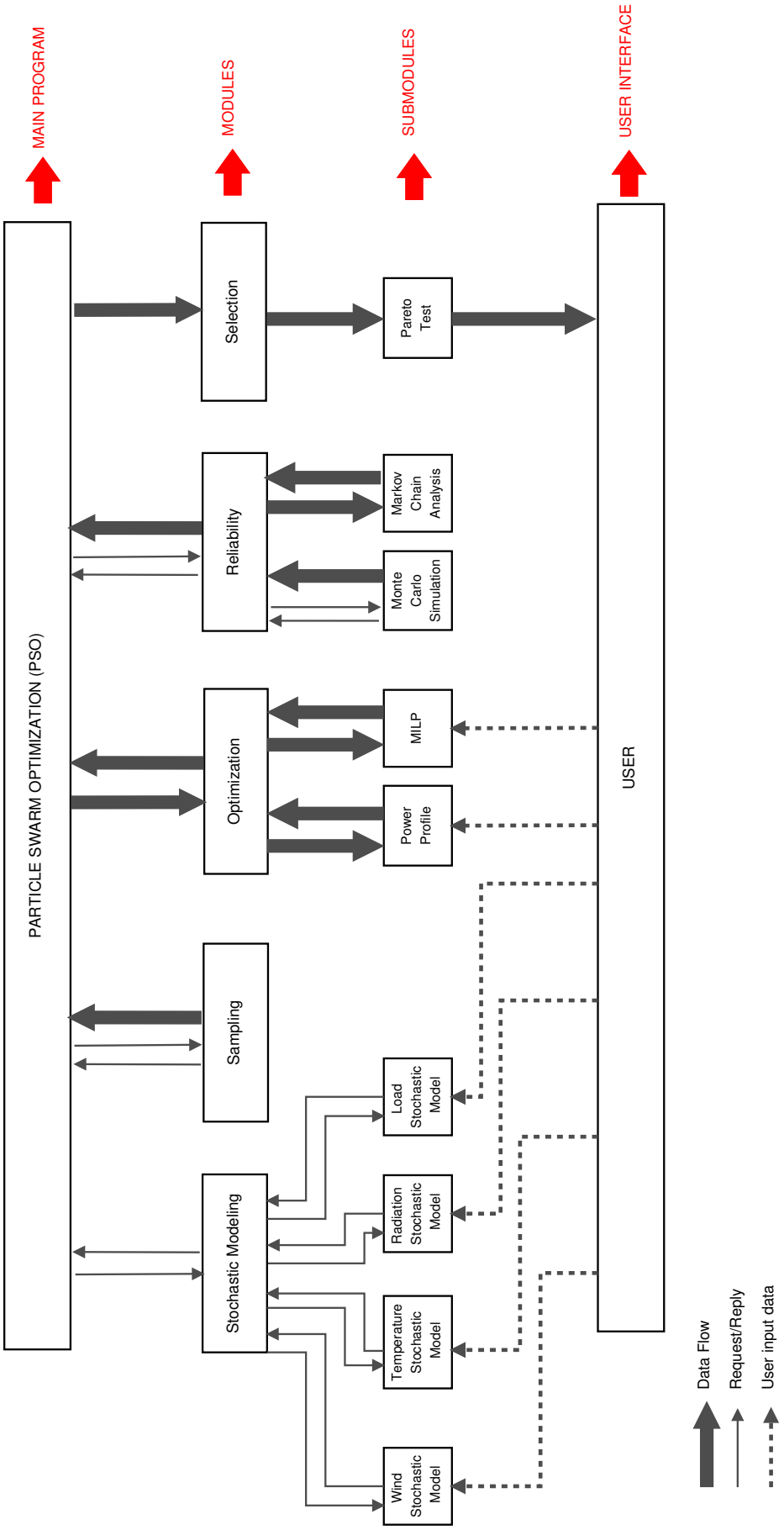

Figure 35 – Framework Software Procedural Design

5 Simulation

The methodology used throughout this study is mainly based on a number of assumptions that each lead to a number of limitations and biased considerations. In this way, the simulation aims to show the results obtained on each step for some considerations. Moreover, the outcomes of complete framework is also demonstrated.

So, following, the simulation outcomes are divided in three main analysis. First, it is presented the results of operation optimization stage, observing the influence of renewable sources penetration and the operational modes of a microgrid (grid-connected and isolated mode). After, it is examined the dependency of failure and repair rates over the distribution power system reliability. Finally, the PSO best microgrid searching is considered in order to complete the global analysis of the framework.

For the proposal of this study, it is assumed a grid-connected IPP-owner microgrid, which is suitable for an university campus - as Federal University of Itajuba (UNIFEI) - allowing the energy trading between microgrid and main network. Thus, two cases are studied. The first one is a base case, where it is presented the results of each stage of the framework. The base case considers a microgrid configured as presented in 3.2 (one wind turbine, one photovoltaic system, an energy storage system, and a set of three diesel generators). The second case studies a specific case of UNIFEI, where the use of wind turbines is not suitable, and the dispatchable generators are already available and installed. So, in the UNIFEI case, only PV generators are considered.

5.1 Case study - base case

5.1.1 Input parameters

It was done an exhaustive investigation in order to have the input parameters for simulation. The database presented in Table 9 is a collection of parameters and costs given in a number of works and reports which are disposed in the bibliography [12, 13, 24, 118–122].

Particularly, for the tariffs, it is considered a specific brazilian electricity charging named *Tarifa Branca*. Table 10 shows the energy tariffs considering the *Tarifa Branca* policy [121, 123] and *Bandeiras Tarifárias* [122] policies.

For simulation, the tariff prices follows the *Green flag* tariffs of class of user *B1* as shown in Table 10. These prices are properly converted to US$ based on the quotation R$ → US$ of the day March 26th of 2018.

Table 9 – Input parameters for simulation

Parameter	**Value**	**Unit**
Peak load	600	kW
Energy storage system capacity	100	kWh
Storage system power	100	kW
Diesel generator 1	200	kW
Diesel generator 2	65	kW
Diesel generator 3	100	kW
Main grid limit	500	kW
Capital Cost PV	4000	$/kW
Capital Cost WT	1882	$/kW
Capital Cost diesel generator	1600	$/kW
Capital Cost storage system (rated power)	423	$/kW
Capital Cost storage system (capacity)	100	$/kWh
Maintenance cost renewable	0.01	$/kWh
Maintenance cost diesel generator	0.016	$/kWh
Maintenance cost storage system	0.01	$/kWh
Selling price	0.08	$/kWh
Buying price	0.16	$/kWh
Fuel cost	0.76	$/L
CO_2 emission tax	30	$/kg$CO_2$
Fuel emission rate	2.64	$kg/L
Lifetime of DERs	20	years
Investment interest rate	8	%/year

Table 10 – Tariffs in R$/kWh considering the *Tarifa Branca* policy - CEMIG March 26th, 2018

Tariffs (Flags)	**Green flag**	**Yellow flag**	**Red flag (level 1)**	**Red flag (level 2)**
B1 - Residential - Peak	0.96096	0.97096	0.99096	1.01096
B1 - Residential - Intermediate	0.61643	0.62643	0.64643	0.66643
B1 - Residential - Out peak	0.38775	0.40775	0.427775	0.44775
B2 - Rural - Peak	0.70001	0.71001	0.73001	0.75001
B2 - Rural - Intermediate	0.44790	0.45790	0.47790	0.49790
B2 - Rural - Out peak	0.28389	0.29389	0.31389	0.33389
B3 - Other classes - Peak	1.00001	1.01001	1.03001	1.05001
B3 - Other classes - Intermediate	0.63986	0.64986	0.66986	0.68986
B3 - Other classes - Out peak	0.40556	0.41556	0.43556	0.45556

5.1.2 Optimal operation of grid-connected microgrid

Following, it is demonstrated the impacts of renewable source penetration (wind turbine and photovoltaic systems) for a grid-connected microgrid operation. The analysis take into account two indexes - operation daily cost and CO_2 emission.

In an environmental and business point of view, the microgrid with the high penetration of wind turbine seems to be the best solution, since with the increasing of such

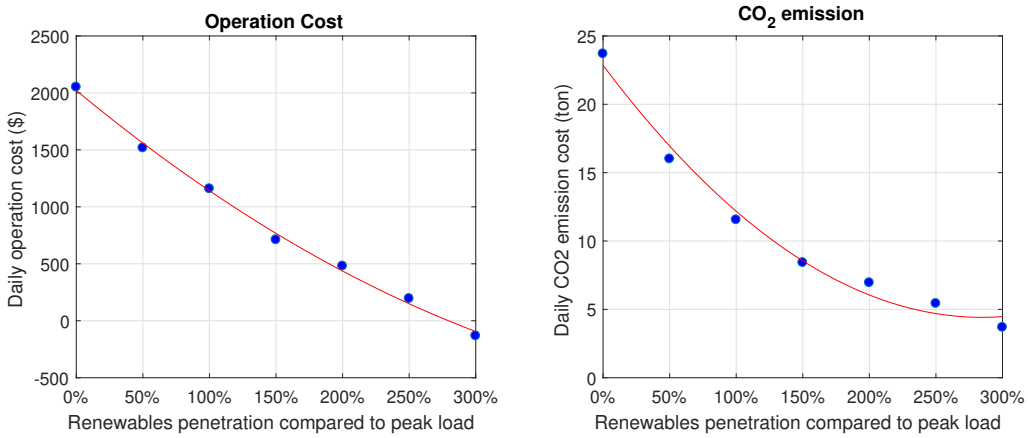

Figure 36 – Analysis of renewable penetration considering daily cost and emission of microgrid operation considering only WT

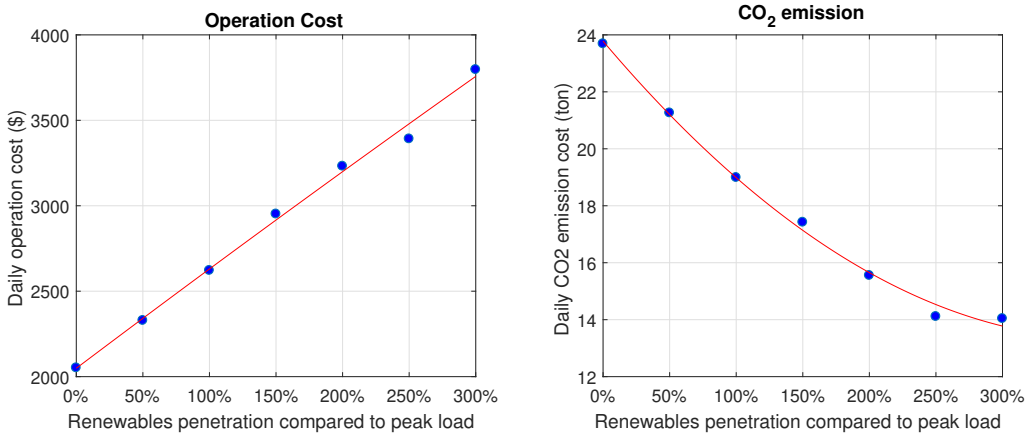

Figure 37 – Analysis of renewable penetration considering daily cost and emission of microgrid operation considering only PV

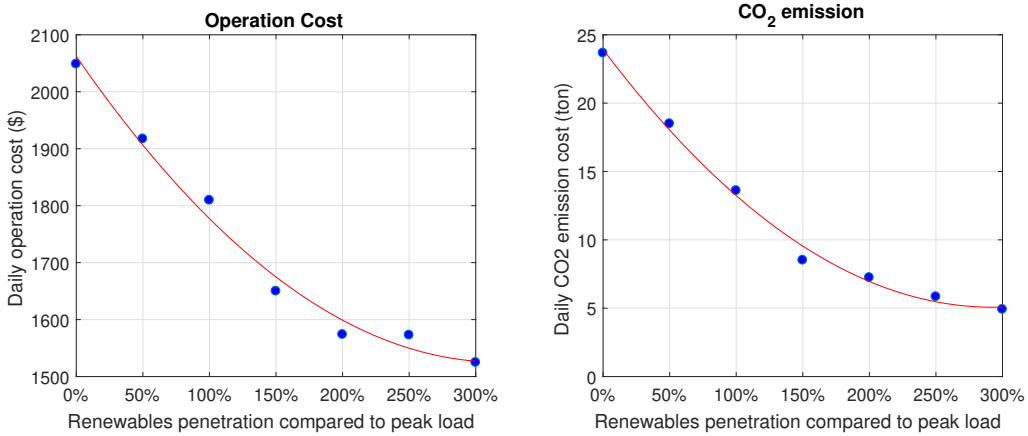

Figure 38 – Analysis of renewable penetration considering daily cost and emission of microgrid operation considering equal penetration of PV and WT generation

technology the CO_2 emission decreases significantly and operation cost becomes negative when the WT penetration is about 300% (refer to Figure 36). Such behavior is justified by the low capital cost of wind generators.

The solution with just PV generation has a trend of increasing the cost operation with the increasing of solar generation, while emissions decrease. This result can be justified by the higher capital price, its daily generation profile (only on sun period - day-time), and green generation (refer to Figure 37). The combination of these two technologies also indicates a descendant trend, mainly because of the WT (refer to Figure 38). But, in this case the decay is not so sharp as the pure wind system.

To illustrate the impacts of RES penetration on real daily operation, Figure 39, 40, and 41 show the generation scheduling for a summer day with and without renewable sources. One can observe in Figure 39 that load demand is sustained by the upstream grid and storage system during the off-peak period, since the grid tariffs are lower than the diesel generator costs. But, on peak hours, the generators are turned on with the intention of overcome the peak tariffs. Besides that, the scheduling indicates a predictable behavior because of dispatchable generators.

In contrast to this, the system with renewable penetration has an unpredictable behavior which is justified by the RES stochastic nature. Figure 40 and Figure 41 show that the microgrid with renewable sources uses less energy from the main grid and in the case of 150% it can even exports some energy. Once again, it is seem the usage of diesel generators on peak-time stead of grid importation.

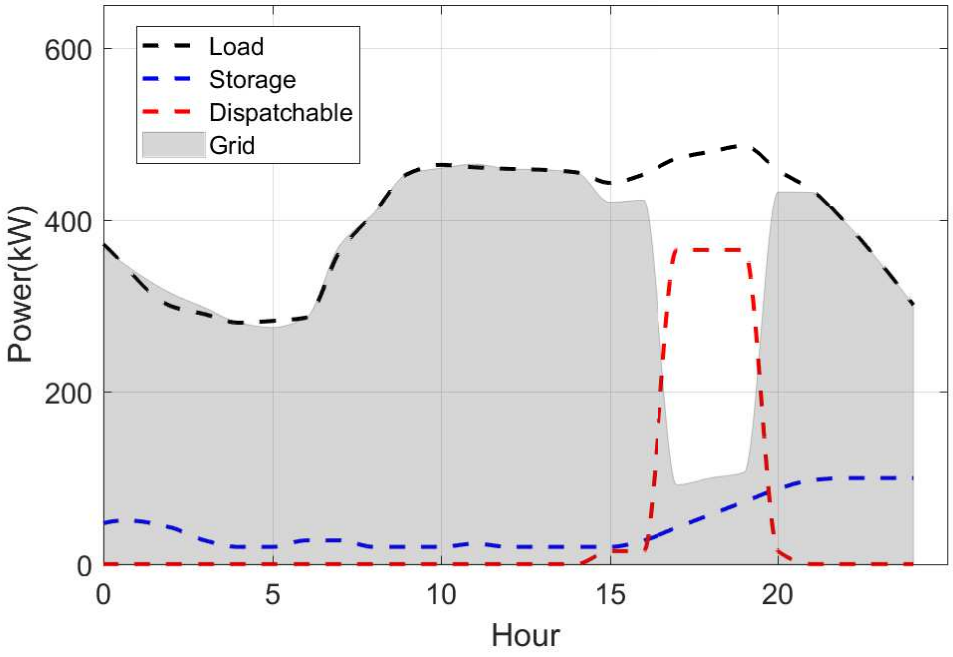

Figure 39 – Electrical power scheduling of the grid-connected microgrid without renewable sources for a summer day

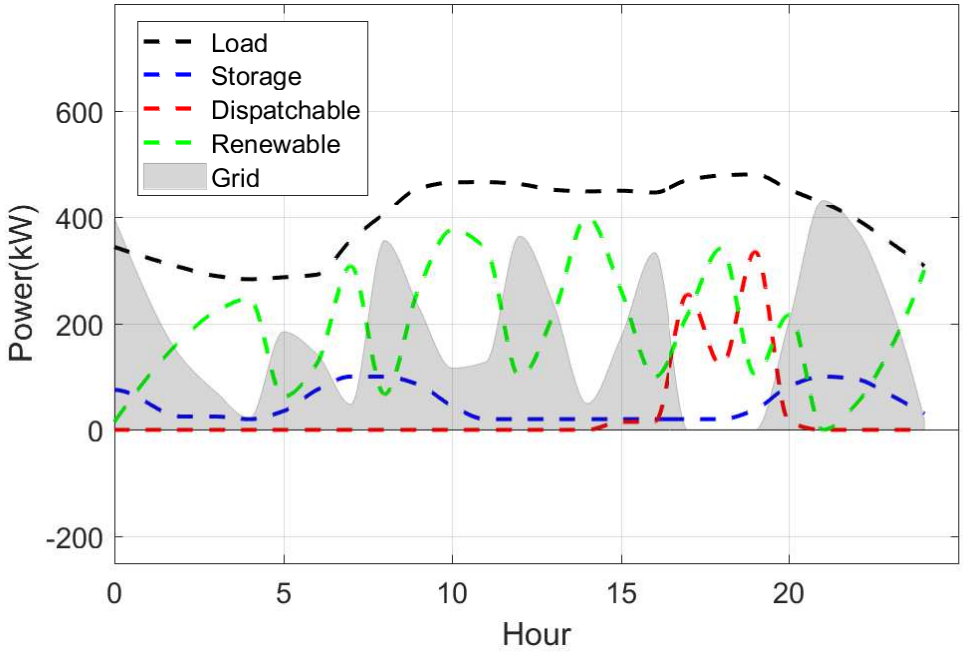

Figure 40 – Electrical power scheduling of the grid-connected microgrid with 100% penetration of renewable sources for a summer day

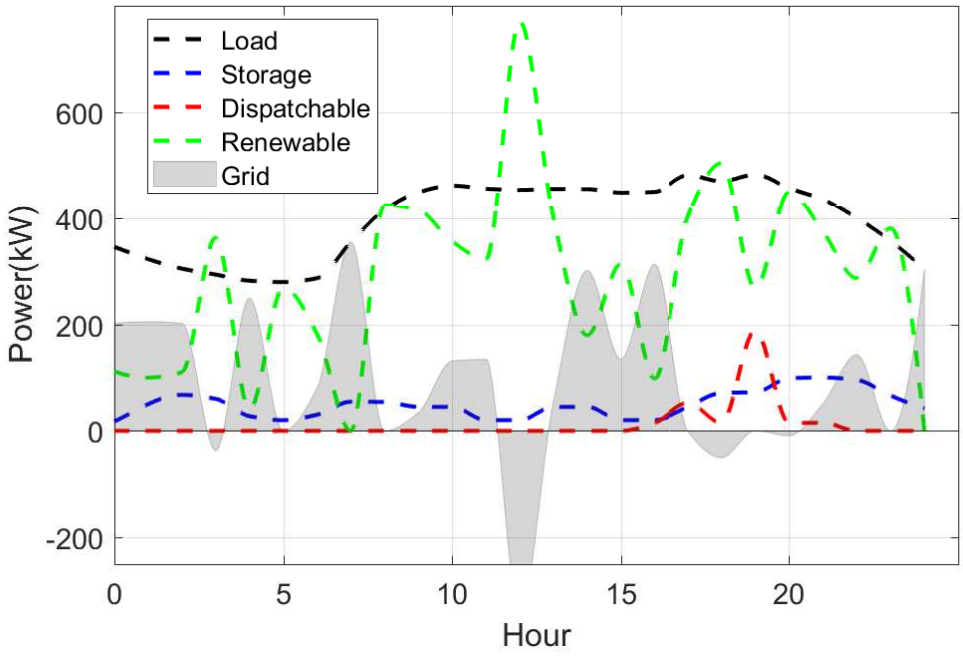

Figure 41 – Electrical power scheduling of the grid-connected microgrid with 150% penetration of renewable sources for a summer day

5.1.3 Optimal operation of isolated microgrid

For the period of microgrid operating in isolated mode, system operators are expected to settle on load shedding decision since there is no support from grid. Such decision

takes into account any or a combination of system security indicator, which can be voltage, current, power balance and frequency restraints [124]. As the suggested framework acts only on strategic plan of microgrid, the power balance is sufficient to characterize the level of security of the system. So, differently from the grid-connected operation, the isolated microgrid needs a proper policy of load shedding in order to maintain this indicator in an appropriate level. For the present work, such policy is the EMS philosophy proposed by the Petri net model shown in 4.1.

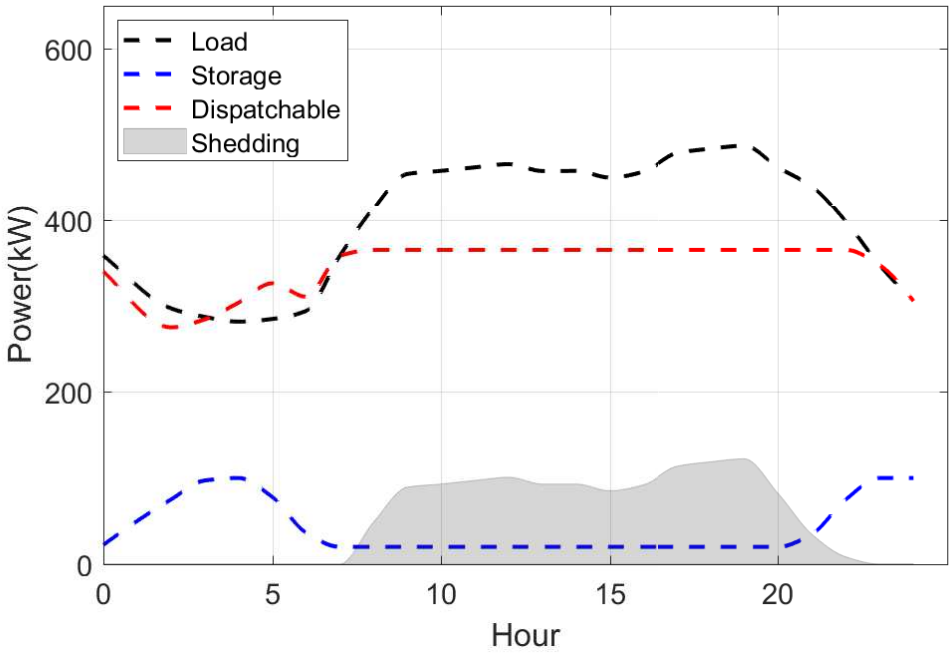

Figure 42 – Electrical power scheduling of the isolated microgrid without renewable sources for a summer day

In the first case, where no renewable energy is considered (refer to Figure 42), the period of load shedding is too large, what is an obvious behavior since there is no grid to support the load demand, particularly at peak hours. In contrast, the second case (refer to Figure 43) where exists the support of renewable sources, the load shedding is just observed in a very short period at the peak hours, since at this time there is low power from the sun and the demand is high. Also, this is an expected result, since in the second scenario there is more generation potential, but, the stochastic behavior of RES introduces an unpredictable scheduling.

5.1.4 Results of RES penetration in both grid-connected and isolated mode

To summarize the impacts of renewables penetration, the Table 11, 12, and 13 indicates the trend of inserting this kind of generators. For this analysis, it is assumed the case of a microgrid with equal penetration of WT and PV (half wind and half solar).

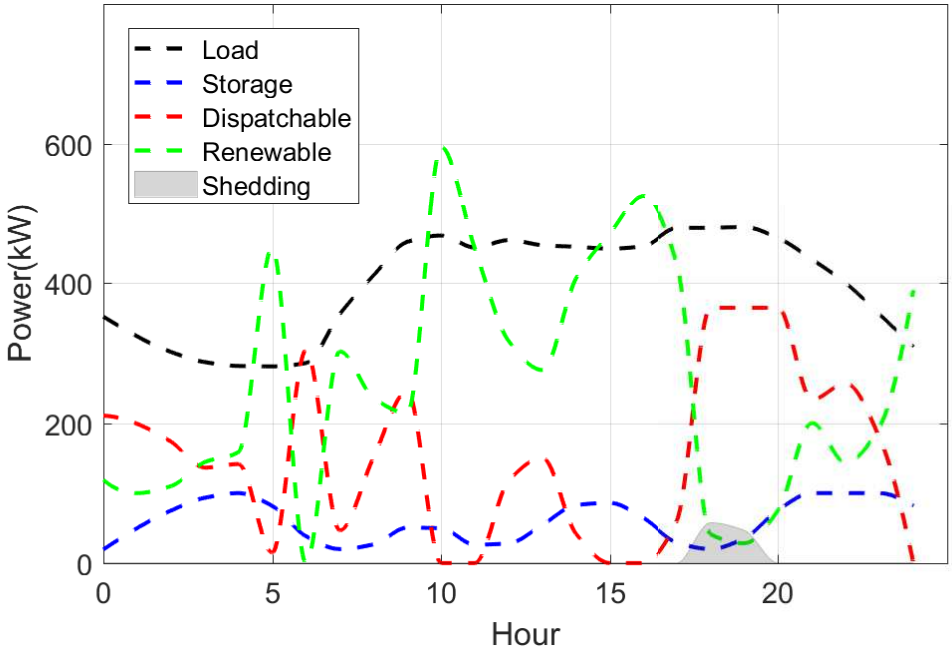

Figure 43 – Electrical power scheduling of the isolated microgrid with 150% renewable sources for a summer day

Table 11 – Microgrid operational daily cost considering tax over CO_2 emission

Mode	**No renewable 0% penetration**	**With renewable 150% penetration**	**With renewable 300% penetration**
Grid-connected	2051.21 $	1686.50 $	1558.52 $
Isolated	10097.01 $	3256.54 $	3558.63 $

Table 12 – Microgrid operational daily cost not considering tax over CO_2 emission

Mode	**No renewable 0% penetration**	**With renewable 150% penetration**	**With renewable 300% penetration**
Grid-connected	1874.70 $	1698.58 $	1393.75 $
Isolated	9712.14 $	2560.06 $	2637.43 $

Table 13 – Microgrid daily CO_2 emission

Mode	**No renewable 0% penetration**	**With renewable 150% penetration**	**With renewable 300% penetration**
Grid-connected	23.67 ton	10.31 ton	5.33 ton
Isolated	20.01 ton	8.96 ton	4.61 ton

As shown in Table 11 and Table 12, the operation cost with grid-connected is significantly smaller than isolated mode. This justifies that the business model where the microgrid is operated by IPP and connected to the main network is the most economically acceptable option. The penetration of renewable energies decreases the operational costs, but as seen in the 150% and 300% penetration, the uncontrolled increase of RESs may

not represent a decrease in costs. Therefore, there is the validity of a study that verifies the optimal insertion of wind and solar generators. Remembering that the percentage of renewable penetration is related to the peak load (*e.g.* 600 kW)

Also, the investigation considers the effects of CO_2 emission. The metrics used to measure such impact was economical (cost with tax), shown in Table 11 and Table 12, and environmental (amount of emitted pollutant) shown in Table 13. It is observed that the increasing of RES represents a decreasing on CO_2, which is an expected result. In fact, it is seen a linear relationship between RES penetration and CO_2 emission.

5.1.5 Reliability assessment

The condition of load shedding is observed only on isolated mode operation. Therefore, the reliability indexes are calculated only when the system is in this condition. The analysis performed for reliability take as basis the results of Monte Carlo simulation (MCS) as proposed in section 4.3.

As presented in Figure 44, 45, and 46, the expected reliability indexes decrease as the insertion of RES increases. But, such results indicate a tendency of stagnation for certain level of penetration (negative exponential tendency), and because of that, an unilateral decision policy can lead to a overestimated microgrid configuration. This conclusion is confirmed analyzing the cases with 250% and 300% of RES penetration.

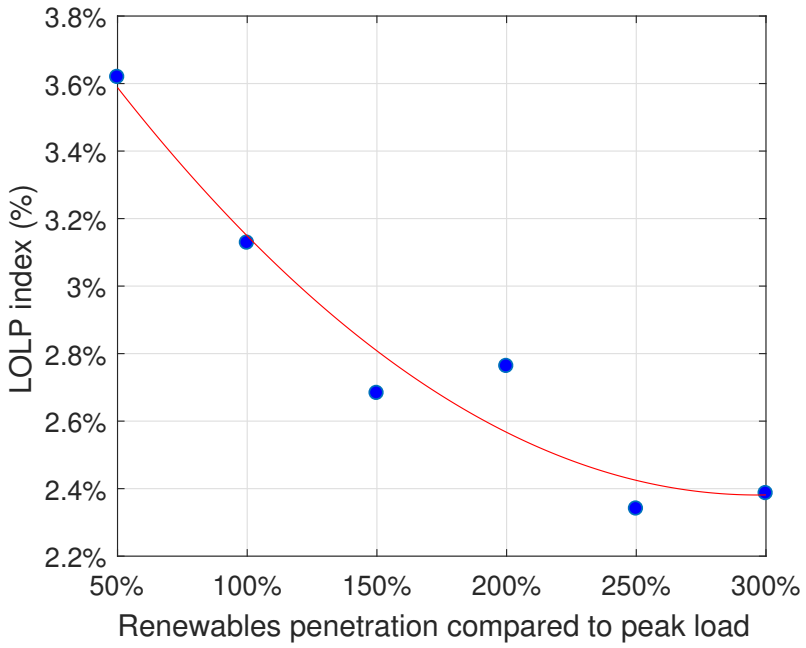

Figure 44 – LOLP index for RES penetration

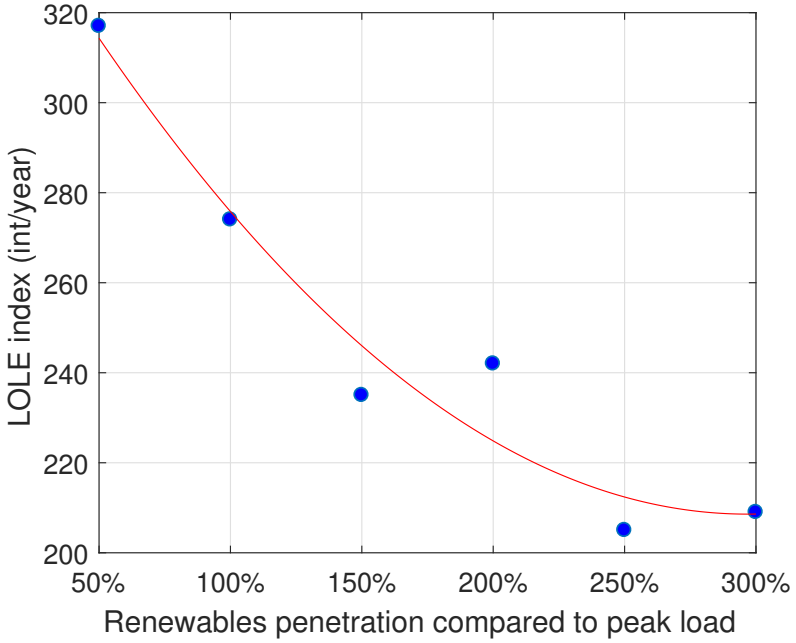

Figure 45 – LOLE index for RES penetration

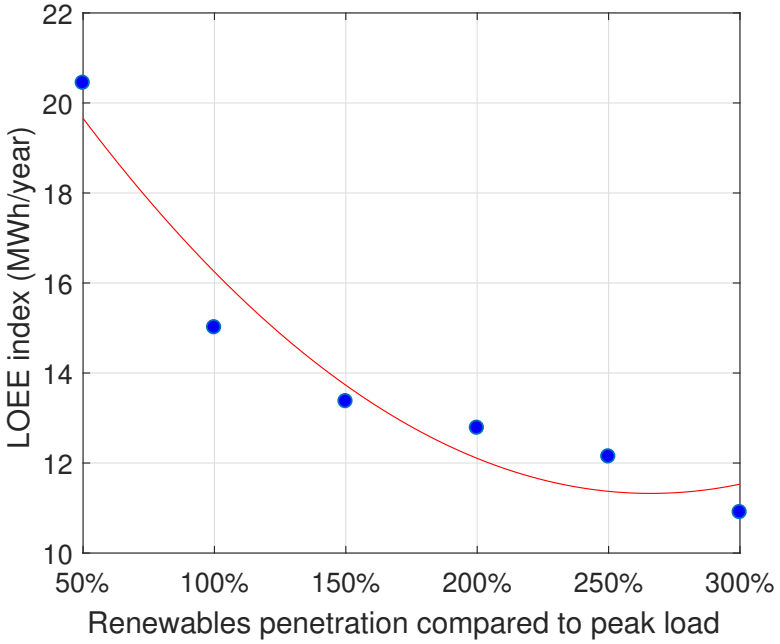

Figure 46 – LOEE index for RES penetration

5.1.6 Contingency assessment

The section above has considered the quality of the power system reliability observing just the isolated microgrid operation. But, since the object of this study is the grid-connected microgrid, then it is necessary to analyze the system as a whole, with all possible operational states. In this way, the contingency analysis is crucial to evaluate the effect that microgrid causes in the power system reliability. Besides, the contingency

assessment explores the effects that rates of failure and repair causes on such system. It is important to remark that the present work considers only operating failures of the main grid and microgrid operating in isolated mode. Therefore, equipment and generator failures are not investigated.

Table 15 and Table 16 depicts the reliability indexes of a traditional power system scenario without the microgrid (refer to Figure 32), and the scenario with the presence of microgrid to support the load demand (refer to Figure 33). Besides, it is also considered the effects that the transition rates of failure/repair of power system causes in such scenarios.

The transition rates can represents typical values of distribution system MTBF and MTTR. For instance, assumes that a typical value to the upstream grid fails is twice a year. Then it comes that the MTBF is 0.5 year. Remembering the relation defined on Markov chain modeling, $\lambda = 1/MTBF$, one can identifies that $\lambda = 2$. For MTTR, the concept is the same. Assumes that the time to repair the network when a extreme event occurs is one day, which represents approximately 0.002739 year, so the relation $\mu = 1/MTTR$ gives a rate of 365. Table 14 illustrates the concept.

For the investigation of the influence of modifying the failure/repair rates, only the transitions connecting *Grid-Connected* state is modified ($\lambda, \mu, \lambda_{1,2}, \mu_{2,1}$), since in the real world the reinforcement of power system is made, usually, on upstream grid (once again, refer to Figure 32 and 33). The other transition rate values are assumed from Table 14. For this investigation, it was considered a microgrid with 150% of renewable penetration related to the peak load, composed by half solar and half wind.

From the results, the distribution network with the incorporation of microgrid has always better outcomes than the traditional model. This is justified by the simple reason that the introduction of microgrid allows the islanding (isolated) operation which supports the demand using the local generators. For MTBF and MTTR values, it is founded the best solution when MTBF is 1 per year, and the MTTR is 12 hours ($\mu, \mu_{2,1} = 730$). This scenario represents the lowest transition rate between normal operation and isolated/contingency operation, and it is the highest rate of repairing. In other words, this scenario has the highest MTBF and the lowest MTTR.

Table 14 – Reliability indexes - typical values for traditional power system

Transition rate	**Typical value**	**Transition rate value**
λ, $\lambda_{1,2}$	1 year	1
$\lambda_{2,3}$	12 hours	730
μ, $\mu_{2,1}$	1 day	365
$\mu_{3,1}$	1 week	52.35
$\mu_{3,2}$	1 hour	8760

Table 15 – Reliability indexes - traditional power system

Transition rate value	**LOLP [%]**	**LOLE [h/yr]**	**LOEE [MWh/yr]**
$\lambda = 1, \mu = 365$	0.273	23.917	10.88
$\lambda = 2, \mu = 365$	0.545	47.738	21.72
$\lambda = 1, \mu = 730$	0.137	11.984	5.46
$\lambda = 2, \mu = 730$	0.272	23.858	10.84
$\lambda = 1, \mu = 182$	0.546	47.869	21.76
$\lambda = 2, \mu = 182$	1.087	95.217	43.34

Table 16 – Reliability indexes - power system incorporating microgrid

Transition rate value	**LOLP [%]**	**LOLE [h/yr]**	**LOEE [MWh/yr]**
$\lambda_{1,2} = 1, \mu_{2,1} = 365$	0.030	2.581	1.19
$\lambda_{1,2} = 2, \mu_{2,1} = 365$	0.059	5.179	2.35
$\lambda_{1,2} = 1, \mu_{2,1} = 730$	0.016	1.372	0.63
$\lambda_{1,2} = 2, \mu_{2,1} = 730$	0.031	2.744	1.23
$\lambda_{1,2} = 1, \mu_{2,1} = 182$	0.053	4.671	2.11
$\lambda_{1,2} = 2, \mu_{2,1} = 182$	0.107	9.335	4.27

5.1.7 PSO best design searching

In order to observe the effects of each aspect identified in the proposed microgrid design, the following section shows the best plan of individual interests of a decision maker. To do so, it is performed the PSO searching process, which is applied in two distinct solvers. The first solver uses the PSO to find a unique best solution, while the second solver uses it to create the feasible region (design space) that will serve to form the Pareto front (set of optimal solutions).

To have a global microgrid design, here, it is also considered that the dispatchable generators (three diesel generators) are also decision variables. So, the space of searching is a 5-dimensional space.

The parameters used on the PSO are a population of 30 particles, inertia weight (w) between 0.4 and 0.9, and the acceleration factors (c_1,c_2) equal to 2. These values assumes some considerations about PSO parameters better discussed in [125]. Also, for the Markov chain analysis, it is assumed the following transition rates: $\lambda_{1,2} = 1$; $\mu_{2,1} = 365$; $\mu_{3,1} = 52.35$; $\mu_{3,2} = 8760$. Rate $\lambda_{2,3}$ comes from the MCS procedure as described on chapter 4.

It was performed a sensibility analysis considering the elapsed time and the number of iteration in relation to the number of particles to choose the appropriate number of particles. As shown in Figure 47, the elapsed time to solve the PSO algorithm is not clearly dependent of the number of particles, since there is no pattern that relates the number of particles and the elapsed time. By the other hand, the number of iteration is reduced when the number of particles increase, as shown in Figure 48. Because of that,

the number of 30 particles seems to be appropriate, since it needs lower elapsed time and lower number of iteration to accomplish the PSO stop criteria.

The complete solution was tested in a Intel Core(TM) i5-3317U CPU @ 1.70GHz PC. The CPU benchmark test indicates a mean time of 24 minutes for each simulation.

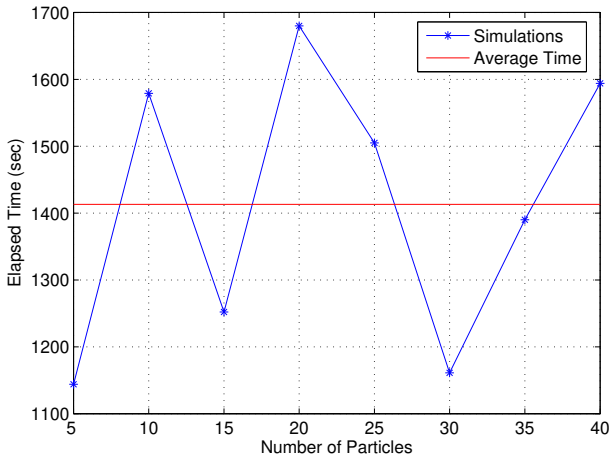

Figure 47 – Sensibility curve of number of particles and elapsed time

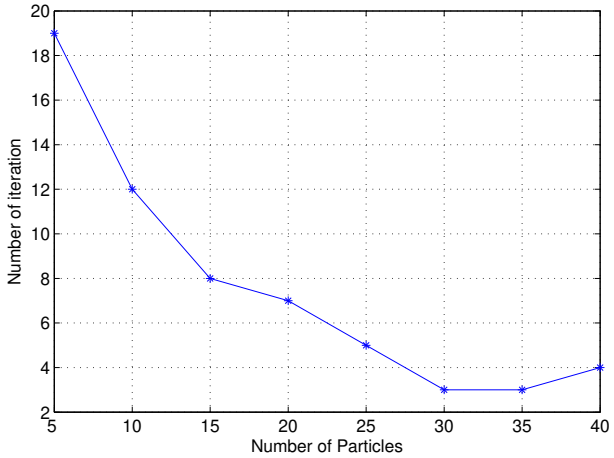

Figure 48 – Sensibility curve of number of particles and number of iteration

The following sensibility analysis indicates if the weighted sum PSO algorithm has proper performance. It was investigated five different scenarios for each decision parameter (cost, emission and unreliability) varying the percentage of one parcel while the others assume an equal distribution. For instance, the scenario in which the weight of cost is 25%, the emission and the unreliability parcels assume 37,5% each. The sensibility of the daily cost varying w_1 is shown in Figure 49. In similar way, the sensibility of the daily emission varying w_2 is shown in Figure 50. Finally, the sensibility of the annual unreliability index varying w_3 is shown in Figure 51

The performance of weighted sum PSO algorithm has presented a proper performance, since the three parameters decreases as the weights (w_1, w_2, and w_3) for given parcel increases. So, the minimization process executed by the PSO is appropriate.

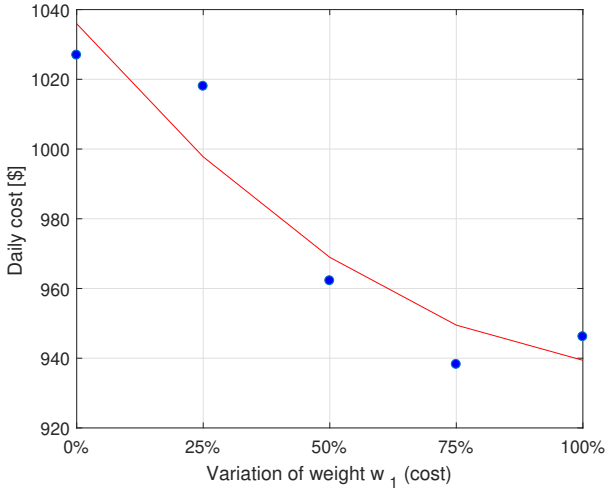

Figure 49 – Sensibility curve of daily cost and the value in percentage of weight w_1 (cost)

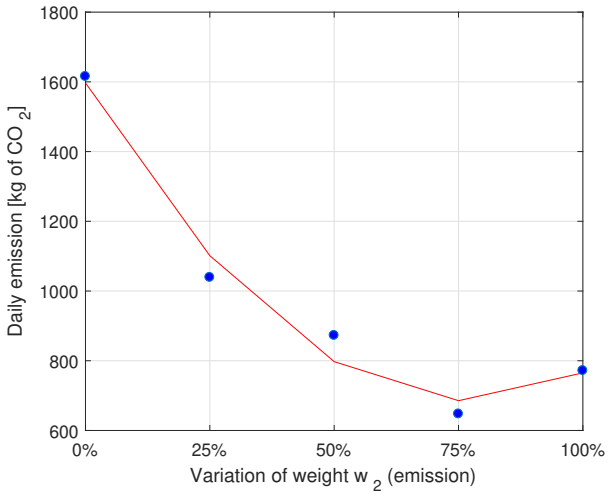

Figure 50 – Sensibility curve of daily emission and the value in percentage of weight w_2 (emission)

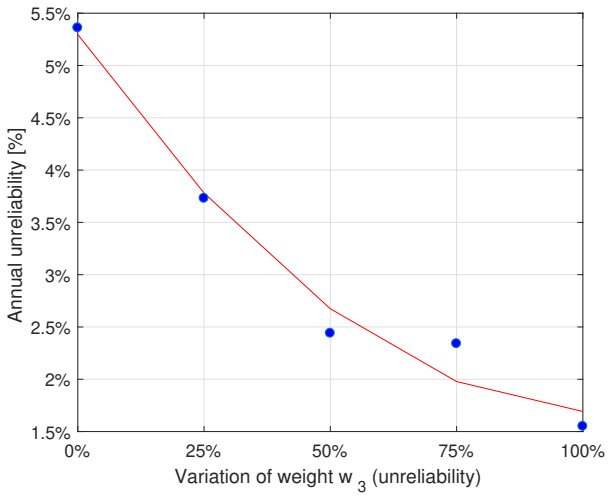

Figure 51 – Sensibility curve of annual unreliability and the value in percentage of weight w_3 (unreliability)

5.1.7.1 PSO - weighted fitness function

For this methodology, the PSO is used to search a unique best solution regarding the weighted fitness function presented in 4.5.1. To have representative solutions, it is assumed weights regarding non-biased and unilateral decisions. The assumptions of each weight and the following best distributed generator combination is shown on Table 17, where w_1, w_2, and w_3 refers to cost, emission, and reliability, respectively. One must note that the first weight division represents the non-biased solution, while the last three indicates an unilateral tendency.

Table 17 – Results for PSO weighted fitness function - best combination of distributed generator

Weights	**Wind Turbine (kW)**	**Photovoltaic (kW)**	**PDG1 (kW)**	**PDG2 (kW)**	**PDG3 (kW)**
$w_1 = 0.33, w_2 = 0.33, w_3 = 0.33$	450	150	117	42	91
$w_1 = 0.8, w_2 = 0.1, w_3 = 0.1$	450	150	117	42	91
$w_1 = 0.1, w_2 = 0.8, w_3 = 0.1$	450	450	146	65	93
$w_1 = 0.1, w_2 = 0.1, w_3 = 0.8$	450	293	200	55	99

Table 18 – Results for PSO weighted fitness function - planning indicators

Weights	**Cost ($)**	**Emission (ton)**	**Unreliability (%)**
$w_1 = 0.33, w_2 = 0.33, w_3 = 0.33$	1759.11	9.63	0.2294
$w_1 = 0.8, w_2 = 0.1, w_3 = 0.1$	1759.11	9.63	0.2294
$w_1 = 0.1, w_2 = 0.8, w_3 = 0.1$	2074.27	8.10	0.1353
$w_1 = 0.1, w_2 = 0.1, w_3 = 0.8$	1981.39	8.81	0.0876

As seen in Table 17, the first two weight distribution returns the same result. This may be explained by a local minima in the problem or a bias in the problem formulation that leads to such result. Ignoring such behavior, one must note that this solution represents the smallest usage of local sources, which means that, for operational cost point of view, it is interesting to use the upstream grid as much as possible. The third weight distribution shows an appropriate response, since the best solution has the maximum usage of renewables sources. Last combination also has an appropriate response for reliability sense, as it is uses the greatest amount of dispatchable sources. Such results are reinforced by the planning indicators shown in Table 18.

5.1.7.2 PSO - Pareto front

It is used the a intuitive method of Pareto frontier [126] to find the best solution. Once again, it is important to be clear that the optimal solution will depend on the interest of the decision maker.

To demonstrate such subjective solution, it is suggested four distinct decision policies. The three first policies indicates an unilateral decision (cost, emission or reliability)

while the fourth presents a specific policy, which takes into account the concept of using the most sun energy as possible. Such strategy makes completely sense in brazilian IPP-owner microgrids, since the government has already approved some incentives to this technology, as demonstrated by the governmental program "Programa de Desenvolvimento da Geração Distribuída de Energia Elétrica (ProGD)".

1. best solution regarding the lowest daily operational cost;
2. best solution regarding the lowest daily CO_2 emission;
3. best solution regarding the lowest yearly reliability;
4. best solution regarding the lowest usage of wind turbine and highest usage of photovoltaic systems;

Table 19 – Results for Pareto front - best combination of distributed generator

Policy	**Wind Turbine (kW)**	**Photovoltaic (kW)**	**PDG1 (kW)**	**PDG2 (kW)**	**PDG3 (kW)**
Policy 1	450	150	200	24	100
Policy 2	450	450	200	65	100
Policy 3	450	450	200	65	100
Policy 4	406	221	189	35	100

Table 20 – Results for Pareto front - planning indicators

Policies	**Cost ($)**	**Emission (ton)**	**Unreliability (%)**
Policy 1	1873.27	10.12	0.1529
Policy 2	2098.11	7.15	0.0755
Policy 3	2112.33	7.62	0.0717
Policy 4	1979.06	10.94	0.1441

The best solution regarding each decision policy is shown in Table 19 and Table 20. As demonstrated in the results, the optimal responses are appropriate. Policies 1, 2, and 3, which represents unilateral decisions, indicates a combination of distributed generators with the lowest operational cost, CO_2 emission, and reliability index, respectively. Policy 4, which represents a more specific condition, also indicates a proper solution, since this is the only response in which the value of the wind turbine is not 450 kW. This value of WT rated power is often seen in the solutions because of its installation price and wind availability.

5.1.7.3 Comparison between weighted function and Pareto front

Observing the results for the proposed optimal decision, both search mechanisms work properly, but there is some variation between then.

For the unilateral tendency, it is possible to assess that there is some differences between the best combination of distributed generators and planning indicators. This is justified because the weighted PSO tries to find a unique solution, while the Pareto front tries to find representative points. Also, the former methodology intend to optimize the problem in a biased way, whereas the latest ignores the best global solution to the detriment of searching for a solution that does not hurt one aspect while improving the other.

The graphs shown below, indicates the similarity between this two techniques. Costs and emission have almost the same pattern, as shown in Figure 52 and Figure 53 respectively, while the reliability presents certain deviation (refer to Figure 54). Thus, the reliability indexes are more sensible than the other aspects, considering these two techniques. A more detailed and specific study over the proposed techniques must be developed in order to identify pros and cons of each solution. However, this is not the main focus of the present work.

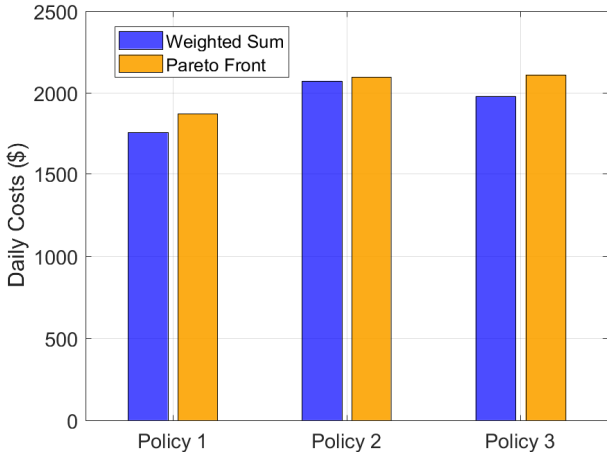

Figure 52 – Comparison between weighted sum and Pareto front techniques - daily operational costs

Regarding the performance, although both strategies have good answers, in case of multi-lateral or more specific decision policies the Pareto front presents more fair responses. For this reason, the following analysis and case of study uses the Pareto front as the PSO solver mechanism.

5.2 Case study - UNIFEI campus Itajubá

The usage of wind turbine for the UNIFEI campus is not convenient since it would be necessary to develop a completely new distribution network to support such power generation technology. In addition, the campus does not have an useful area for the installation of these generators. In contrast to this, the use of photovoltaic panels is

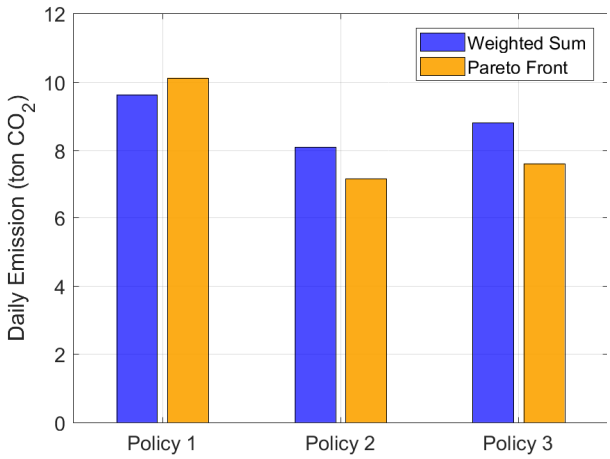

Figure 53 – Comparison between weighted sum and Pareto front techniques - daily CO_2 emission

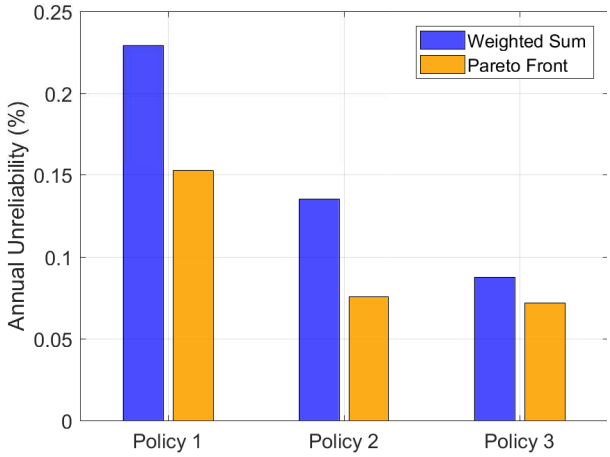

Figure 54 – Comparison between weighted sum and Pareto front techniques - annual unreliability

entirely justifiable, since the roofs of buildings represent a significant area where rooftop panels can be installed.

Thus, the configuration of the microgrid considered for this case of study is slightly different of the base case. It is still a grid-connected microgrid composed by a set of three different diesel generators, which is considered already installed and available. However, the wind generator is no longer available. Renewable sources are represented only by rooftop photovoltaic panels. The microgrid also has an energy storage system, exactly as the base case.

For the UNIFEI case, the power scheduling is presented in Figure 55. As seem in this figure, the renewable source impacts mainly the day period. It is a completly reasonable answer, since it is considered only PV generators. Once again, the dispatchable source play a significant role in the peak hour.

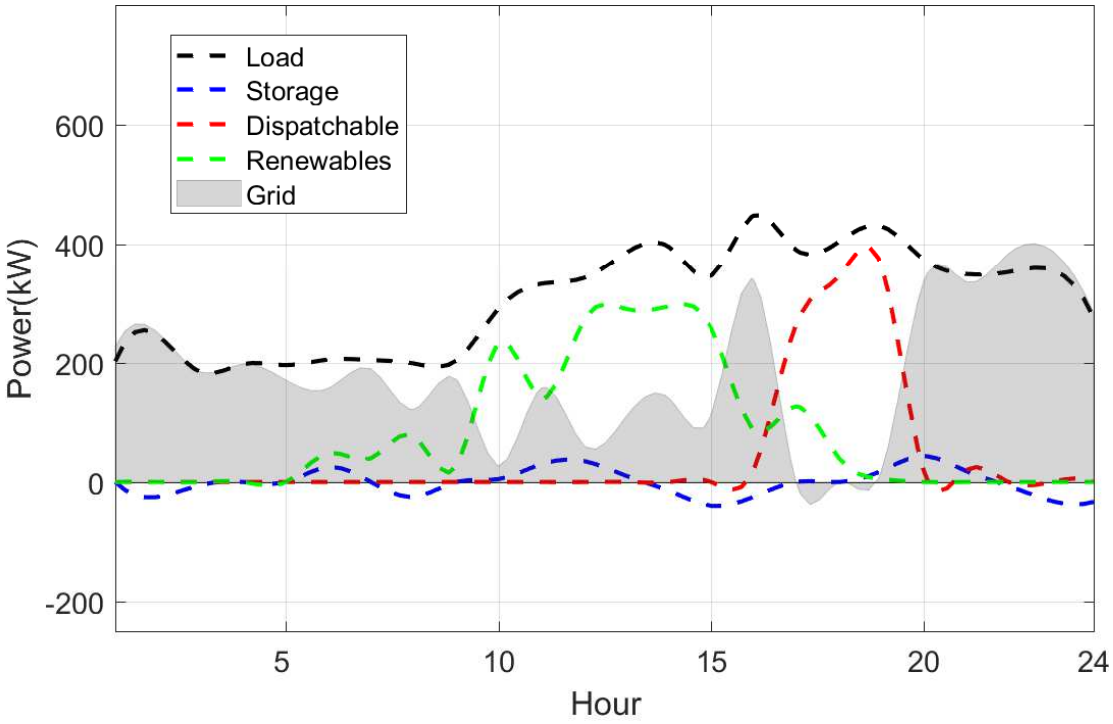

Figure 55 – Electrical power scheduling of grid-connected microgrid with best PV set for a week day in the period of classes - UNIFEI case

5.3 Benchmarking analysis

In order to validate the proposed framework, it was promoted a benchmarking analysis comparing the PSO with the DER-CAM. Thus, Figure 56 and Figure 57 identify the similarity between the Pareto front created using the DER-CAM and the proposed framework solution. As shown, the curves have similar trend, including points with almost the same value. Essentially, the difference between them is because the DER-CAM uses ε-constrained method [127]. Such method optimizes one of the objective functions using the other objective functions as constraints, incorporating them in the constraint part of the model. In each iteration, the ε changes, also changing the constraints. That is why the points of DER-CAM curve seems regularly distributed. In contrast to this, the PSO has a random distribution, which is typical of a meta-heuristic approach.

Numerically, the generational distance (GD) is an appropriate method to assess the difference between two Pareto curves. In this way, the following analysis indicates the sensibility of GD considering the number of particle considered in the PSO.

5.3.1 Performance metrics - Generational distance (GD)

In order to give a numerical comparison between DER-CAM and the proposed framework, it is adopted a useful metric named generational distance (GD) [128, 129]. Generational distance is a way of estimating how far are the elements in the Pareto front

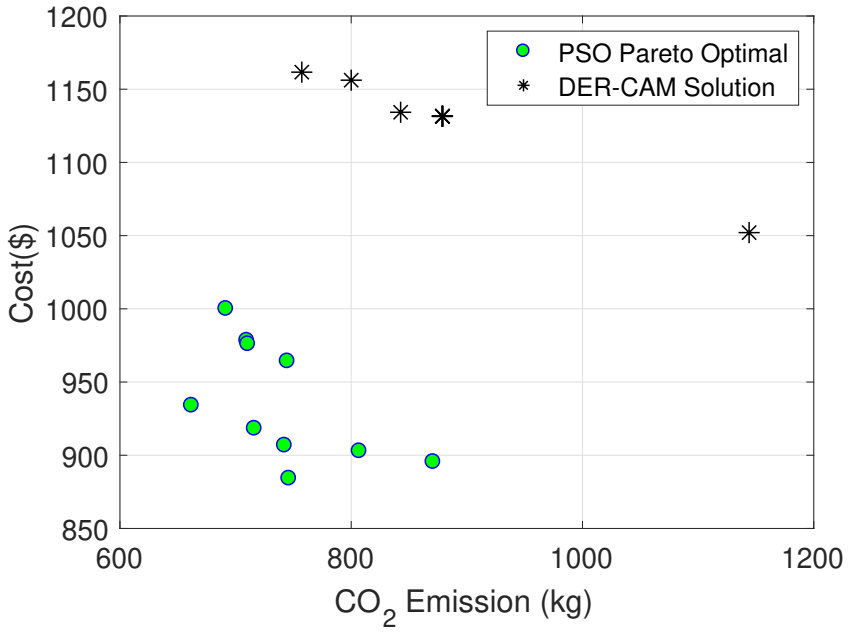

Figure 56 – Benchmarking analysis - comparison between the proposed PSO and DER-CAM considering the Pareto front for base case

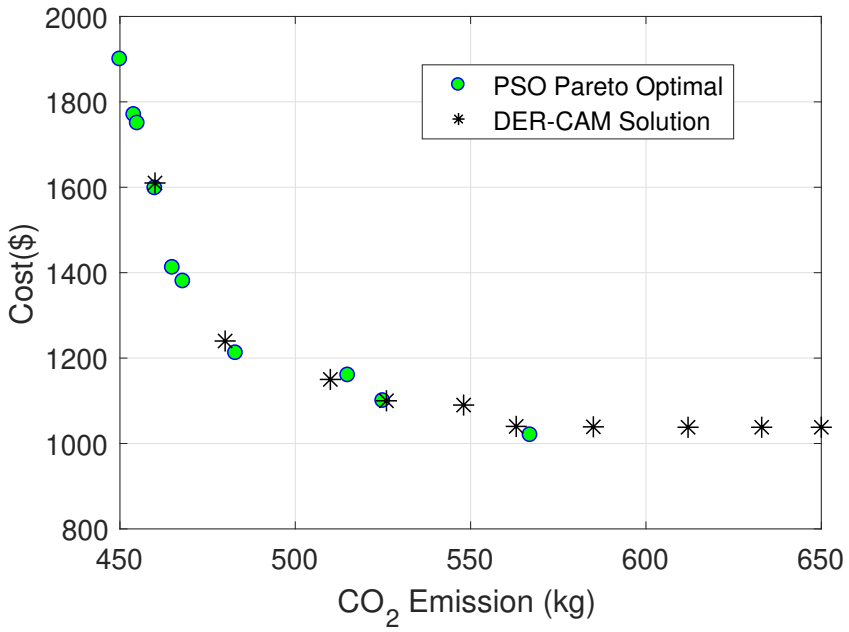

Figure 57 – Benchmarking analysis - comparison between the proposed PSO and DER-CAM considering the Pareto front for UNIFEI case

produced by a test algorithm (PSO solution) from those in the Pareto optimal set (DER-CAM solution). In other words, the GD procedure calculates the distance between the PSO curve to the DER-CAM curve. The description and mathematical representation of this metric is shown below in (5.1).

$$GD = \frac{\sqrt{\sum_{i=1}^{n} d_i^2}}{n} \tag{5.1}$$

where n is the number of non-dominated vectors found by the algorithm being analyzed (PSO solution) and d_i is the Euclidean distance (measured in criterion space) between each of these and the nearest member of the true Pareto front (DER-CAM solution). It should be clear that a value of $GD = 0$ indicates that all the elements generated are in the true Pareto front of the problem. Therefore, any other value will indicate how "far" the proposed solution is from the true Pareto front. Figure 58 illustrates the GD concept.

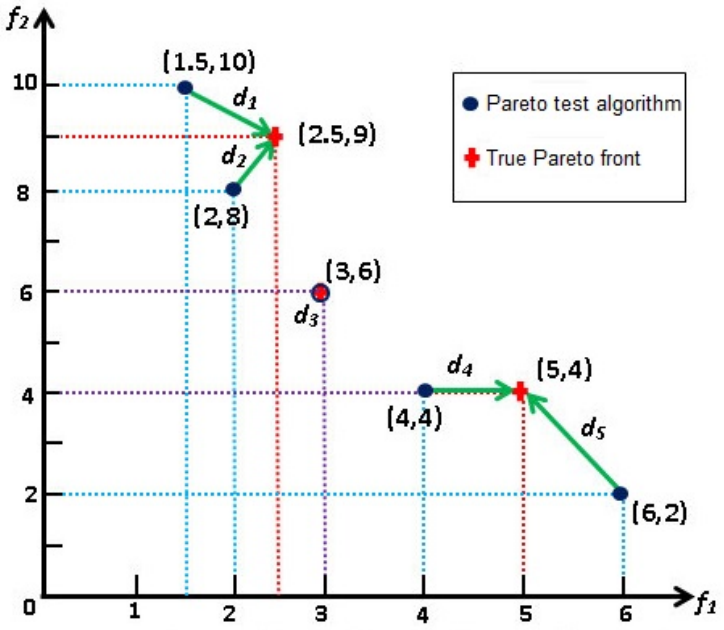

Figure 58 – Example illustration of the generational distance (GD) metric (adapted from [130])

Thus, applying the GD performance metrics in the results of benchmark analysis presented in Figure 56 and Figure 57, the GD index are calculated and exposed as shown in Table 21.

Table 21 – Performance metrics - Generational distance (GD)

Case of Study	**GD index**
Case base	230.28
Case UNIFEI	134.45

Table 22 – Benchmark analysis of DER-CAM and PSO Pareto front - case base

Approaches	**Wind Turbine (kW)**	**Photovoltaic (kW)**	**PDG1 (kW)**	**PDG2 (kW)**	**PDG3 (kW)**
DER-CAM	450	150	20	30	100
PSO	450	224	53	86	127

The GD index for case base and case UNIFEI indicates that the distance between DER-CAM and the proposed framework is quite significant. In fact, the difference of

Table 23 – Benchmark analysis of DER-CAM and PSO Pareto front - case UNIFEI

Approaches	**Wind Turbine (kW)**	**Photovoltaic (kW)**	**PDG1 (kW)**	**PDG2 (kW)**	**PDG3 (kW)**
DER-CAM	0	770	0	0	0
PSO	0	569	0	0	0

DER-CAM and the PSO in the case base is graphically notorious. In the case UNIFEI, the answer in both strategies has almost the same pattern, although exists significant difference in the most extreme points. Such difference is justified because the implementation of the multi-criteria solver is completely distinct. Also, the MILP formula implemented in the present framework is a bit more general than the applied in the DER-CAM. The solution for the best microgrid design has also significant difference as shown in Table 22 and Table 23.

For proper comparison, it is necessary some modifications in the MILP formula in order to reproduce, exactly, the behavior presented in DER-CAM. Thus, the benchmark analysis is relevant in the sense of indicating the coherence of the proposed framework, but it is not completely fair to indicate which of the solutions is ideal, as the methodology of the DER-CAM and the proposed PSO approach are quite distinct.

6 Conclusion

This thesis focused on developing a multidisciplinary optimal planning of grid-connected microgrid systems under uncertainty and multi-criteria decision. In this way, it was intended to provide a framework with a full package of suitable tools to deal with such problem.

In reference to microgrid planning, there has been much research which mention about the uncertainty in the resources, but no models have incorporated the uncertainty explicitly into the model. The proposed framework addresses the issue of uncertainty in the resources modeling the parameters and considering them explicitly into the model.

Attending a more sustainable approach, the planning process developed in this work considers, at the same time, environmental, economical, and technical aspects, which means a multi-lateral decision.

In this way, the main contribution of this thesis was to present a set of tools suitable for the treatment of microgrid planning problem, more specifically, for the case of hybrid renewable generation at a prosumer connecting point. The implementation of this procedure conduces to results that shows substantial reduction in costs, emission and unreliability indexes of the distribution power system when considering the insertion of microgrids based on RES generation.

The results also indicates that a hybrid microgrid composed by distinct generators (dispatchable and renewable sources) allows a flexible solution. Such flexibility is suitable for a decision process with divergent stakeholders.

From that, it is possible to say that such framework provides greater security in the decision-making process.

6.1 Implementation and Results Discussion

The modular approach that was used to build the Matlab program allows decouple the subproblems in many parts as necessary. Thus, each problem (stochastic modeling, sampling, mixed integer programming optimization, reliability and PSO algorithm) can be treated separately and independently without any harm.

The results indicates adequate answers. The sensibility analysis of RES penetration indicates that the wind turbine seems to be an appropriate solution considering both cost and emission. The PV penetration indicates a positive effect in reducing CO_2 emission, however, its initial investment costs returns an increase in operational daily costs.

In conclusion to this, the combination of PV and wind turbine seems to be a proper arrangement.

Even if there are positive impacts with RES penetration, the unpredictability due to their stochastic behavior, continues to be a challenge. In the proposed framework, the stochasticity of such sources was properly managed using stochastic modeling and appropriate sampling. This strategy guarantees convenient answers.

In similar way, the reliability and contingency analysis have used Monte Carlo Simulation and Markov chain as tools to solve the reliability issues. The analysis over these two techniques indicates that both tools are also appropriate to deal with the probabilistic scenarios caused by the RES penetration.

As main program, the PSO algorithm is quite efficient in returning the best microgrid design. Also, the Pareto front approach has presented as better strategy than the weighted sum, since the latter one does not produces flexible multi-lateral answers.

Comparing the proposed framework with DER-CAM (benchmark platform) it was observed significant difference between them, especially in the base case, where it was considered five types of generators. Such difference is justified by the fact that the MILP formulation and the way to solve the multi-criteria problem are quite different. Besides that, DER-CAM does not consider the reliability explicitly in the multi-criteria formula. The second case, where it was used only the size of PV as decision variable, the answer in the DER-CAM has certain similarity with the answer given by the proposed framework.

To have a more fair comparison, it is necessary to implement exactly the MILP formula presented in DER-CAM and ignore the reliability part of the multi-criteria formulation. A more accurate comparison is offered as a further work.

6.2 Further studies and investigations

As suggested, this thesis is an effort in constructing a multidisciplinary arrange capable to treat the microgrid planning in a more sustainable way. Since this is the initial step of a possible commercial software, the framework needs a polished investigation in some parts.

In technical aspects, the proposed framework has eyes only for the planning stage of microgrid implementation. In this way, the approach makes some assumptions to reduce the complexity of the problem. For instance, the real-time control and protection of the microgrid are not considered, which means a complete off-line solution. Also, in the present work it was only used the energy balance as security operation parameter. A more complete solution must also consider frequency and voltage. As further work, the framework will properly treat the voltage and frequency security parameters incorpo-

rating appropriate power flow analysis. Computationally, the PSO and the Monte Carlo simulation algorithms must be investigated in order to get improvements in simulation time. The potentials of Petri net modeling should also be explored, in order to develop generic models of energy management for different stakeholders.

In terms of sustainability, more accurate models for CO_2 emission, energy tariffs policy, society participation and global political guidelines must be discussed and introduced to the framework. To implement such aspects, it is necessary to create a multidisciplinary research group, which is one of the most interesting points that the this thesis has revealed.

As a last consideration, the present work has tried to promote a more sustainable and flexible solution for microgrid planning. It can be said that this objective has been achieved, although future improvements are necessary.

Bibliography

1 HARTONO, B.; SETIABUDY, R. et al. Review of microgrid technology. In: IEEE. *QiR (Quality in Research), 2013 International Conference on*. [S.l.], 2013. p. 127–132. 22

2 PARHIZI, S. et al. State of the art in research on microgrids: A review. *Ieee Access*, v. 3, n. 1, p. 890–925, 2015. 22

3 TAO, L. et al. From laboratory microgrid to real markets. *ICPE (ISPE)*, p. 264–271, 2011. 22

4 BRUINENBERG, J. et al. Cen-cenelec-etsi smart grid coordination group smart grid reference architecture. *CEN, CENELEC, ETSI, Tech. Rep*, 2012. 23, 24

5 NIST FRAMEWORK. Roadmap for smart grid interoperability standards. *National Institute of Standards and Technology*, 2010. 23

6 CS-SGVP: Computer Society - Smart Grid Vision Project. *Smart Grid Research: Computing - IEEE Smart Grid Vision for Computing: 2030 and Beyond*. [S.l.]: IEEE, 2013. ISBN 978-0-7381-8382-4. 23

7 ANNASWAMY, A. M.; AMIN, M. *Smart Grid Research: Control Systems - IEEE Vision for Smart Grid Controls: 2030 and Beyond*. [S.l.]: IEEE, 2013. ISBN 978-0-7381-8458-6. 23

8 TAIBER, J. et al. *Smart Grid Research: Vehicular - IEEE Smart Grid Vision for Vehicular Technology: 2030 and Beyond*. [S.l.]: IEEE, 2014. ISBN 978-0-7381-8835-5. 23

9 LU, D. et al. Application of petri nets for the energy management of a photovoltaic based power station including storage units. *Renewable energy*, Elsevier, v. 35, n. 6, p. 1117–1124, 2010. 24, 34

10 JUNG, J.; VILLARAN, M. Optimal planning and design of hybrid renewable energy systems for microgrids. *Renewable and Sustainable Energy Reviews*, Elsevier, v. 75, p. 180–191, 2017. 24, 30

11 KAVIANI, A. K.; RIAHY, G.; KOUHSARI, S. M. Optimal design of a reliable hydrogen-based stand-alone wind/pv generating system, considering component outages. *Renewable energy*, Elsevier, v. 34, n. 11, p. 2380–2390, 2009. 24, 30, 56

12 MIZANI, S.; YAZDANI, A. Optimal design and operation of a grid-connected microgrid. In: IEEE. *Electrical Power & Energy Conference (EPEC), 2009 IEEE*. [S.l.], 2009. p. 1–6. 24, 30, 89

13 QUASHIE, M.; BOUFFARD, F.; JOÓS, G. Business cases for isolated and grid connected microgrids: Methodology and applications. *Applied Energy*, Elsevier, v. 205, p. 105–115, 2017. 24, 30, 32, 89

14 BAHRAMIRAD, S.; REDER, W.; KHODAEI, A. Reliability-constrained optimal sizing of energy storage system in a microgrid. *IEEE Transactions on Smart Grid*, IEEE, v. 3, n. 4, p. 2056–2062, 2012. 24, 30

15 LIU, X. et al. Microgrids for enhancing the power grid resilience in extreme conditions. *IEEE Transactions on Smart Grid*, IEEE, v. 8, n. 2, p. 589–597, 2017. 24, 30, 33

16 BERKELEY LAB. *Distributed Energy Resources Customer Adoption Model - DER-CAM*. 2018. <https://building-microgrid.lbl.gov/projects/der-cam>. Online; accessed 17 October 2018. 25

17 HOMER ENERGY. *The HOMER Pro microgrid software by HOMER Energy*. 2018. <https://www.homerenergy.com/>. Online; accessed 17 October 2018. 25

18 SIDDIQUI, A. S. et al. Distributed generation with heat recovery and storage. *Journal of Energy Engineering*, American Society of Civil Engineers, v. 133, n. 3, p. 181–210, 2007. 25

19 MARNAY, C. et al. Optimal technology selection and operation of commercial-building microgrids. *IEEE Transactions on Power Systems*, IEEE, v. 23, n. 3, p. 975–982, 2008. 25

20 LOTFI, H.; KHODAEI, A. Ac versus dc microgrid planning. *IEEE Transactions on Smart Grid*, IEEE, v. 8, n. 1, p. 296–304, 2017. 27, 61

21 STŘELEC, M.; MACEK, K.; ABATE, A. Modeling and simulation of a microgrid as a stochastic hybrid system. In: IEEE. *Innovative Smart Grid Technologies (ISGT Europe), 2012 3rd IEEE PES International Conference and Exhibition on*. [S.l.], 2012. p. 1–9. 27, 30, 35, 38

22 MOREMICROGRIDS - U-Cluster "Integration of RES + DG" MICROGRIDS - part of the European Research Project Cluster "Integration of RES + DG" of the EU projects SUSTELNET, DGNET, INVESTIRE, DISPOWER, CRISP and DGFACTS. 2008. <http://www.microgrids.eu/index.php>. Online; accessed 03 April 2018. 29

23 KRKOLEVA, A. et al. Social aspects of wider microgrids deployment. IET, 2010. 29

24 WU, X.; WANG, X.; QU, C. A hierarchical framework for generation scheduling of microgrids. *IEEE Transactions on Power Delivery*, IEEE, v. 29, n. 6, p. 2448–2457, 2014. 29, 89

25 SOARES, J. et al. Multi-objective robust optimization to solve energy scheduling in buildings under uncertainty. In: IEEE. *Intelligent System Application to Power Systems (ISAP), 2017 19th International Conference on*. [S.l.], 2017. p. 1–6. 29, 56

26 MATTLET, B.; MAUN, J.-C. Assessing the benefits for the distribution system of a scheduling of flexible residential loads. In: IEEE. *Energy Conference (ENERGYCON), 2016 IEEE International*. [S.l.], 2016. p. 1–6. 29

27 DISTRIBUTED Energy Resources - Customer Adoption Model (DER-CAM). 2018. <https://building-microgrid.lbl.gov/projects/der-cam>. 30

28 AHMADIAN, A. et al. Optimal wdg planning in active distribution networks based on possibilistic–probabilistic pevs load modelling. *IET Generation, Transmission & Distribution*, IET, v. 11, n. 4, p. 865–875, 2017. 30, 56, 72

29 BEER, S. et al. An economic analysis of used electric vehicle batteries integrated into commercial building microgrids. *IEEE Transactions on Smart Grid*, IEEE, v. 3, n. 1, p. 517–525, 2012. 30

30 GUO, Y. et al. Two-stage economic operation of microgrid-like electric vehicle parking deck. *IEEE Transactions on Smart Grid*, IEEE, v. 7, n. 3, p. 1703–1712, 2016. 30

31 LI, X.; CAO, J.; DU, D. Probabilistic optimal power flow for power systems considering wind uncertainty and load correlation. *Neurocomputing*, Elsevier, v. 148, p. 240–247, 2015. 30

32 ARRIAGADA, E. et al. A probabilistic economic dispatch model and methodology considering renewable energy, demand and generator uncertainties. *Electric Power Systems Research*, Elsevier, v. 121, p. 325–332, 2015. 30, 40, 41, 72

33 YU, H. et al. Probabilistic load flow evaluation with hybrid latin hypercube sampling and cholesky decomposition. *IEEE Transactions on Power Systems*, IEEE, v. 24, n. 2, p. 661–667, 2009. 30

34 HARRIS, W.; EHSANI, M. Socioeconomically sustainable rural microgrid engineering design. In: IEEE. *Global Humanitarian Technology Conference (GHTC), 2017 IEEE*. [S.l.], 2017. 31

35 BRENNA, M.; LONGO, M.; YAICI, W. Simulation and optimization of integration of hybrid renewable energy sources and storages for remote communities electrification. In: IEEE. *Innovative Smart Grid Technologies Conference Europe (ISGT-Europe), 2017 IEEE PES*. [S.l.], 2017. 31

36 USTUN, T. S. The importance of microgrids & renewable energy in meeting energy needs of the brazilian amazon. In: IEEE. *Power and Energy (PECon), 2016 IEEE International Conference on*. [S.l.], 2016. p. 1–6. 31

37 GRABER, S. et al. Solar microgrids in rural india: Consumers' willingness to pay for attributes of electricity. *Energy for Sustainable Development*, Elsevier, v. 42, p. 32–43, 2018. 31

38 ADEFARATI, T.; BANSAL, R. C.; JUSTO, J. J. Reliability and economic evaluation of a microgrid power system. *Energy Procedia*, Elsevier, v. 142, p. 43–48, 2017. 31

39 AL-SHAALAN, A. M. Essential aspects of power system planning in developing countries. *Journal of King Saud University-Engineering Sciences*, Elsevier, v. 23, n. 1, p. 27–32, 2011. 31

40 MENGOLINI, A.; VASILJEVSKA, J. The social dimension of smart grids. *Consumer, community, society. Luxembourg: EU Commission, JRC Scientific and Policy Reports*, 2013. 31

41 RIFKIN, J. *The third industrial revolution: how lateral power is transforming energy, the economy, and the world*. [S.l.]: Macmillan, 2011. 31

42 MORRIS, G. Y. et al. Evaluation of the costs and benefits of microgrids with consideration of services beyond energy supply. In: IEEE. *Power and Energy Society General Meeting, 2012 IEEE*. [S.l.], 2012. p. 1–9. 32

43 VAAHEDI, E. et al. The emerging transactive microgrid controller: Illustrating its concept, functionality, and business case. *IEEE Power and Energy Magazine*, IEEE, v. 15, n. 4, p. 80–87, 2017. 32

44 VASILJEVSKA, J.; LOPES, J. P. On the micro-grid and multi micro-grid impact assessment: Cost and benefits evaluation. 2011. 32

45 LI, J.; WU, L. et al. Optimal operation for community based multi-party microgrid in grid-connected and islanded modes. *IEEE Transactions on Smart Grid*, IEEE, 2016. 33

46 LU, X.; WANG, J.; GUO, L. Using microgrids to enhance energy security and resilience. *The Electricity Journal*, Elsevier, v. 29, n. 10, p. 8–15, 2016. 33

47 GHOLAMI, A. et al. Microgrid scheduling with uncertainty: The quest for resilience. *IEEE Transactions on Smart Grid*, IEEE, v. 7, n. 6, p. 2849–2858, 2016. 33

48 SHU, Z.; JIRUTITIJAROEN, P. Latin hypercube sampling techniques for power systems reliability analysis with renewable energy sources. *IEEE Transactions on Power Systems*, IEEE, v. 26, n. 4, p. 2066–2073, 2011. 34

49 MACHADO, P.; SOUZA, L. E. de; MAUN, J.-C. Long-term reliability analysis of a microgrid on isolated mode using cpn formalism. In: SPRINGER. *International Conference on Practical Applications of Agents and Multi-Agent Systems*. [S.l.], 2017. p. 53–62. 34

50 OLIVARES, D. E.; CAÑIZARES, C. A.; KAZERANI, M. A centralized optimal energy management system for microgrids. In: IEEE. *Power and Energy Society General Meeting, 2011 IEEE*. [S.l.], 2011. p. 1–6. 34

51 LIN, Z. et al. A survey on the applications of petri net theory in power systems. In: IEEE. *Power Engineering Society General Meeting, 2006. IEEE*. [S.l.], 2006. p. 7–pp. 34

52 KARAVAS, C.-S. et al. A multi-agent decentralized energy management system based on distributed intelligence for the design and control of autonomous polygeneration microgrids. *Energy Conversion and Management*, Elsevier, v. 103, p. 166–179, 2015. 34

53 NUNNA, H. K.; DOOLLA, S. Multiagent-based distributed-energy-resource management for intelligent microgrids. *IEEE Transactions on Industrial Electronics*, IEEE, v. 60, n. 4, p. 1678–1687, 2013. 34

54 QACHCHACHI, N.; MAHMOUDI, H.; HASNAOUI, A. E. Smart hybrid ac/dc microgrid: Power management based petri nets. In: IEEE. *Information Technology for Organizations Development (IT4OD), 2016 International Conference on*. [S.l.], 2016. p. 1–6. 34

55 SECHILARIU, M.; WANG, B.; LOCMENT, F. Building integrated photovoltaic system with energy storage and smart grid communication. *IEEE Transactions on Industrial Electronics*, IEEE, v. 60, n. 4, p. 1607–1618, 2013. 34, 63

56 DOU, C.-X.; LIU, B. Multi-agent based hierarchical hybrid control for smart microgrid. *IEEE transactions on smart grid*, IEEE, v. 4, n. 2, p. 771–778, 2013. 35

57 DOU, C.-x.; LIU, B.; GUERRERO, J. M. Event-triggered hybrid control based on multi-agent system for microgrids. *IET Generation, Transmission & Distribution*, IET, v. 8, n. 12, p. 1987–1997, 2014. 35

58 DOU, C. et al. Decentralised coordinated control of microgrid based on multi-agent system. *IET Generation, Transmission & Distribution*, IET, v. 9, n. 16, p. 2474–2484, 2015. 35, 63

59 LU, X. et al. Hybrid petri nets for modeling and analysis of microgrid systems. *IEEE/CAA Journal of Automatica Sinica*, IEEE, v. 3, n. 4, p. 349–356, 2016. 35

60 SALEH, M.; ESA, Y.; MOHAMED, A. Centralized control for dc microgrid using finite state machine. In: IEEE. *Power & Energy Society Innovative Smart Grid Technologies Conference (ISGT), 2017 IEEE*. [S.l.], 2017. p. 1–5. 35

61 TURNER, G. et al. Design and active control of a microgrid testbed. *IEEE Transactions on Smart Grid*, IEEE, v. 6, n. 1, p. 73–81, 2015. 35

62 MACHADO, P. et al. Modeling using colored petri net of communication networks based on iec 61850 in a microgrid context. *Journal of Control, Automation and Electrical Systems*, Springer, p. 1–15, 2018. 35

63 SANKARAKRISHNAN, A.; BILLINTON, R. Sequential monte carlo simulation for composite power system reliability analysis with time varying loads. *IEEE Transactions on Power Systems*, IEEE, v. 10, n. 3, p. 1540–1545, 1995. 36, 37, 42

64 SILVA, A. L. D. et al. Pseudo-chronological simulation for composite reliability analysis with time varying loads. *IEEE Transactions on Power Systems*, IEEE, v. 15, n. 1, p. 73–80, 2000. 37

65 BILLINTON, R.; SANKARAKRISHNAN, A. A comparison of monte carlo simulation techniques for composite power system reliability assessment. In: IEEE. *WESCANEX 95. Communications, Power, and Computing. Conference Proceedings., IEEE*. [S.l.], 1995. v. 1, p. 145–150. 37

66 JUSTUS, C. et al. Methods for estimating wind speed frequency distributions. *Journal of applied meteorology*, v. 17, n. 3, p. 350–353, 1978. 38

67 BILLINTON, R.; BAI, G. Generating capacity adequacy associated with wind energy. *IEEE transactions on energy conversion*, IEEE, v. 19, n. 3, p. 641–646, 2004. 39

68 KATSIGIANNIS, Y. A.; GEORGILAKIS, P. S.; TSINARAKIS, G. J. A novel colored fluid stochastic petri net simulation model for reliability evaluation of wind/pv/diesel small isolated power systems. *IEEE Transactions on Systems, Man, and Cybernetics-Part A: Systems and Humans*, IEEE, v. 40, n. 6, p. 1296–1309, 2010. 39, 40, 41

69 ZUBO, R. H.; MOKRYANI, G.; ABD-ALHAMEED, R. Optimal operation of distribution networks with high penetration of wind and solar power within a joint active and reactive distribution market environment. *Applied Energy*, Elsevier, v. 220, p. 713–722, 2018. 40

70 LV, Y. et al. A probability model of pv for the middle-term to long-term power system analysis and its application. *Energy Procedia*, Elsevier, v. 103, p. 28–33, 2016. 40

71 THOMSON, M.; INFIELD, D. Impact of widespread photovoltaics generation on distribution systems. *IET Renewable Power Generation*, IET, v. 1, n. 1, p. 33–40, 2007. 40

72 SONG, J. et al. Development of a markov-chain-based energy storage model for power supply availability assessment of photovoltaic generation plants. *IEEE Transactions on Sustainable Energy*, IEEE, v. 4, n. 2, p. 491–500, 2013. 41, 71

73 GRIGG, C. et al. The ieee reliability test system-1996. a report prepared by the reliability test system task force of the application of probability methods subcommittee. *IEEE Transactions on power systems*, IEEE, v. 14, n. 3, p. 1010–1020, 1999. 41, 74

74 KRISHNAMURTHY, S.; JAHNS, T.; LASSETER, R. The operation of diesel gensets in a certs microgrid. In: IEEE. *Power and Energy Society General Meeting-Conversion and Delivery of Electrical Energy in the 21st Century, 2008 IEEE*. [S.l.], 2008. p. 1–8. 42

75 PETERSON, J. L. Petri nets. *ACM Computing Surveys (CSUR)*, ACM, v. 9, n. 3, p. 223–252, 1977. 42, 43

76 DAVID, R.; ALLA, H. Petri nets for modeling of dynamic systems: A survey. *Automatica*, Elsevier, v. 30, n. 2, p. 175–202, 1994. 42

77 MURATA, T. Petri nets: Properties, analysis and applications. *Proceedings of the IEEE*, IEEE, v. 77, n. 4, p. 541–580, 1989. 43, 69

78 BILLINTON, R.; ALLAN, R. N. *Reliability evaluation of engineering systems*. [S.l.]: Springer, 1992. 45, 78

79 PRIVAULT, N. *Understanding Markov chains: examples and applications*. [S.l.]: Springer Science & Business Media, 2013. 45

80 BRÉMAUD, P. *Markov chains: Gibbs fields, Monte Carlo simulation, and queues*. [S.l.]: Springer Science & Business Media, 2001. v. 31. 45

81 SMITH, J. C.; TASKIN, Z. C. A tutorial guide to mixed-integer programming models and solution techniques. *Optimization in Medicine and Biology*, Taylor and Francis Auerbach Publications, p. 521–548, 2008. 50, 52, 54, 55

82 GENOVA, K.; GULIASHKI, V. Linear integer programming methods and approaches–a survey. *Journal of Cybernetics and Information Technologies*, v. 11, n. 1, 2011. 50, 51

83 CAVANINI, L. et al. Microgrid sizing via profit maximization: a population based optimization approach. In: IEEE. *Industrial Informatics (INDIN), 2016 IEEE 14th International Conference on*. [S.l.], 2016. p. 663–668. 56

84 CHEN, J. et al. Optimal sizing for grid-tied microgrids with consideration of joint optimization of planning and operation. *IEEE Transactions on Sustainable Energy*, IEEE, v. 9, n. 1, p. 237–248, 2018. 56

85 CHATTERJEE, A.; KEYHANI, A. Neural network estimation of microgrid maximum solar power. *IEEE Transactions on Smart Grid*, IEEE, v. 3, n. 4, p. 1860–1866, 2012. 56

86 METAXIOTIS, K. et al. Artificial intelligence in short term electric load forecasting: a state-of-the-art survey for the researcher. *Energy conversion and Management*, Elsevier, v. 44, n. 9, p. 1525–1534, 2003. 56

87 MORALES, R. et al. Microgrid planning based on fuzzy interval models of renewable resources. In: IEEE. *Fuzzy Systems (FUZZ-IEEE), 2016 IEEE International Conference on*. [S.l.], 2016. p. 336–343. 56

88 GAZIJAHANI, F. S.; SALEHI, J. Stochastic multi-objective framework for optimal dynamic planning of interconnected microgrids. *IET Renewable Power Generation*, IET, v. 11, n. 14, p. 1749–1759, 2017. 56

89 CHEN, S. H.; JAKEMAN, A. J.; NORTON, J. P. Artificial intelligence techniques: an introduction to their use for modelling environmental systems. *Mathematics and computers in simulation*, Elsevier, v. 78, n. 2-3, p. 379–400, 2008. 56

90 HUANG, C.-L. A particle-based simplified swarm optimization algorithm for reliability redundancy allocation problems. *Reliability Engineering & System Safety*, Elsevier, v. 142, p. 221–230, 2015. 56

91 PANT, S.; SINGH, S. Particle swarm optimization to reliability optimization in complex system. In: IEEE. *Quality and Reliability (ICQR), 2011 IEEE International Conference on*. [S.l.], 2011. p. 211–215. 56, 57

92 ABBAS, G. et al. Solution of an economic dispatch problem through particle swarm optimization: A detailed survey-part i. *IEEE Access*, IEEE, v. 5, p. 15105–15141, 2017. 57

93 MATTSON, C. A.; MESSAC, A. Pareto frontier based concept selection under uncertainty, with visualization. *Optimization and Engineering*, Springer, v. 6, n. 1, p. 85–115, 2005. 58, 59, 82

94 BAUMGARTNER, U.; MAGELE, C.; RENHART, W. Pareto optimality and particle swarm optimization. *IEEE Transactions on magnetics*, IEEE, v. 40, n. 2, p. 1172–1175, 2004. 58

95 XUE, B.; ZHANG, M.; BROWNE, W. N. Particle swarm optimization for feature selection in classification: A multi-objective approach. *IEEE transactions on cybernetics*, IEEE, v. 43, n. 6, p. 1656–1671, 2013. 58

96 LI, B.-B.; WANG, L.; LIU, B. An effective pso-based hybrid algorithm for multi-objective permutation flow shop scheduling. *IEEE transactions on systems, man, and cybernetics-part A: systems and humans*, IEEE, v. 38, n. 4, p. 818–831, 2008. 58

97 HIWA, S.; HIROYASU, T.; MIKI, M. Design mode analysis of pareto solution set for decision-making support. *Journal of Applied Mathematics*, Hindawi, v. 2014, 2014. 58

98 CAO, X.; WANG, J.; ZENG, B. A chance constrained information-gap decision model for multi-period microgrid planning. *IEEE Transactions on Power Systems*, IEEE, v. 33, n. 3, p. 2684–2695, 2018. 61

99 VIANA, A.; PEDROSO, J. P. A new milp-based approach for unit commitment in power production planning. *International Journal of Electrical Power & Energy Systems*, Elsevier, v. 44, n. 1, p. 997–1005, 2013. 61, 77

100 BALL, M. O. Computational complexity of network reliability analysis: An overview. *IEEE Transactions on Reliability*, IEEE, v. 35, n. 3, p. 230–239, 1986. 61

101 MACHADO, P.; SOUZA, L. E. de; NETTO, R. S. Framework to support grid-connected microgrid optimal planning. In: IEEE. *Environment and Electrical Engineering and 2017 IEEE Industrial and Commercial Power Systems Europe (EEEIC/I&CPS Europe), 2018 IEEE International Conference on*. [S.l.], 2018. p. 1–6. 62

102 PATEL, M. R. *Wind and solar power systems: design, analysis, and operation*. [S.l.]: CRC press, 2005. 72

103 GHAHDERIJANI, M. M.; BARAKATI, S. M.; TAVAKOLI, S. Reliability evaluation of stand-alone hybrid microgrid using sequential monte carlo simulation. In: IEEE. *Renewable Energy and Distributed Generation (ICREDG), 2012 Second Iranian Conference on*. [S.l.], 2012. p. 33–38. 72

104 CLEMENT-NYNS, K.; HAESEN, E.; DRIESEN, J. The impact of charging plug-in hybrid electric vehicles on a residential distribution grid. *IEEE Transactions on power systems*, IEEE, v. 25, n. 1, p. 371–380, 2010. 72

105 WOUTERS, C.; FRAGA, E. S.; JAMES, A. M. An energy integrated, multi-microgrid, milp (mixed-integer linear programming) approach for residential distributed energy system planning–a south australian case-study. *Energy*, Elsevier, v. 85, p. 30–44, 2015. 72

106 CPLEX Optimizer - IBM Analytics. 2018. <https://www.ibm.com/analytics/data-science/prescriptive-analytics/cplex-optimizer>. Online; accessed 12 April 2018. 75

107 LOFBERG, J. Yalmip: A toolbox for modeling and optimization in matlab. In: IEEE. *Computer Aided Control Systems Design, 2004 IEEE International Symposium on*. [S.l.], 2004. p. 284–289. 75

108 ZAHMATI, A. S.; FERNANDO, X.; GRAMI, A. Steady-state markov chain analysis for heterogeneous cognitive radio networks. In: IEEE. *Sarnoff Symposium, 2010 IEEE*. [S.l.], 2010. p. 1–5. 80

109 ZADEH, L. Optimality and non-scalar-valued performance criteria. *IEEE transactions on Automatic Control*, IEEE, v. 8, n. 1, p. 59–60, 1963. 81

110 CHIANDUSSI, G. et al. Comparison of multi-objective optimization methodologies for engineering applications. *Computers & Mathematics with Applications*, Elsevier, v. 63, n. 5, p. 912–942, 2012. 81

111 COELLO, C. A. C. A comprehensive survey of evolutionary-based multiobjective optimization techniques. *Knowledge and Information systems*, Springer, v. 1, n. 3, p. 269–308, 1999. 81

112 JIA, L.; TONG, L. Renewables and storage in distribution systems: Centralized vs. decentralized integration. *IEEE Journal on Selected Areas in Communications*, IEEE, v. 34, n. 3, p. 665–674, 2016. 82

113 KUMAR, D.; SAMANTARAY, S. R.; KAMWA, I. Multi-objective design of advanced power distribution networks using restricted-population-based multi-objective seeker-optimisation-algorithm and fuzzy-operator. *IET Generation, Transmission & Distribution*, IET, v. 9, n. 11, p. 1195–1215, 2015. 82

114 JAVADI, M. S. et al. Multi-objective expansion planning approach: distant wind farms and limited energy resources integration. *IET Renewable Power Generation*, IET, v. 7, n. 6, p. 652–668, 2013. 82

115 MARQUES, L. T.; DELBEM, A. C.; LONDON, J. B. A. Towards the improvement of multi-objective evolutionary algorithms for service restoration. In: IEEE. *Power & Energy Society Innovative Smart Grid Technologies Conference (ISGT), 2017 IEEE*. [S.l.], 2017. p. 1–5. 82

116 SHEN, G. et al. Micro grid scheduling optimization model based on multi-objective genetic algorithm. In: IEEE. *Intelligent Transportation, Big Data & Smart City (ICITBS), 2016 International Conference on*. [S.l.], 2016. p. 513–516. 82

117 MATTSON, C.; MESSAC, A. Concept selection in n-dimension using s-pareto frontiers and visualization. In: *9th AIAA/ISSMO Symposium on Multidisciplinary Analysis and Optimization*. [S.l.: s.n.], 2002. p. 5418. 82

118 ASSOCIATION, A. A. W. E. *AWEA small turbine global market study - American Wind Energy Association (AWEA)*. 2010. 89

119 LAZARD. *Lazard's levelized cost of energy analysis - version 8.0*. 2013. 89

120 TSIKALAKIS, A. G.; HATZIARGYRIOU, N. D. Centralized control for optimizing microgrids operation. In: IEEE. *Power and Energy Society General Meeting, 2011 IEEE*. [S.l.], 2011. p. 1–8. 89

121 ANEEL. *Resolucao normativa 733 - Tarifa Branca*. 2015. <http://www.aneel.gov.br/tarifa-branca>. Online; accessed 02 March 2018. 89

122 ANEEL. *Resolucao normativa 547 - Bandeiras tarifarias*. 2013. <http://www.aneel.gov.br/bandeiras-tarifarias>. Online; accessed 02 March 2018. 89

123 CEMIG - Tarifa Branca. 2018. <http://www.cemig.com.br/pt-br/atendimento/Paginas/valores_de_tarifa_e_servicos.aspx>. 89

124 BAKAR, N. N. A. et al. Microgrid and load shedding scheme during islanded mode: A review. *Renewable and Sustainable Energy Reviews*, Elsevier, v. 71, p. 161–169, 2017. 94

125 POLI, R.; KENNEDY, J.; BLACKWELL, T. Particle swarm optimization. *Swarm intelligence*, Springer, v. 1, n. 1, p. 33–57, 2007. 99

126 AGRAWAL, G. et al. Intuitive visualization of pareto frontier for multiobjective optimization in n-dimensional performance space. In: *10th AIAA/ISSMO multidisciplinary analysis and optimization conference*. [S.l.: s.n.], 2004. p. 4434. 102

127 MAVROTAS, G. Effective implementation of the ε-constraint method in multi-objective mathematical programming problems. *Applied mathematics and computation*, Elsevier, v. 213, n. 2, p. 455–465, 2009. 106

128 FONSECA, C. M. et al. Evolutionary multi-criterion optimization. In: SPRINGER. *Second International Conference, EMO 2003*. [S.l.], 2003. 106

129 COELLO, C. A. C.; CORTÉS, N. C. Solving multiobjective optimization problems using an artificial immune system. *Genetic Programming and Evolvable Machines*, Springer, v. 6, n. 2, p. 163–190, 2005. 106

130 LWIN, K. T.; QU, R.; MACCARTHY, B. L. Mean-var portfolio optimization: A nonparametric approach. *European Journal of Operational Research*, Elsevier, v. 260, n. 2, p. 751–766, 2017. 108